ՀՀ ԳԱԱ Վ. Համբարձումյանի անվան Բյուրականի աստղադիտարան

Անդրեասյան Հասմիկ Ռուբենի

«Երիտասարդ էրուպտիվ աստղերի ուսումնասիրություն»

ԱՏԵՆԱԽՈՍՈՒԹՅՈՒՆ

Ա. 03. 02 – «Աստղաֆիզիկա, ռադիոաստղագիտություն» մասնագիտությամբ ֆիզիկամաթեմատիկական գիտությունների թեկնածուի գիտական աստիճանի համար

Գիտական ղեկավար՝

Ֆ. մ. գ. դ. Մաղաքյան Տիգրան Յուրիի

Բյուրական – 2021

NATIONAL ACADEMY OF SCIENCES OF THE REPUBLIC OF ARMENIA

BYURAKAN ASTROPHYSICAL OBSERVATORY
AFTER V. AMBARTSUMIAN

HASMIK ANDREASYAN

THE INVESTIGATION OF YOUNG ERUPTIVE STARS

PhD Thesis

A thesis submitted in fulfillment of the requirements for the degree of Doctor of Philosophy in specialization
01.03.02 – Astrophysics and Radioastronomy

Scientific adviser:
Dr. Tigran Yu. Magakian

Byurakan 2021

CONTENT

1. GENERAL INTRODUCTION

The discovery of the Stellar Associations by Viktor Ambartsumian in 1947 opened a new era in our understanding of the star formation processes [1]. It was a "sowing the seeds" of a revolutionary theory, which defined our modern view on the star formation and led to many subsequent discoveries. The idea that star formation is an ongoing process, i.e., continues at all stages of the evolution of our Galaxy, was like a "bolt from the blue", as the first hypothesis about the star formation supposed, that all stars were created or formed at the same time. The second discovery in the star formation theory was that stars formed not individually, but in physical groups or clusters, which create the stellar associations (groups of hot O, B giant and T-Tauri stars, with the maximum lifetime of 10^7 yrs.) during the initial phases of their evolution [2]. These associations contain gigantic amount of diffuse matter in a form of molecular clouds, with masses of an order of 10^4 $M_\odot$ and more. Stars are born within these giant molecular clouds (GMCs) of dust and gas. Under the gravitational turbulences the dust and gas begin to collapse in clumps. The gravitational pressure slowly heats up the material in their centers. Stars are formed in hot core centers called **"Protostars"**, or so called **Class 0** sources (in figure 1.1 the model of the stellar birth is presented). They are not visible in optical range, because they are still deeply embedded in dense clouds, however, we can detect such objects in infrared bands. This youngest stage lasts until the accretion of infalling material warms up a protostar to a temperature, sufficient for the start of a thermonuclear fusion. By then, the central object has accumulated most of its final mass and we can say, that "a star is born", namely when it becomes visible in the optical range. Those are called **Class I** objects. They are still surrounded by the significant residual envelopes of the circumstellar material and at least 60% of all young stellar objects have a circumstellar disk [3]. At this evolutionary stage the newly born star is named as **Pre-Main Sequence (PMS)** star and it is located above the Main Sequence in **Hertzsprung-Russell (HR)** diagram.

In general, the evolutionary path of low mass young stellar objects (**YSOs**) is going through Class 0 to Class III, where **"Class 0"** sources correspond to the youngest protostar stage known so far and **Class III** sources are the most evolved ones [4,5]. Quantitatively, **Class 0** sources have ages $t<10^4$ yrs, **Class I** sources are estimated to be typically $t\approx10^5$ yrs, **Class II** sources correspond to classical T Tauri type stars (CTTS) and have ages ranging from 10^5 yrs to several times 10^6 yrs and more. The much later epochs ($>10^7$yr), when the central star has consumed or has dispersed most of its circumstellar material, correspond to the **Class III** sources. Practically, they are more evolved CTTS stars and are called weak-line T Tauri stars (WTTS).

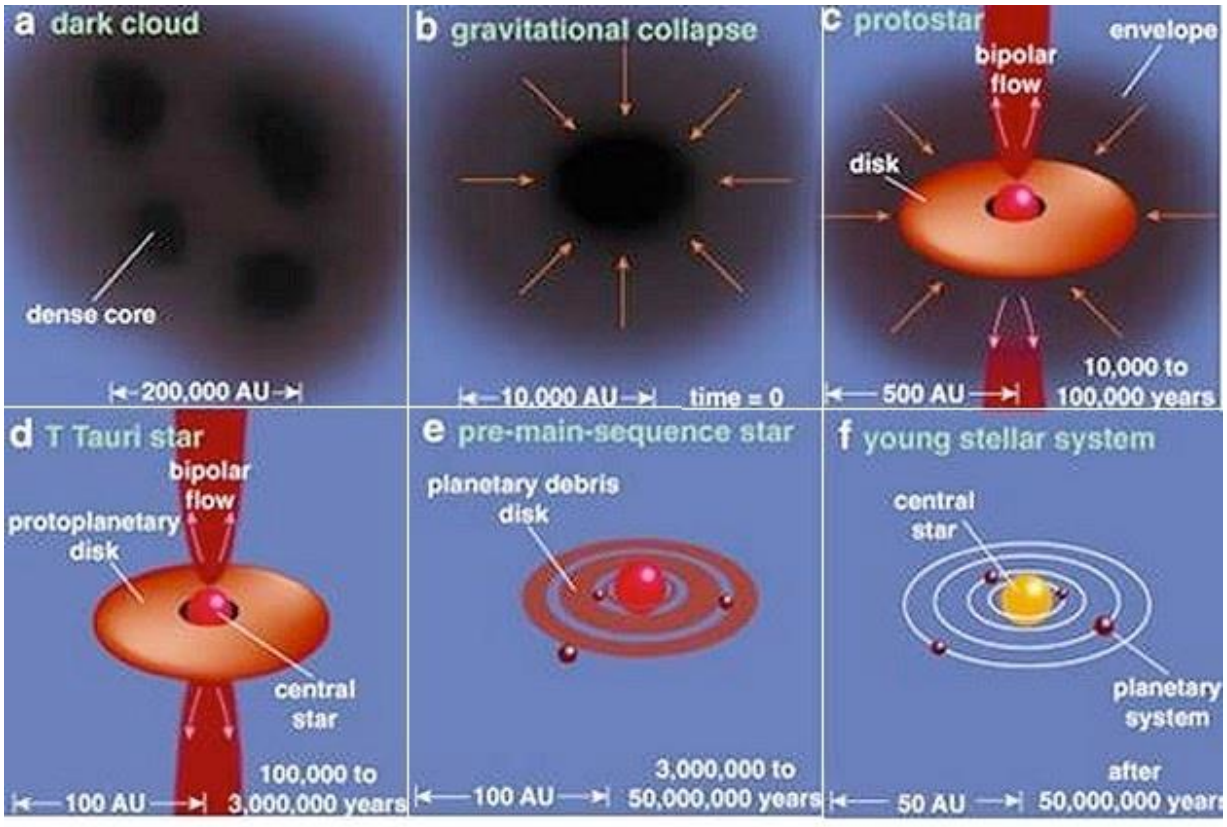

Figure 1.1 The model of a stellar birth

Based on their masses, PMS stars are divided into two classes – the **T Tauri (TTS)** ($M<2M_\odot$) and the **Herbig Ae/Be (HAeBe)** ($2M_\odot<M<8M_\odot$) type stars and both classes show

various types of variability. More massive stars ($M>8M_{\odot}$) skip the PMS phase, because they evolve very quickly.

The most prevalent type of PMS objects are TTS stars, a common interest in which began after the pioneering work of Joy [6]. At that time there were only eleven stars known with similar variability and physical characteristics, which differ from already known classes of variable stars. So they were considered as a new class, which are named now as **"T Tauri variables"** after their prototype T Tauri (TT) star – the brightest member of the group, variations of which were detected a long before [7]. The distinctive characteristics of TTS are:

- Irregular variability for about 3 magnitudes
- Spectral types F5-G5, with emission spectrum
- Low luminosity and the association with nebulosity.

Presently, the number of TTSs has increased to hundreds and many studies are being conducted for revealing the uncertain physical causes of light variations of TTSs. One of the distinguishable characteristics of the spectra of TTs is the photospheric line Li λ6707, which indicates their young age.

Nowadays it is generally accepted that TTSs can be separated into two main subclasses: Classical T Tauri stars (CTTSs), which are surrounded by circumstellar disk and Weak line T Tauri stars (WTTSs), which lack the evidence of the accretion disk [8,9]. A huge variety of the photometric and spectroscopic variabilities observed in young stars, makes their classification very difficult. A detailed study of various causes of TTS variability has been carried out in work of Herbst [10], based on a large catalog, including details of several hundred stars. Consequently, the additional class of early type stars with spectral type of K1 and earlier **(early-type T Tauri stars (ETTS))** was added, in order to separate the particularities in their variability. Let's discuss these classes one by one.

The periods of variability of **WTTSs** (**variability type I**) are on time scales of days, with the amplitudes up to $0^m.8$ in V band and they are caused by the rotation of large dark magnetic spots on the surface of the star. In the case of **CTTSs** (variability type II) we

observe non-periodic variability, with the amplitudes of up to 3^m in V band, which is caused by a superposition of cool and hot surface spots. In general, the idea that hot and cool spots, analogically with the Sun, can exist on the surfaces of T Tauri stars and could cause light variations as the stars rotate, for the first time was suggested by Hoffmeister [11]. According to models, approximately 20% of the TT stars are covered by dark spots, with a lifetime that varies from days to a few years [12]. Also, it is well known that many T Tauri stars have so called "veiling continuum" [7], i.e. excess of continuous emission which can cover the absorption lines in some regions of the spectrum. It is also known, that the degree of veiling can be changed with time, also causing the light variations in CTTSs.

Regarding **ETTSs (variability type III)**, the general picture is more confused. Period of irregular variations of ETTSs is on timescales of days to weeks, with amplitudes typically less than one magnitude. It is probably caused by the circumstellar obscurations due to the dust clumps or clouds passing by the star. Such kind of variability is typical also for HAeBe stars [13], which are discussed later.

Besides of slow variations, there are CTTSs, which demonstrate also powerful outbursts of up to five magnitudes. These objects are classified into two main classes of eruptive variables: **FUors** and **EXors** (see a review by Audard et al. [14]). These stars are among the most intriguing PMS objects, since the identification of their origin could potentially lead to the consistent picture of the early phases of stellar evolution. Although, they were discovered relatively lately, many studies have been performed in order to understand the nature of these outbursts. Let us take a closer look at each class, separately.

The prototype of the class of eruptive variables **FUors** is a variable star **FU Ori**, which in 1937-1939 gradually raised its brightness from m_{pg}= 16 to 10 and since then it appeared in the spotlight [15,16]. By its designation this group was named as FUors by V. Ambartsumian [17]. FUors can be found in the regions of star formation and usually, are associated with reflection nebulae and dark clouds. Up to now, only few objects have been generally classified as members of the class of classical FUors: FU Ori itself, V1057 Cyg, V1515 Cyg and V1735 Cyg (fig. 1.2). The characteristic feature of all of them is the strong outburst of 5-6 magnitudes on a timescales of a year, following by a very slow fading. Moreover, in the

case of FU Ori we see that the star is remaining in high-luminosity state until now, i.e. almost 90 years. Besides the powerful outburst and subsequent spectral variability, also short-term photometric variability with amplitude of approximately 0.2 mag. and duration of a few days took place in FU Ori [18]. Spectroscopically, FUors have non-emission type spectra, dominated by the deep CO overtone absorption, with broad blue-shifted Balmer lines, P Cygni profiles in Hα and the Na I lines, which imply a mass-lose rate of about 10^{-5} $M_{\odot}$ yr^{-1}. In general, the spectral type of FUors is attributed to F-G type giants/supergiants in the visible and M type in the near IR ranges. As the ionization level in FUor atmospheres is low, we do not see lines with a degree of ionization higher than Fe II and He I.

But what is the generator of these outbursts? This question has triggered different hypotheses and it is still open. Based on the accredited theory of Hartmann & Kenyon, the protostellar accretion proceeds as follows: more or less steady accretion matter falls from the envelope onto the protostellar disk, then from the protostellar disk onto the central star [19,20]. As a result we observe short but very powerful episodes of flow, which manifest FUori outbursts.

Thus, FUors outbursts happen when the circumstellar accretion disk is increasing its surface brightness as the external envelope falling onto it, i.e., disk accretion rate greatly increases. The spectral features of FUors in the optical and in the near-infrared wavelengths (the typical double peak absorption lines from a rotating disc) are considered in favor of this interpretation.

The opposite theory suggests that the star itself is the reason of such flare-ups [21]: referring to the broad absorption lines of FUors, Larson deduces that as a result of rapid rotations, the outer layers of the star can be heated enough to evoke outbursts and a mass loss via powerful winds. In [22] authors also support this idea. In this context, we also have to take into account the possibility of a presence of a companion star, example of which is the FU Ori itself [23]. Fig. 1.2 presents four classical FU Ori stars.

Figure 1.2 Color image of a field around FU Ori, V1057 Cyg, V1515 Cyg and V1735 Cyg, taken from PanSTARRS DR 1 survey (i, r, g filters). The stars are shown with the cross.

The class of FUors is not numerous. The problem lies in observational inconveniences: It is hard to follow the star for decades to confirm its FUor type outburst. There are many known objects, which spectroscopically can be classified as FUors, but the outburst event has not been documented for them. It is possible, that for such objects an outburst has occurred too long ago and we did not have opportunity to detect it. It is not surprising, since we know that the timescale of the decline phase of FUors can last decades. For such objects, which show the main spectral characteristics of classical FUors, but the outburst phase has not been witnessed, the label **FUor-like** is adopted. The possible differences and similarities of these two classes of eruptive objects were discussed in many works (e.g.,

[23,24]). Both of them are young stars undergoing episodes of high accretion, however they can be at different phases of their outburst activity or decay phases.

Although we know the evolutionary phases of FUors, it is interesting to state that they are mostly located in regions with relatively low star-formation activity [22, 24]. It could indicate that in high density environments either FUors, in general, are not frequent, or they have fewer stated outbursts. To address this issue we have to understand on which protostellar evolutionary phases the objects with FUor type outbursting activity could be found. Estimations show that a solar-type star can undergo 10-100 FUor outbursts during its pre-main-sequence phase [25]. Such recurrent outbursts can be explained by instabilities in massive accretion disks. But this idea requires more massive disks, than those typically detected in the T Tauri phase. As we have evidences for large, massive disk structures around the FUors [26], we have then a support for the idea that FUor outbursts primarily happen in an early phases of protostellar evolution. It is also confirmed, that FUors often are the source of molecular outflows, which are also youth's indicators. Both these characteristics are common among Class 0 and Class I objects, but not among Class II PMS stars. Even though Class 0 sources have active accretion disks and show outflows, it is unlikely that a FUori type outburst can be seen from Class 0 objects, even if such an outburst occurred. The reason is that Class 0 sources are deeply embedded in massive dusty clouds and envelopes, which do not allow the star to be visible in the optical range, i.e. being detected. In [27], authors support the idea that FUors show alike correlation between the disk mass and the outflow, as seen in Class I sources. So, it means that the protostars can go through several FUor outbursting events before they throw off their surrounding clouds and reach the T Tau phase. Moreover, only the low-mass protostars during their first few hundred - thousand years can exhibit FUor or FUor-like events.

The molecular outflows from FUors can produce the bright knots of emission: so called **Herbig-Haro (HH)** objects. **HH** objects are formed when jets of partially ionized gas, ejected by the star, meet nearby clouds of gas and dust [28]. Indeed, the studies confirm the existence of a strong relation of HH objects with episodic outbursts of FUors [29]. Appositely, it was Ambartsumian, who proposed to name these objects "Herbig-Haro".

There are also a significant number of stars that kind of mimic the FUors, but in smaller scale. This group of eruptive variable stars is named **EXors** [25], after their prototype **EX Lupi**. The members of this group show occasional flare-ups like FUors, but during their maximum brightness their spectroscopic behavior is different. In contrast to FUors, their spectra are dominated by T-Tauri like emission spectra, with no stellar absorption lines. In addition, they are less luminous and their outbursts are relatively short-term in comparison with FUors, lasting months to year. Thereby EXors are ideal candidates to investigate both on quiescence vs outburst phases for the same objects on relatively short time scales, which could help to find answers for many questions about the evolutionary studies of individual objects. Even though around two dozens of EXors are known, only some of them are well-studied, for example EX Lupi itself and two other objects - V1118 Ori and VY Ori, which all together demonstrate the diversity of outburst properties of EXors. It should be noted, that this class of eruptive variables was actively studied by prof. Elma Parsamian in Byurakan and in Mexico [30].

The explanation of EXor type outbursts is thought to be similar to FUor phenomenon. Until now the most successful model remains the one suggested in [19] for FUor type outbursts: accretion matter is passing through the circumstellar disk toward its inner edge, from where this matter along the magnetic lines pours on the central star. However, the mechanism responsible for the EXors accretion outburst is still a controversial issue: two scenarios are proposed:

1. disk instabilities, as a sequel of thermal instabilities causing the changes on the disk viscosity [31], or, alternatively:

2. accretion bursts could be caused by external reasons, such as an existence of a close binary pair [32]. Indeed, many EXors are located in binary systems, including the EX Lupi. EX Lup is a young low-mass ($0.6M_{\odot}$) M0 V type star, with bolometric luminosity in quiescent phase $L_{bol}=0.7L_{\odot}$. Last time it underwent the strong outburst in 2008: it raised its brightness for five magnitudes and kept this high level for six months with a slight fading, and afterwards returned to its initial state. The quick recovery of EX Lup after the outburst and the similarity between its pre-outburst and post-outburst states let us to presume, that

during the outburst only the accretion rate has varied. Its study revealed that accretion was also present in quiescence stage, but it has delivered less material onto the star than in the outburst phase.

Except for the individual objects such as EX Lupi, not many studies exist on obtaining the data for EXor candidates. The most complete investigation of EXor type objects was done by the group which carried out the program called EXORCISM (EXOR Optical and Infrared Systematic Monitoring, [33,34]), intended to perform photometric and spectroscopic long-term monitoring of eruptive variables/candidates. The analysis of the large amount of data obtained by this monitoring program shows that typical values for accretion rate of EXors during the quiescent stage are $m_{acc} = 10^{-10} - 10^{-8}\ M_{\odot}\ yr^{-1}$ and $m_{acc} = 10^{-8} - 10^{-6}\ M_{\odot}\ yr^{-1}$ during the outburst. As was mentioned above, during the outburst the number of emission lines increases and undergoes striking variations. Many emission lines exhibit asymmetric profiles. P Cyg profiles at the higher Balmer lines indicate the presence of strong winds of quite high velocities up to hundreds km/s. During both quiescence and outburst phases metallic neutral and ionized lines (FeI and FeII) are detected. Forbidden emission lines ([OI], [SII], [FeII]) usually exhibit blueshifted profiles, which indicate the presence of shocked gas and jets originating from the star.

Herbig Ae/Be stars are the class of objects described by Herbig [35]. In his pioneering work Herbig listed 26 Ae and Be PMS stars of intermediate masses, satisfying three criteria:

- Having the spectral type A or earlier, with emission spectrum
- The star must have been situated in an obscured region
- It has to illuminate fairly bright nebulosity in its immediate vicinity.

The 2nd criterion is natural, because YSOs are located in the regions associated with molecular clouds. The 3th requirement is pointing out the difference between an “ordinary” Be and “Herbig” Be star, which relies on the necessity in the association with the nebulosity of the latter. It turns out, that there are physical differences between these two classes of objects. For example, infrared (IR) excesses of Herbig Ae/Be stars are much stronger than those of ordinary Be stars [36,37].

A mass range of HAeBe stars places them in between Solar-type stars and high mass stars. Therefore, they play an important role in the studies of the evolution of star formation from actively accreting discs towards to debris discs and mature planetary systems. So they could be the key in understanding both the formation of stars and of the planets. Unfortunately, there were not many large-scale systematic surveys of HAeBe stars and they have mostly been found serendipitously. But nowadays there are known more than two hundreds of HAeBe stars, which makes the analysis of these objects much easier and reliable.

HAeBe stars are known to show irregular photometric and spectroscopic variations, similar to ETTS class of variables [38,39], as mentioned above. It is accepted, that their variability is caused by the extinction, for example due to rotating circumstellar disk. In [39] studied more than 250 HAeBe stars, concluding that ≈25% of all HAeBes show strong variability, which correlates with Hα line profile and ≈ 70% of them display double peaked Hα line profiles, which is an indicator of an edge-on disk. Moreover, they point out the possibility of similar accretion mechanisms in Herbig Ae and T Tauri type stars by studying the variations of Hα line profiles. A break in properties at around $3M_{\odot}$ and at around $7M_{\odot}$ was indicated by the same team. Hence, in general, high mass stars have very small infrared excess and low variability. And vice versa, lower mass HAeBe objects show stronger variability and IR excess. There could be different reasons beyond that. For example, high mass objects have a more efficient dust dispersal mechanism [41], or their evolutionary track is passed faster. Basically, variations seen in HAeBe stars are not very large, i.e., of the order of one magnitude in the optical range, but an extreme cases of non-periodic variability with sudden quasi-Algol-type drops in brightness of two-three magnitudes have been also observed [42]. These objects form a small group of PMS stars of intermediate mass and they are named **UXors,** after their prototype **UX Ori** star [43]. Many objects of this group of irregular variables are catalogued as HAeBes. As a separate class of objects, UXors have received an attention only in the last thirty years, however, at the present they became a subject of many photometric and spectroscopic investigations [44,45]. Observations in the IR and in the millimeter ranges have shown that UXors are surrounded by optically thick circumstellar

disks, alike TTSs. It is generally established, that edge-on disks are responsible for the large variability observed in UXors [44,46]. Their defining characteristic is not only photometric and spectroscopic variability, but also so called "reddening and blueing effect". It has been observationally confirmed that with a change in brightness, a star becomes redder when its apparent magnitude increases. Then, at some brightness level, these stars reverse this redward trend and become bluer. This effect was first observed by Wenzel [47] and later by many others [48,49]. This, at first sight unexpected phenomenon was explained by the assumption, that variations in brightness are caused by a dust cloud spinning around the star, in the outer part of stars' circumstellar disk. So, if the disk is oriented nearly edge-on with respect to the observer, then the dust cloud passing in front of the star will obscure the object. As a result we observe the star reddened and with reduced brightness, so we detect Algol-like minimum of two-three magnitudes. Afterwards, when the obscuring cloud passes away from the line of sight, the star becomes brighter and its color index decreases. Many largely irregular variable HAeBe stars, including UX Ori itself, exhibit this blueing effect. This could lead us to the idea that the circumstellar environment of UXors is more evolved, so they are important in studies of the evolutionary processes of circumstellar disks. However, as it was shown in [42] UXor features depend only on the favorable relative position between line of sight and equatorial plane. Detailed spectral investigations of UXors are presented in [46]. Overall picture is the following: spectra consist by many redshifted absorption metallic lines and the Hα line is strong and double-peaked. It is explained by the infall of gas from the disk material onto the star, just like in the magnetospheric accretion models proposed for TTSs. Using these assumptions, one could show that the accretion rate for UXors is $M_{acc} \approx 10^{-7} M_{\odot}$ yr^{-1}.

Despite all the great progress made in the field of eruptive variables, there are still many open questions. Even the origin of the outburst is a matter of debate. While the reason of the UXor type variability is more or less clear, we cannot say the same about the FUors and EXors. It is uncertain whether the same mechanism is responsible for both FUor and EXor type outbursts, or they occur in different ways. Maybe both classes are presenting the same phenomena in different evolutionary stages. The discussion of these and many other

questions are in fact the subject of many studies (e.g. [14]) The undoubted classification of the objects as FUor, EXor or UXor is another problem, taking into account that some recently discovered examples of eruptive stars somehow filled the gap between long-term (FUor) and short-term (EXor) outburst manifestations. These newly discovered objects display a kind of intermediate timescale of outburst decay and other characteristics in comparison of classical FUors and EXors. It is not excluded, that the same object at the same time can represent both, for example FUor and UXor type variability. For revealing the nature of the outbursts it is also very important to study the associated with the FUor or EXor stars reflection nebulae, HH objects and jets, as their main driven forces. The difficulty concerning the understanding of their evolutionary framework is probably due to the fact that the modeling of the evolution of the entire disk is far from being an easy task. The theoretical models are usually focused on either the inner or outer disks. As a result, the outcome does not entirely satisfy for both classes. Moreover, up to now only few attempts have been made to compare the theoretical models with actual observations.

Consequently for further discoveries of possible new type of eruptive YSOs and PMS objects, firstly, we need a comprehensive, long-term, multi–wavelength monitoring of eruptive variables, including both photometric and spectroscopic investigations. Nowadays many space-based telescopes are operating, carrying out surveys in different wavelength and thus covering the whole range. Indeed, large-field monitoring facilities enlarge our arsenal of observational data, but, despite that, we are reliant that the ground-based telescopes still have great potential. The observational material of the individually taken object in this case is extremely important, particularly if observations are systematic and include photometry and spectroscopy. Consequently we decided to start our project of investigation for both previously and newly identified eruptive objects.

In this sense, very important work also is done by the group of American Association of Variable Star Observers (AAVSO) [50].

2. METHODS

In 2015 our group decided to start the new observational program of optical investigation of eruptive stars. The aim was to re-observe young stars, which traditionally show odd and peculiar variations, thus obtaining new observational material on them. Also we were intended to find new possible candidates of different classes of eruptive variables. The spectral data were obtained mainly with the 2.6-m telescope of the Byurakan Astrophysical Observatory (BAO) and with the 6-m. telescope of the Special Astrophysical Observatory (SAO), in collaboration with our Russian colleagues (in 2020). The photometric data were obtained with 2.6-m telescope and also with the 1-m telescope of (BAO)[1].

2.6-m optical telescope is the largest in BAO, and 2nd in Caucasus, after 6-m. in (SAO). It is located at the altitude of 1406 m. above the sea level with the coordinates: longitude 40°20′29″ and latitude +44°16′29″. We used SCORPIO (Spectral Camera with Optical Reducer) multi-mode camera with focal reducer at the prime focus of the telescope [51], thus having the opportunity to obtain both direct images and long-slit spectra (fig. 2.1). It was equipped with the TK SI-003A 1044 x 1044 CCD matrix before, and after August 2016 with the E2V CCD42-40 2080 x 2048 CCD matrix (see tab. 2.1). In fact, our observational program started immediately after the end of the refurbishing works on 2.6-meter telescope.

Detectors					
TK SI-003A 1044 x 1044			E2V CCD42-40 2080 x 2048		
Spec. ranges	R (resolution)	Å/pix	Spec. ranges	R (resolution)	Å/pix
4100-6800	800	2.7	4100-7100	800	1.5
5900-6800	2500	0.9	5800-6950	2500	0.5
5800-7300	1500	1.5	5700-7350	1500	0.8

Table 2.1 The specifics of CCD detectors, utilized during the observations in BAO.

[1] https://www.bao.am/index.php

Figure 2.1. The design of SCORPIO spectral camera

Since 2017 practically all photometric observations were conducted on 1-meter telescope. It is one of the largest Schmidt-type telescopes in the world and is famous for its many successfully conducted projects, including First Byurakan Survey (FBS, Markarian survey) and Second Byurakan Survey (SBS).

Several spectra were obtained with the 6-m. BTA telescope in SAO. It is situated at the altitude of 2070 m. above the sea level, in the Zelenchuksky District on the north side of the Caucasus Mountains in southern Russia. Its coordinates are: longitude 43°38′48″ and latitude +41°26′26″. During our observations the aperture reducer SCORPIO-2, which is the modernized version of SCORPIO [52], in the prime focus of the telescope, was used. It was equipped with E2V 261-84 CCD matrix as a detector. The reduction of the data, obtained with SCORPIO-2, was carried out in the IDL environment, using programs developed at SAO.

The list of targets included mainly the objects, for which we have found or at least suspected the eruptive activity in the PMS evolutional stage. Several objects in the course of observations were demonstrating significant variations, and therefore became the main targets for the further investigation.

Thus, in dissertation I present the detailed investigation of five objects: LkHα 225, LkHα 224, V565 Mon, PV Cep and V350 Cep. In each of chapters individual observations and corresponding analysis for these objects are given. In table 2.2 the general information of the observational time, spent on all targets, is listed.

Object	Total exposure (hour)
LkHα 225	11
LkHα 224	11
V565 Mon	4
PV Cep	5
V350 Cep	1

Table 2.2 The general information on observations. In the 2nd column a total exposure of spectral and photometric observations is shown.

In addition to our own observations, data from the following virtual observatories, electronic databases and large surveys played a very important role in my works. Definitely, one of the most applicable programs for me was the Aladin interactive sky atlas [53], which gives the immediate interactive access to all the databases and archives (like Simbad [54] and VizieR [55]). It gives an opportunity to easily compare the images of the same field taken from different surveys, which was very useful for my work. Surveys which I was mainly using were Gaia project[2] (Gaia) [56,57], The Two Micron All-Sky Survey (2MASS)[3],

[2] The data from the European Space Agency (ESA) mission Gaia (https://www.cosmos.esa.int/gaia) were processed by the Gaia Data Processing and Analysis Consortium (DPAC) https://www.cosmos.esa.int/web/gaia/dpac/consortium). Funding for the DPAC has been provided by national institutions, in particular the institutions participating in the Gaia Multilateral Agreement.

The Digitized Sky Survey (DSS)[4], Wide-field Infrared Survey Explorer (WISE)[5], The Panoramic Survey Telescope and Rapid Response System (Pan-STARRS)[6]. Below I will present the information and usage of each of them in my works.

Gaia DR2 was released on 2018 and it provides the most complete and reliable list of parameters of stars, available heretofore. It includes parallaxes and proper motions for more than 1.3 billion of stars and G magnitudes (which are matching with V magnitudes from the Johnson-Cousins photometric system) for more than 1.69 billion sources. For recalculation of distances I was using mostly the parallaxes of Gaia. Also, in some cases I checked the extinction estimates.

2MASS astronomical survey was published on 2003. It was conducted in three infrared wavelengths: 1.25 (J), 1.65 (H), 2.17 (K_s) micrometers. There are "2MASS" and "2MASSX" (extended) catalogues which, in total, include more than 300 million objects. I used 2MASS to obtain the infrared photometric data when needed.

DSS1 and *DSS2* are the digitized releases of several all-sky photographic surveys, including Palomar Observatory Sky Surveys I and II. They were prepared by the Space Telescope Science Institute between 1983 and 2006. The data are available in blue, red and IR bands. In optical band it is a useful guide, which can help to set the observations' direction.

WISE space survey was launched in 2009, then reactivated and renamed as NEOWISE in 2013. It imaged the entire sky in the middle-infrared 3.4, 4.6, 12 and 22 μm wavelengths bands. I used it to compare the optical and the infrared images, which in case of YSO's is very important.

---

[3] Two Micron All Sky Survey is a joint project of the University of Massachusetts and the Infrared Processing and Analysis Center/California Institute of Technology, funded by the National Aeronautics and Space Administration and the National Science Foundation.

[4] The Digitized Sky Surveys were produced at the Space Telescope Science Institute under U.S. Government grant NAG W-2166. The images of these surveys are based on photographic data obtained using the Oschin Schmidt Telescope on Palomar Mountain and the UK Schmidt Telescope. The plates were processed into the present compressed digital form with the permission of these institutions.

[5] Wide-field Infrared Survey Explorer is a joint project of the University of California, Los Angeles, and the Jet Propulsion Laboratory/California Institute of Technology, funded by the National Aeronautics and Space Administration.

[6] The Pan-STARRS1 Surveys (PS1) and the PS1 public science archive have been made possible through contributions by the Institute for Astronomy, the University of Hawaii, the Pan-STARRS Project Office, and participating institutions.

Pan-STARRS 1 and *2* surveys provide huge amount of the sky images in five bands (g, r, I, z, y). The telescopes of Pan-STARRS project, situated in Hawaii, have very large field of view (3 degree diameter, 7 square degrees FOV). The accompanying catalogue with precise astrometric and photometric values is also presented. For my tasks this survey has a great importance, because its particularly focuses on young variable stars.

The data reduction was done using IRAF (Image Reduction and Analysis Facility)[7] and ESO-MIDAS[8] software packages, which are primarily working on Linux operating system. They provide general tools for data reduction, which are organized into separate packages, including imaging and spectral reduction ones. Photometry of LkHα 225 and LkHα 224 was done mainly with IRAF, and the photometry of the V565 Mon, PV Cep and V350 Cep was performed using MIDAS.

For photometry in IRAF I was using Phot => apphot packages, which allowed me to do photometric estimations for individual stars. In the course of this, I also took a time to examine the facilities of the command "DAOfind" for the photometry of crowded fields. For the photometry of individual objects in MIDAS program, I was running appropriate "daophot" package. All spectral reductions were done with MIDAS system in the "spec" and "long" contexts. As a first step I removed the cosmic rays and noises, and then I calibrated the spectra. For the calibration of wavelengths the comparison spectra of Ne+Ar lamp were used. At the last step, the rebining of the spectra and the sky subtraction were performed to transform the pixels into the Angstroms. In order to estimate equivalent widths, radial velocities or other parameters the spectra were normalized to the continuum.

To create illustrative graphics, mainly the Origin 2017 Pro [58] and the program Inkscape [59] were used.

[7] IRAF is distributed by the National Optical Astronomy Observatories, which is operated by the Association of Universities for Research in Astronomy, Inc. (AURA) under cooperative agreement with the National Science Foundation

[8] ESO-MIDAS system is developed by European Southern Observatory

3. UNUSUAL YOUNG STAR V1318 CYGNI S (LkHα 225): NEW POWERFUL OUTBURST

3.1 Introduction

In 1960 George Herbig published his famous paper about the Ae/Be stars connected with nebulae (lately designated as HAeBe stars; [35]), which were suggested to represent the more massive and luminous young stellar objects in comparison to T Tauri stars. Among them he listed the bright BD+40°4124 star, surrounded by several objects with fainter emission lines. One of them was designated as LkHα 225. Only Hα emission lines of moderate intensity were found in its medium-resolution spectrum. A general view of this group is presented in Fig. 3.1.

This star attracted further attention when significant variability was found [60,61,62]. As a variable star it received V1318 Cyg designation. At the same time, the area around BD+40°4124 was recognized as a star-forming region, where several bright IR sources were discovered. Among them, LkHα 225 was also listed [63]. This object demonstrated prominent variability even in K band [64].

It is nearly impossible to draw certain conclusions about the photometric behavior of V1318 Cyg from early brightness estimations, as was pointed out by Wenzel [65]. Usually the object demonstrated erratic variations around V=17.0, with occasional brightening up to 2^m [62]. One cannot exclude the longer period of high brightness in the 1950s, as such a level can be seen on POSS-1 plate (1953) (Fig. 3.2a) and on the plate shown in [35], obtained in 1956. In both cases LkHα 225 is equal in brightness to or brighter than nearby LkHα 224.

In the 1980s, studies of the variability of V1318 Cyg continued in a more organized way, including systematic electrophotometric observations [66,67,68]. It was shown that the star fluctuated near a certain mean brightness level, sometimes demonstrating deep minima. The mean level itself was slowly decreasing from year to year, and in 1987-1988 the star brightness was always lower than V=17 [67].

Even in the DSS-1 images one can see that the shape of LkHα 225 is slightly elongated

in the north-south (N-S) direction (Fig. 3.2a). However, the probable duplicity of this object was mentioned for the first time only by Ibragimov et al., [66]. After the deep decline in brightness, the study of the inner structure of LkHα 225 became easier. As was shown in [69], the object actually consists of two stars - V1318 Cyg N and V1318 Cyg S – and a nebulous knot between them, all placed in the N-S direction, with a total separation of 5″. This discovery immediately raised a question about the role of both components in the high-amplitude variations of visible brightness. Below we consider this point in detail.

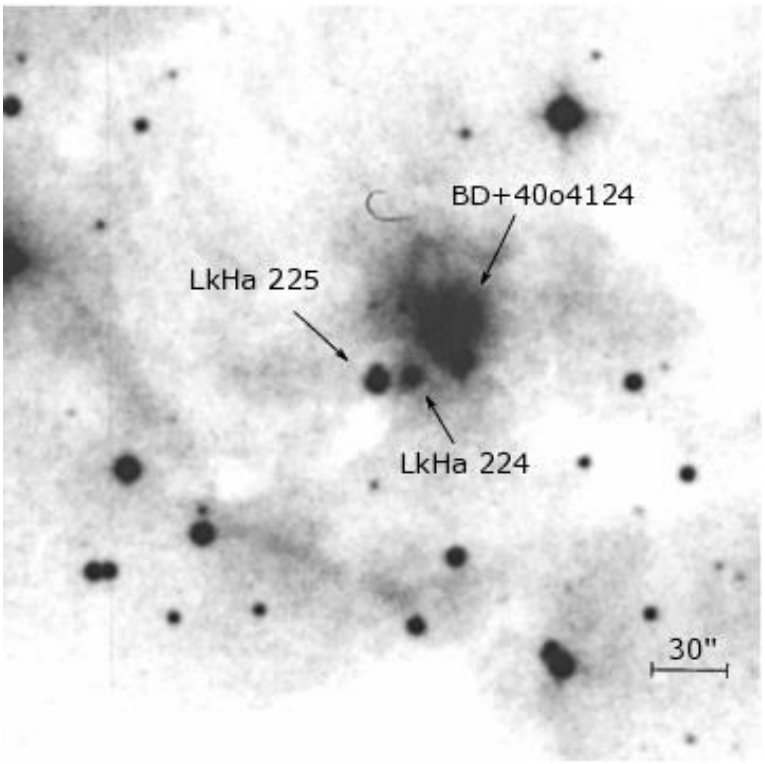

Fig. 3.1 Direct image of the BD+40°4124 region in POSS-1 red plate (14.06.1953), taken from SuperCOSMOS sky survey

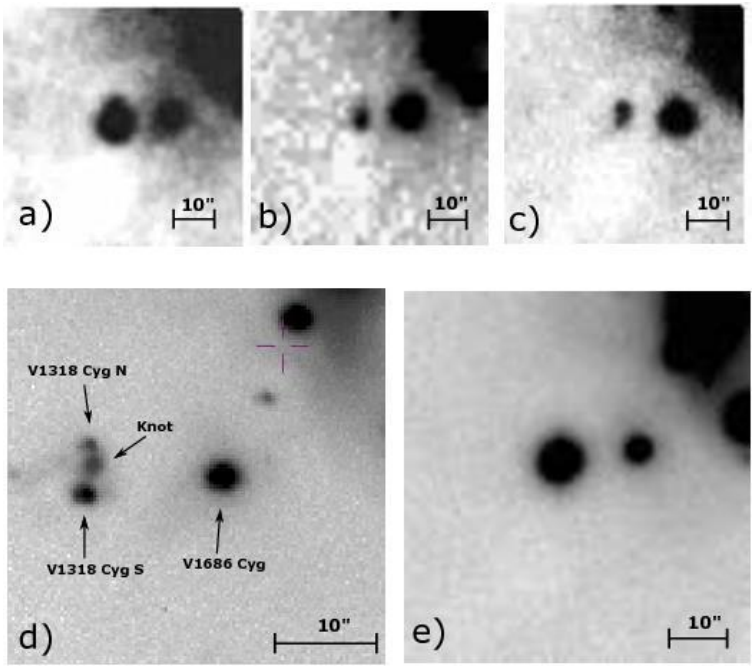

Fig. 3.2 Enlarged direct images of V1318 Cyg field. *(a)*: POSS-1 red plate (14.06.1953), SuperCOSMOS sky survey. *(b)*: Quick-V plate (3.09.1983), STScI digitized sky survey. *(c)*: POSS-2 red plate (29.06.1992), SuperCOSMOS sky survey. *(d)*: IPHAS survey image in R band (11.10.2006), objects discussed here are marked by arrows. *(e)*: ZTA-2.6 image in R band (22.09.2015). BD+40°4124 is hidden under the bright reflection nebula in the upper-right corner of all images.

Spectral data presented in [70,71], confirmed that both objects belong to the young stars of A-F spectral type with specific emissions, including prominent forbidden lines produced by Herbig-Haro type outflow, which was found by Magakyan & Movsesyan [71]. Pronounced differences between the spectra of V1318 Cyg S in maximal and minimal brightness levels were pointed out in the same study.

3.2 Observations and data reduction

Observations of V1318 Cyg were implemented on the 2.6-m telescope. The field of view in the imagery mode was 11.5′ (with 0.68″ pix^{-1}) and 13′ (with 0.38″ pix^{-1}) with TK and EEV

detectors, respectively. Direct CCD images were obtained in BVRI bands, usually with two or three exposures for each color. The seeing was 2.5-3″.

In the long-slit mode the width of the slit was 1.5″ and the length was about 5′. As dispersive elements, the grism with 600 gmm^{-1} as well as two grisms equipped with volume phase holographic gratings with 1200 and 1800 gmm^{-1} were used.

Date	Spectral range (in Å)	Resolution (λ/Δλ)	Total exposure (min)	Label
22.09.2015	5880-6740	2500	60	A
18.11.2015	5785-7315	1500	60	B
22.11.2015	5785-7315	1500	60	C
16.05.2016	5880-6880	2500	30	D
10.06.2016	5890-6795	2500	40	E
08.08.2016	5780-7300	1500	30	F
23.08.2016	4120-6810	800	60	G
24.08.2016	5895-6795	2500	40	H
29.08.2016	4070-7055	800	20	I
30.08.2016	5870-6875	2500	40	J
06.11.2016	5695-7360	1500	45	K
28.11.2016	4025-6995	800	30	L
20.12.2016	4025-6995	800	45	M
21.12.2016	5850-6850	2500	30	N

Table 3.1. Full log of the V1318 Cyg spectral observations.

Notes. Spectra A-H were acquired with TK SI-003A CCD matrix, and spectra I-N with E2V CCD42-40 matrix.

In the period from 2015 Sept. to 2016 Dec. fourteen spectra were obtained. A full log of the spectral observations is presented in Table 3.1.
Exposure times were selected to provide a signal-to-noise ratio of about 50-100 in the final spectra after the processing and optimal extraction.

For the data calibration we used several stars in the field, covering various magnitude ranges to avoid the effects of saturation. Stars were selected from the papers [70,67], and in some cases also the magnitudes from USNO-B1 catalogue were used. A special comparison confirmed that the magnitudes of calibration stars had good internal consistency. For each date the brightness of the objects was estimated separately for all exposures, after which results were averaged to obtain mean magnitudes. Typical internal scatter of results is $0^m.005$-$0^m.01$, and typical errors of final estimates are about $0^m.02$-$0^m.03$. In several cases, especially for I band, we excluded from the calibration partially saturated images of standard stars; this raised errors up to $0^m.07$-$0^m.08$.

3.3 Results: Photometric history and the new outburst of V1318 Cyg

As mentioned above, at the end of the 1980s the total visible brightness of V1318 Cyg started descending and at the beginning of the 1990s its visible brightness fell rapidly. This fading can be seen very well in Fig. 14 from [72]. The question regarding which of the stars in the pair is responsible for such high-amplitude variations can be solved by comparison of the images of the object on DSS-1 and DSS-2 plates (see Fig. 3.2a and c), and the data from [69]. Obvious differences in morphology even on half-resolved survey images point to the significant variability of V1318 Cyg S. Its low brightness in the 1990s, confirmed by observations presented in [70,71], allowed for photometric and spectral observations to be performed for both stars separately. In particular, the brightness of both stars was estimated as V=18.58, R_c=16.88, I_c=15.41 (V1318 Cyg N) and V=19.17:, R_c=17.34;, I_c=15.68; (V1318 Cyg S) [70]. This corresponds to an integral brightness of the double star of about V=18.1. Such value is in good compliance with the measurements in [67] for 1987-1988,

which in turn means that by the end of the 1980s V1318 Cyg S has possibly reached a minimal level of brightness.

One cannot exclude the variability of V1318 Cyg N however, and indeed the extreme faintness of V1318 Cyg in the falls of 1995 (V≈21) and 1997 (V≈24), according to the estimates from [72] is evidence supporting this statement.

Beginning new observations of V1318 Cyg field in 2015 September, we immediately found that the star underwent a new powerful outburst and its brightness reached the level of the 1960s or even higher (Fig. 3.2e). The position of the photometric peak of the image was pointing to V1318 Cyg S as the outbursted star. The faint northern star was lost in its glare in our very short (to avoid saturation effects) exposures.

To find precise coordinates of both stars we consulted the *Gaia* DR2 catalogue [56,57], where both V1318 Cyg N and V1318 Cyg S stars are resolved and listed (DR1 did not include these objects). We performed the astrometric calibration of our images, obtained within the years of 2015-2017, with the aid of the *astrometry.net* system [73], and measured the position of the outbursting star. All images demonstrated very good internal agreement and the dispersion of stellar position was ≈0.27″ (which is about half a pixel) in both coordinates, for V and I colors. Our coordinates agree with the *Gaia* DR 2 position of the V1318 Cyg S star within 0.3″. *Gaia* DR2 photometry also confirmed the outburst of the southern star: *G* magnitudes are 13.23 for the southern star and 18.92 for the northern star, that is, they currently differ in brightness by about 6^m.

Though we have found on our exposures the faint trace of V1318 Cyg N near the northern edge of the bright southern star, it was not possible to resolve both objects to measure them separately. Therefore, the photometry presented below is related to both stars and the nebula between. Photometric data are presented in Table 3.2. Their errors do not exceed $0^m.02$-$0^m.03$, as was already noted above; if errors are higher (up to $0^m.08$), values are marked with ":". In any case, taking into account the *Gaia* magnitude for V1318 Cyg N, it is easy to estimate that its contamination affects the values in Table 3.2 no more than $0^m.01$.

Date	B	V	R	I
22.09.2015	16.95	14.61	12.53	11.06
18.11.2015	17.18	14.76	12.72	11.16
31.03.2016	17.38	14.98	12.95	11.20
10.06.2016	16.78	14.40	12.43	10.85
23.08.2016	16.77	14.38	12.49	10.96
20.12.2016	16.81	14.46	12.59	10.92
20.07.2017	17.48	15.03	13.12	11.29

Table 3.2 V1318 Cyg (LkHα 225) photometry

As can be seen from our photometric data, the star presently remains at an almost constant level of brightness. To find an answer to the immediate question of when this new large-amplitude increase of the brightness of V1318 Cyg S started, we checked various surveys and found the images of IPHAS survey [74], obtained from 2003 to 2006, where both stars are resolved and V1318 Cyg S in R band is already brighter than V1318 Cyg N by at least one magnitude. We performed photometry for both stars using all suitable IPHAS images. Because of the relative faintness of the stars, the influence of the central nebular knot (Fig. 3.2d) on the photometric results was significant. This fact as well as the varying quality of IPHAS exposures led to significant measurement errors, reaching several tenths of a magnitude. We tried to minimize these errors as much as possible, and present the best of our estimates in Table 3.3.

These data, when we compare them with the measurements from [70], lead us to two important conclusions. On the one hand, V1318 Cyg N became about two magnitudes fainter in comparison with 1993 Jan. This confirms the appreciable variability of the northern star. On the other hand, we see that the brightness of V1318 Cyg S in 2003-2006 also is lower than in 1993 Jan. by several tenths of magnitude. This means that after the great minimum of the second half of the 1990s its level of brightness was restored to the

values observed at the end of the 1980s, and until the end of 2006 there was no further increase.

The V1318 Cyg field was also observed on 2003 Sept. 20 in the SDSS survey - see Data Release 12 [75]. We do not show this image here, because the appearance of the object does not significantly differ from IPHAS images. SDSS photometric data related to V1318 Cyg S do not exist, since the image- recognizing program mistook the pair of stars with the middle nebula for a galaxy and integrated all their fluxes.

V1318 Cyg S			V1318 Cyg N		
Date	R	I	Date	R	I
09.08.2003	17.66	16.45	09.08.2003	18.48	17.44
10.08.2003	17.67	16.45	18.10.2003	19.17	17.58
18.10.2003	18.01	16.04	08.08.2004	18.93	18.02
08.08.2004	17.72	16.23	11.10.2006	18.79	17.21
11.10.2006	17.86	15.94	---	---	---

Table 3.3 V1318 Cyg S and V1318 Cyg N brightness on the IPHAS images.

The most recent images of the region around BD+40°4124 that precede our new observations are available in the Pan-STARRS1 data archive [76]. They show both the N and S stars resolved, and V1318 Cyg S seems definitely brighter than in IPHAS images. In view of the "stacked" nature of DR1 images (i.e., they represent co-added images made from the multiple exposures taken over the survey), only the mean epoch of observations for V1318 Cyg (May 2012) was given. The new data release (DR2) of the Pan-STARRS survey contains the separate images of this area, and the dates of observations span 2010 Aug. – 2014 Oct. Analyzing these images, we found that even in 2010 the star V1318 Cyg S was brighter than on SDSS images of 2003, and a further perceptible increase in its brightness took place in the middle of 2013. Photometric estimates (magnitudes in *grizy* bands) provided by Pan-

STARRS DR1 were converted to BVRI magnitudes using the transformations suggested in [77], which resulted in the following values for the brightness of both stars: V1318Cyg S – B=18.73; V=16.38; R=14.57; I=12.90; V1318Cyg N – B=21.14; V=19.65; R=17.91; I=16.30. One can see that these R and I magnitudes are brighter than IPHAS values by more than 3^m for V1318Cyg S and by about 1^m for V1318 Cyg N. On the other hand, they are still about 2^m lower than the present level. These estimates however should be used with some caution because as we found by comparison with other available photometric data, highly variable emission background in the central part of BD+40°4124 cloud can introduce serious systematic errors in Pan-STARRS photometry.

We placed all measurements of V1318 Cyg S on the light curve (Fig. 3.3). Taking all results into account, we come to the following conclusions. Somewhere between 2000 and 2003 V1318 Cyg S came out of its minimum and returned to the mean brightness level of 1988. This star then remained at the same brightness for at least three years without pronounced changes. In the period between 2006 and 2010 the brightness of V1318 Cyg S started to rise to more than 5 mag (at an unknown speed), reaching a maximum by the second half of 2015, and remains at this level for at least two years. Another long maximum possibly took place in the 1950s, but no systematic observations were performed at that time (see above). We also see that small fluctuations near the present maximum do not lead to noticeable changes of color indices of the star, in contrast with its behavior at the lower level of brightness in the 1980s [66,72].

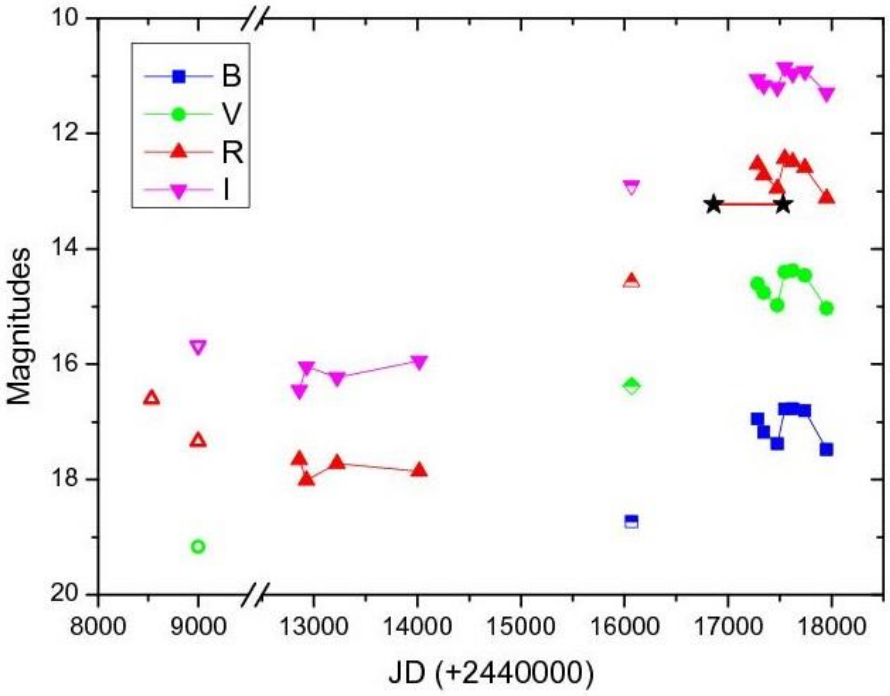

Fig. 3.3 BVRI light curve of V1318 Cyg S for the period of 1991-2017. Filled symbols show our measurements for IPHAS and Byurakan images; open symbols show data from [69] and [70]; half-open symbols show mean estimates for the four-year period of time from PanSTARRS survey (see text); and the line bounded by asterisks shows the level in G magnitude and the period of observations from *Gaia* DR2.

3.3.1 Spectrum of V1318 Cyg S at its maximum: General appearance

All our spectrograms of V1318 Cyg at maximal brightness are remarkably similar and do not show any prominent changes during the 1.5 year time interval of observations. Furthermore, they resemble the star spectrum during its previous maximum in the 1970s, which was briefly described in [71], but on the other hand noticeably differ from the spectrum at minimum brightness [70]. The general appearance of the V1318 Cyg spectrum is shown in Figs. 3.4 and 3.5. Due to the difference of almost six magnitudes in brightness,

the influence of V1318 Cyg N should be negligible; in any case, slit width was significantly lower than the distance between the stars. In the following discussion we consider these data as the V1318 Cyg S spectra.

One can see a very red continuum with both emission and absorption features. The only line with a complex profile is Hα. More detail is shown in Fig. 3.6 where we present Hα profiles obtained from all our better-resolution spectra. To compensate small positional differences between spectra introduced by rebinning, for some of them we added slight (≤ 0.1Å) shifts to adjust all spectra by two nearby Fe emission lines. Iron emission in T Tau and HAe/Be stars usually has low variations in radial velocity, with one being close to stellar velocity (see, e.g. [78]). As one can see, this profile has the typical appearance of rather broad (nearly 800 kms^{-1} in total width) Hα emission, divided by a blue-shifted, relatively narrow absorption component, which goes well down the continuum; we did not find any significant changes in its structure or radial velocities, though the equivalent widths (EWs) of both red-shifted and blue-shifted emission components vary to some extent. Such double-peaked Hα profiles are common in young active stars, but their central absorptions often do not reach the continuum level. Besides the P Cyg component of the Hα line, we see prominent absorptions of NaI D and, in the blue part of the spectrum, strong absorptions of Hβ, Fe II (42), and (48), Mg I (2) as well as several weaker ones (Fig. 3.4; at the shorter wavelengths weakness of continuum prevents detection of any lines except for the trace of Hγ absorption). These lines are typical for the early A spectral type but, having negative radial velocities (see details below), they definitely belong to the outflowing envelope of the star. In addition, we detected a prominent diffuse interstellar band (DIB) λ6284 Å, which easily resolves from the nearby atmospheric absorption λ6278 Å, and is among the strongest ones [79].

In the red part of the spectrum the only undoubtedly observed metallic absorption is λ6456 of Fe II (75); there is no convincing evidence of the existence of the famous Li I λ6707 absorption.

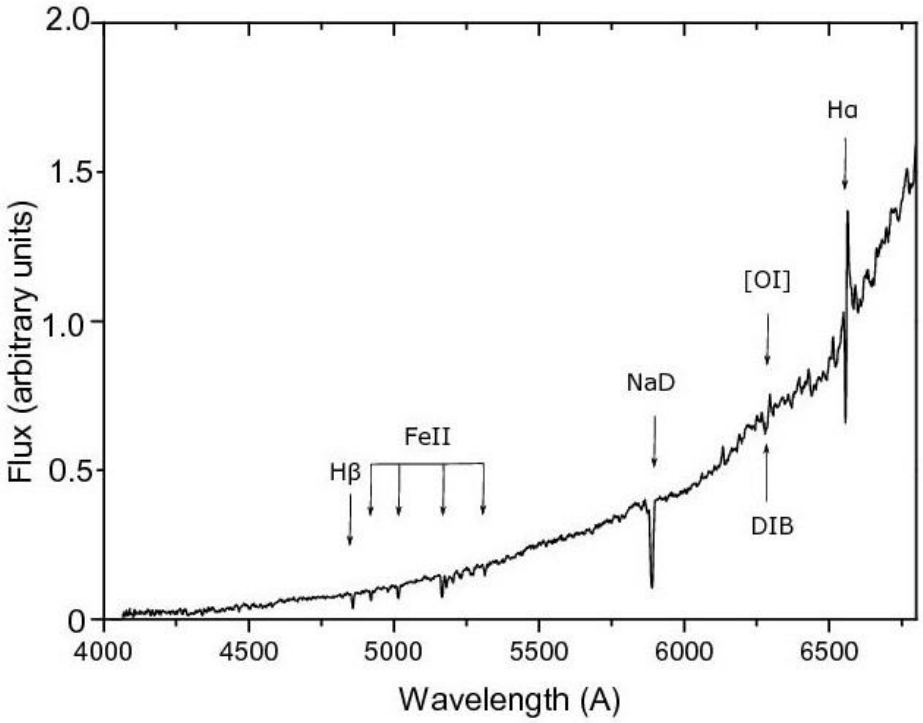

Fig. 3.4 Low-dispersion spectrum of V1318 Cyg, obtained with the 2.6m telescope. Main features are identified.

In fact, with our resolution we did not detect any photospheric absorption lines, which make the spectral type of V1318 Cyg S difficult to estimate. This question is discussed in detail in the following section.

3.3.1.1 Emission lines

Virtually all emission lines in the spectrum of V1318 Cyg S in maximal brightness, covered by our spectrograms, are located in the λλ6000-7000 Å range (see Fig. 3.5). They can be divided into three groups: Hα (the only hydrogen line with an emission component), which was described above, forbidden lines of [OI] and [SII], and a large number of low-excitation Fe I and Fe II lines.

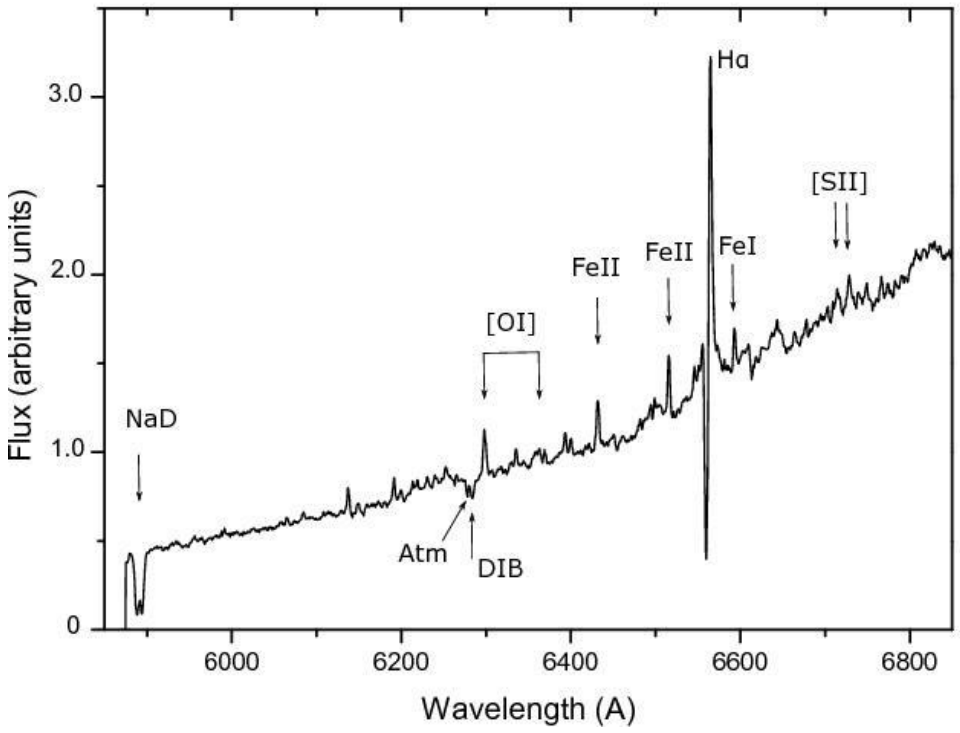

Fig. 3.5 Red part of V1318 Cyg spectrum with better dispersion. The spectrum was obtained with the 2.6m telescope. P Cyg profile of Hα line and strong NaI D absorptions are prominent. Several other features, including forbidden lines, are also identified. A part of this spectrum is shown in more detail in Fig. 3.7.

Forbidden emissions are contaminated not only by night sky lines of [OI], but also by lines of the diffuse emission background. Lines belonging to the star itself are not especially prominent and are produced in the HH outflow originating from V1318 Cyg S or perhaps from both stars in the pair [71].

It is worth mentioning that [SII] lines are wide and probably consist of two poorly resolved components, though they do not show particularly conspicuous variations as in PV Cep ([80]; but the period, encompassed by present observations of V1318 Cyg S, is also shorter).

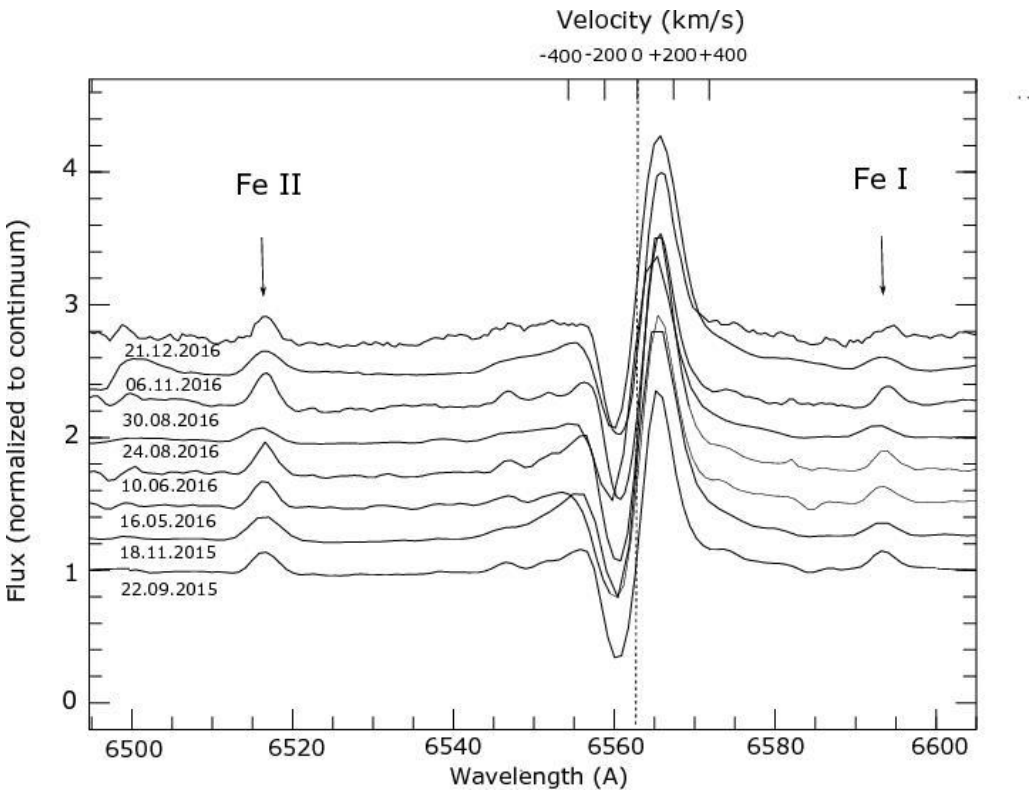

Fig. 3.6 Hα line in V1318 Cyg spectrum: comparison for various dates.

Nearly all other emissions in the red range of the V1318 Cyg S spectrum belong to iron, especially Fe I, which makes it similar to T Tau-type stars. We show this in more detail in Fig. 3.7, with matched spectra of well-known eruptive young stars PV Cep and V350 Cep, obtained in Byurakan with the same equipment on 24.08.2016 and 22.09.2015, respectively. All emission features seen in this range were identified with lines of Fe I and Fe II using the spectrum of VY Tau at maximum brightness for reference [81].

One can see the remarkable similarity between the spectra of both active stars, which closely resemble each other even in fine detail (though V350 Cep presumably belongs to T Tau-type with spectral type M2, while the probable spectral type of PV Cep is A5); on the other hand, V1318 Cyg S differs from its counterparts in that it has significantly lower EWs of emission lines and obviously lower excitation level.

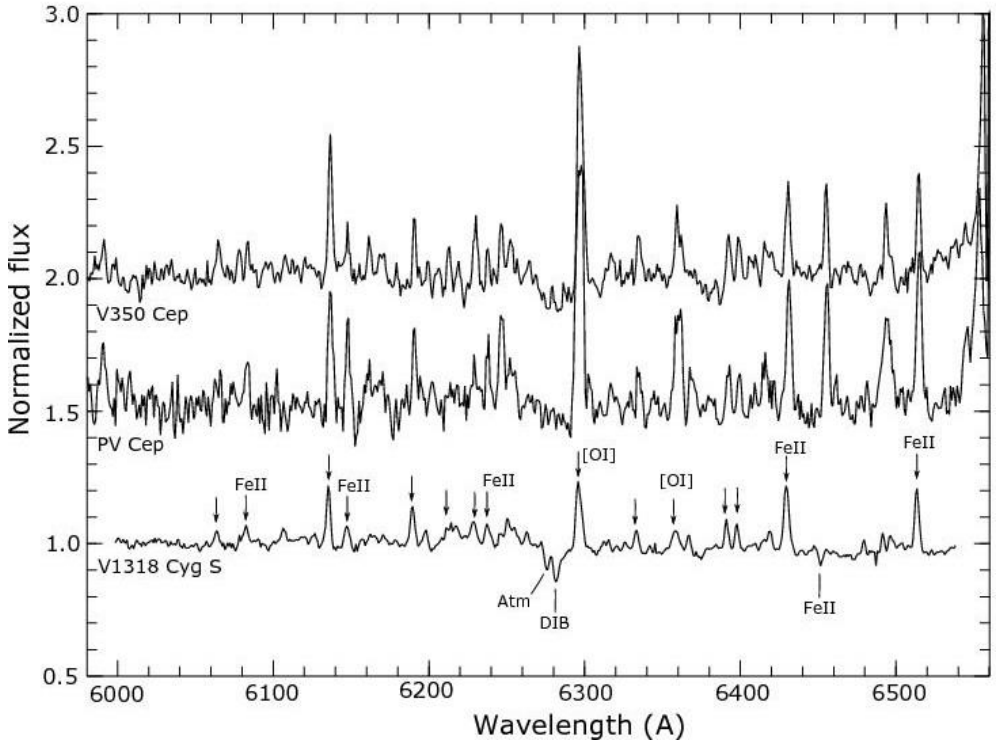

Fig. 3.7 Emission lines in V1318 Cyg, PV Cep and V350 Cep: comparison.
All main features are identified; lines, marked only by arrows, belong to Fe I.

Especially spectacular is the absence of intense emissions of λ6456.38 Å Fe II (74) (this line is actually seen in absorption) and of the strong blend of λ6493.78 and λ6499.65 Å Ca I (18). Beyond the range shown in Fig. 3.7, the spectra of the three stars completely differ: for example, both V350 Cep and PV Cep demonstrate rich emission spectra also at shorter wavelengths.

3.3.1.2 Equivalent widths and radial velocities

Estimations of EWs of selected emission and absorption lines were performed using the best 12 spectra from our data set. In Table 3.4 we present their averaged values, taking into account that the spectrum of V1318 Cyg S at maximal brightness has not significantly changed in two years. Especially noteworthy is the almost constant strength of the NaI D doublet, which is the most intense absorption in the star spectrum. Significant variations of

intensities (which can also be seen from the standard deviations from Tab. 3.4) were only detected in the components of the Hα line: their EWs were changing in the range of 4-10Å (emission) and 1-3Å (absorption).

Line	EW, Å	Spectra [a]	PV Cep [b]	V350 Cep [b]
λ6731 [SII] (2F)	-0.36±0.11	A-F, H, J-K	---	---
λ6717 [SII] (2F)	-0.25±0.06	A-F, H, J-K	---	---
Hα (em)	-6.86±1.50	A-F, H, J-K	---	---
Hα (abs)	1.91±0.61	A-F, H, J-K	---	---
λ6517 Fe II (40)	-0.55±0.13	A-F, H, J-K	-2.34	-1.23
λ6456 Fe II (74)	0.43±0.14	A-F, H, J-K	---	---
λ6430 Fe I (62)	-0.72±0.10	A-F, H, J-K	-1.99	-1.27
λ6300 [OI] (1F)	-1.28±0.20	A-F, H, J-K	-5.26	-3.92
λ6278 DIB	0.64±0.10	A-F, H, J-K	---	---
λ6137 Fe I (207)	-0.69±0.08	A-F, H, J-K	-1.69	-1.61
NaI D	8.44±0.23	B-C, F-G, J-M	---	---
λ5018 Fe II (42)	2.47±0.07	G, L-M	---	---
λ4923 Fe II (42)	1.89±0.18	G, L-M	---	---
Hβ	4.26±0.38	G, L-M	---	---

Table 3.4 Equivalent widths of selected V1318 Cyg S spectral lines.

Notes. EW values of emission lines are negative. [a] Spectra, used for averaging, are indicated by letters, which correspond to the Table 3.1. [b] PV Cep was observed at 24.08.2016 and V350 Cep at 22.09.2015.

In general the strength of emission spectrum of V1318 Cyg S is not high. For comparison in the Tab. 3.4 we present EW values for typical lines in the spectra of PV Cep and V350 Cep, shown also in Fig. 3.7. As one can see, they vastly exceed those of V1318 Cyg S.

Line	V_R kms^{-1}	Dates [a]
Hα (em)	+107±30	A, D, E, H, J, K, N
Hα (abs)	-150±29	A, D, E, H, J, K, N
NaI D (abs)	-81±16	J, K, N
Hβ (abs)	-90±41	I, L, M
FeII, MgI (abs, blue range)	-45±23	I, L, M
FeII (abs, red range) [b]	-68±32	A, E, H, J, N
FeI (em)	-14±17	A, E, H, J, N
FeII (em)	-21±22	A, E, H, J, N
λ6300 [OI] (em)	-89±22	A, D, E, H, J, K, N
[SII] (em)	-127±20	A, D, E, H, J

Table 3.5 Mean heliocentric radial velocities of V1318 Cyg S spectral lines. Notes. [a] Spectra used for measurement and averaging are indicated by letters, which are the same as in Table 3.1. [b] Only λ6456 Fe II (74) line.

We also estimated the heliocentric radial velocities of strong and well-defined lines in the V1318 Cyg S spectrum, separately measuring emission and absorption components of Balmer lines, the NaI D pair, the forbidden line of [OI] and [SII], the four strongest Fe II

lines and λ5183 Mg I, observed in absorption in the blue range, and λ6456 Fe II observed in red range, as well as selected unblended emissions of Fe I (λλ6137, 6191, 6393, 6400) and Fe II (λλ6432, 6516). We would like to mention that for the measurements of lines in the red range we used 0.80 and 0.50 Å pix^{-1} resolution spectra; on the other hand, we had only 1.50 Å pix^{-1} spectra to measure Hβ and metallic absorptions in the blue spectral range. Radial velocities, averaged over all available measurements, are collected in Tab. 3.5. Standard deviations of mean radial velocities of hydrogen lines are clearly larger than observational errors (which are about 15-20 kms^{-1}), definitely confirming some variations in time. However, within the accuracy of our data we did not find any reliable trends in such variations. We further discuss radial velocities in the following section.

3.4 Discussion and conclusions

Starting from the paper of Aspin et al., [69], V1318 Cyg S was considered a luminous ($L_{bol}\approx1600L_{\odot}$) and strongly reddened object. However, all these estimates are based on the studies in infrared and sub-millimeter ranges [82,83]. On the other hand, spectral classification of HAeBe stars may encounter problems, which can lead to serious discrepancies in spectral types (see [84], for detailed discussion).

Comparing the optical spectra of V1318 Cyg S during the period of maximal brightness with spectral atlases and surveys of HAeBe stars, we found that in the blue spectral range well noticeable Fe II (42) absorptions and several other features make its spectrum remarkably similar to that of XY Per Herbig Ae star (A5), shown in the atlas of Gray [85], as well as to such HAeBe stars as UX Ori (A3) [84] and RR Tau (A0) near the maximum [86,87] (spectral classes are given according to [84]). On the other hand, typical HAeBe stars have more prominent broad absorption wings of Balmer lines, and certain details, especially the powerful NaI D absorptions, seem to contradict the early spectral type. However, such “anomalous” [84] NaI D and Fe II absorption features in some HAeBe stars have a non-photospheric origin, being caused by material surrounding the star. In the case

of V1318 Cyg S, high negative radial velocities of these lines (see Tab. 3.5) confirm their formation in the envelope or in the dense stellar wind.

Assuming that V1318 Cyg S indeed belongs to HAeBe stars, it should be noted that given the strength of spectral lines it is not similar to the majority of these stars. Comparing equivalent widths from Tab. 3.4 and corresponding values from Table 8 from [84], one can see that the greatest resemblance (both in strength of Fe II absorptions and weakness of Hα emission) to V1318 Cyg S demonstrate XY Per, UX Ori, RR Tau, BF Ori and LkHα 208 stars. As one can see, all these stars belong to the group of UXors. We return to this topic below.

On the other hand, emission lines in the red part of the spectral range and strong NaI D absorption make V1318 Cyg S somewhat similar to T Tau-type stars, though there is no evidence for a later-type spectrum, at least at maximal brightness. In fact, the observed combination of Fe absorption in the blue spectral range and Fe emissions in the red is quite unusual. The key to the problem could be the difference between their radial velocities (Tab. 3.5). Taking into account the heliocentric velocity of the BD+40°4124 molecular cloud (-9kms^{-1}; [88]), one can see that low radial velocities of Fe emissions (which very probably originate near the stellar surface) are close to this value. In fact, it is reasonable to consider their mean value of -18kms^{-1} as the systematic radial velocity of V1318 Cyg S. Consequently, the higher negative values from Tab. 3.5 will correspond to the speed of various layers of the expanding envelope and collimated outflow.

The existence and features of the matter outflow near V1318 Cyg S were studied in detail in the optical [71], infrared, sub-mm [83,89,90,91] and radio ranges [82,92]. All studies of CO emission confirm the existence of a molecular outflow, oriented close to the line of sight, though there is ambiguity about its possible source: it could be V1318 Cyg S [92] or could be heavily embedded and non-detectable in the optical range protostar located nearby [90]. In any case, the presence of high-velocity wind from V1318 Cyg S itself is obvious in view of many shock-excited spectral lines detected in optical [71] and infrared [83] ranges. One can assume that V1318 Cyg S, like a great number of HAeBe and T Tau stars, is driving a more or less collimated outflow, creating Herbig-Haro-type emission in its vicinities. Indeed,

forbidden emissions in the nebula between both stars have radial velocities of about –80kms^{-1} [71], which agrees well with results from Tab. 3.5 (one should keep in mind that other measurements from this latter paper refer in fact to V1318 Cyg N because the southern star was very faint during that period). Absence of [NII] lines and moderate equivalent widths of outflow emissions point to the low excitation level, corresponding to a shock velocity about 100 km s^{-1} or lower. Low inclination of the V1318 Cyg S flow to the line of sight is also corroborated by the shape of stellar Hα line profile: as is shown in [93], such kinds of profiles (type III-B by the classification in [94]) require slow accelerating wind viewed near pole-on. The significant equivalent width of blue-shifted absorption lines, which presumably arise in dense wind or/and envelope, should also be taken into account.

Independent evidence for a near pole-on orientation of V1318 Cyg S is provided by a high-resolution polarization map from [95], showing low polarization at the position of V1318 Cyg S and the centrosymmetric pattern of polarization vectors around it, without any traces of a circumstellar dust disk.

To understand the main parameters of the star we should first of all find the amount of interstellar extinction toward V1318 Cyg S as well as toward two other more massive members of this small association, namely BD+40°4124 and V1686 Cyg (LkHα 224). However, up to now almost all such estimates have been indirect and uncertain. For example, analysis of the molecular emissions in the infrared and radio ranges resulted in improbably high values of A_v of 25 [69] and even 50 [82], which contradict the direct visibility of V1318 Cyg S in the optical range. The estimation of A_v=10, based on the approximation of the spectral energy distribution [69] is more reliable. In the same way, in [70] it is estimated A_v>8 and A_v>7 for V1318 Cyg S and V1318 Cyg N, respectively. However, in the same work the extinction values for the brightest stars were calculated in a straightforward way on the basis of established spectral types and previously observed (B-V) colors. These latter authors found A_v=3.6-3.8 for BD+40°4124 and 4.2-6.7 for V1686 Cyg, that is much lower values. In the same way, the value of A_v=3.0 for these stars was obtained in the comprehensive paper of van den Ancker et al., [83]; but for V1318 Cyg S they get A_v=15.4, again based on the analysis of the features in the infrared spectrum.

Presently, while V1318 Cyg S remains at a stable maximum its spectral type could be more or less reliably assigned as early A. Furthermore, since the current colors are well determined, we can directly derive A_v. We computed mean (B-V) and (R-I) from Table 3.2 and compared them with intrinsic colors of A2V and A5V stars from the tables from [96,97], following the procedure and corrections described in [70]. As a result we derived A_v=7.22 (for A2V star) or 7.00 (for A5V star) using (B-V), and 7.57 or 7.38, respectively, using (R-I). The excellent agreement of these values however contradicts the larger estimates listed above. It is possible to assume that after prominent brightening, some amount of absorbing dust was cleared from the line of view. Thus, it will be interesting to repeat the observations of the object in the infrared range and to compare them with previous data.

Gaia project DR2 allows for reliable estimates to be made of the V1318 Cyg group distance. Indeed, one should assume that at least BD+40°4124, the brightest star in this small cluster, V1686 Cyg, and both stars of V1318 Cyg are close neighbors in space. The trigonometric parallax of BD+40°4124, taken from *Gaia* DR2, is 1.092±0.031 mas, which corresponds to a distance of 916 pc. V1686 Cyg, as well as V1318 Cyg S and V1318 Cyg N, were also detected and measured by *Gaia*, but with errors one order higher, probably due to their relative faintness. For completeness we list these data here: 0.785±0.122, 1.393±0.292, and 1.490±0.735 mas, respectively. It seems reasonable to use the value of 920 pc. as the distance of the group, which is also in excellent agreement with the value of 980 pc. estimated in [67] and used by other researchers. With V_{mean}=14.66, A_v=7.2, and this new distance, for V1318 Cyg S at maximum one can derive M_v=-2.36 and L=750$L_\odot$ in the optical range. This value, though naturally higher, agrees reasonably well with 590$L_\odot$ estimated in [83], and confirms that V1318 Cyg S should be sufficiently massive YSO. The value of bolometric luminosity is of course at least two times larger according to the previous estimates.

It is not easy to attribute V1318 Cyg S to one of the known types of erupting medium-mass young stars. Let us discuss the existing options.

FUor-type star. FUors and FUor-like stars are very rare. Their specific features are now well-defined, being described in recent reviews [14,98]. The star V1318 Cyg S can be considered as a FUor, because it keeps its high brightness level after the outbursts for already six years. Although its spectrum in both optical and infrared range is not similar to typical FUors and it is definitely a more massive object. However, new observations show that the spectrum of V1318 Cyg S is slowly developing to the one characteristic for FUors.

EXor-type star. EXors are usually considered to be lower-scale versions of FUors, but this class is loosely defined and probably not homogeneous [14,99]. The light curve of V1318 Cyg S bears a resemblance to those of some EXors; another young eruptive star with developed Fe I emission spectrum at maximum brightness is VY Tau [81], also an EXor. However, the high luminosity of V1318 Cyg S rules out such a classification: the luminosity of all known and probable EXors is lower by at least in one order of magnitude even in outburst.

Intermediate (V1647 Ori-like) object. This is poorly defined and yet-to be properly characterized class of young eruptive objects. However, they have some common features, namely they are connected with small nebulae and collimated outflows (like FUors); show outbursts with durations of several years (in between FUors and EXors); have T Tau-type spectra (like EXors); and their bolometric luminosities are moderate. In fact, V1318 Cyg S satisfies the first two criteria, and its emission spectrum shows a partial similarity to T Tau type. However, the bolometric luminosity of V1318 Cyg S cannot be considered as moderate. It could be a larger-mass member of this class (if such a class indeed exists); one should keep this option in mind.

HAeBe/UXor-type variability. We mentioned above that the intensity of the main emission and absorption lines in the V1318 Cyg S spectrum resemble those of known UXors. However, many arguments suggest that V1318 Cyg S is observed close to polar regions; thus, UXor-type occultations by clumps, moving close to the equatorial plane, are impossible. Naturally, one cannot exclude a role of another kind of obscuration event in the unusual photometric behavior of V1318 Cyg S.

In any case, when considering possible explanations for the variability of V1318 Cyg S, one should take into account such features as a very large brightness amplitude in the optical range (more than 5 mag, possibly even more than 7 mag), large amplitude variations even in near-infrared, very long duration minimum (10 years or more), and pronounced spectral changes between minimum and maximum. The duration of the recent outburst, which is still in progress, should also be regarded as unusual, comparing it to previous, though incomplete photometrical data for this star.

We hope that continued observations, especially collecting and analyzing high-resolution optical spectroscopic data, will shed more light on the nature of this star.

4. NEW OUTBURST OF V1686 CYG: SIMULTANEOUS PHOTOMETRIC AND SPECTRAL ANALYSIS

4.1 Introduction

Among the fields we studied, was a group of HAebe stars in the vicinity of the bright BD+40°4124 star, which itself is Herbig Be star with very strong emission Hα line. One of them is LkHα 224 which also is HAeBe star (the image of the field around the LkHα 224 is the same as for LkHα 225, hence we do not present it here: see Chapter 3). Along with nearby LkHα 225 all three stars for the first time were mentioned by Herbig [35] in his famous paper about Ae/Be stars, connected with bright nebula. With several fainter stars they create a small young cluster, embedded in the dense molecular cloud. In [67] a distance to this group is estimated as 980pc.

The photometric variability of LkHα 224 was detected by Wenzel [65]; as the variable this star received V1686 Cyg designation. The most complete information about its photometric behavior so far was collected in [67,68,72]. According to these data, the star fluctuates near the mean brightness level, sometimes (usually one time per year) demonstrating irregular Algol-like minima, which lasts one-two months: steep and rapid drop by 2-2.5 mag and afterwards more slow and oscillating raise in brightness to the mean value. We can take into account that many Herbig AeBe stars with the A0 or later spectral type show this kind of variability [100]. Besides, also long-term variations exist: mean brightness of V1686 Cyg in V decreased in about 8 years by ≈2.5 mag, achieving minimum in 1993 and in subsequent 4 years restored to previous level; thus, its mean level of brightness itself varies from V=12.5 down to V=15 [70,72,38].

V1686 Cyg was the subject of many spectral studies, but prominent variations of absorption features make its spectral classification very problematic. Estimates of its spectral type vary from B2 to F9 (see [84], and references therein). As it is stated in the same work, shorter term photometric variations of V1686 Cyg could be related to the spectroscopic variability, but this question is not investigated yet. It should be noted that emission lines in

the V1686 Cyg spectrum also demonstrate significant variability [101]. In [71] the broad asymmetric profile of Hα emission with several superposed narrow absorption-like features is shown, suggesting the existence of expanding envelopes.

In 2015 we started systematic observations of BD+40°4124 field, since the new outburst of V1318 Cyg S was detected [102]. In parallel to these studies the V1686 Cyg star also was observed photometrically and spectrally. The unusual and unsuspected brightening of V1686 Cyg up to almost 3 mags was found and traced. This chapter describes the results of these observations.

4.2 Observations and Data Reduction

Observations of V1686 Cyg were implemented from September 2015 to July 2017. For calibration we used some stars in the field, while for comparison stars we used data from [70] and [67]. The typical errors for our data are about $0.^{m}02$-$0.^{m}03$. We also obtained spectra for this star from Sept. 2015 to Dec. 2016, with different spectral resolutions: 0.50, 0.80, 1.50 and 2.65 A/pix.

More details about the methods of observation and data reduction can be found in [102]. Here, in Tab. 4.1, we present the log of the spectral observations.

4.3 Results: The new outburst of V1686 Cyg

The analysis of the historical light curve of V1686 Cyg (based on the encompassing eleven years photometric database [72]) with VizieR service shows, that from the mean level of brightness this star time to time decreases its brightness by 1-1.5 mag amplitudes, which last 10-20 days and then it returns to mean value.

In our case we had the contrary behavior: during the period from Sept. 2015 to Aug. 2016, i.e. almost 1 year of regular observations any significant photometric variability of

V1686 Cyg was not detected. But in Aug. 2016 we noticed that the star significantly rose in brightness.

Date	Spec. range (Å)	Resolution (λ/Δλ)	Total exp. (min.)
22.09.2015	5880-6740	2500	60
18.11.2015	5785-7315	1500	60
22.11.2015	5785-7315	1500	60
16.05.2016	5880-6880	2500	30
10.06.2016	5890-6795	2500	40
08.08.2016	5780-7300	1500	30
23.08.2016	4120-6810	800	60
24.08.2016	5895-6795	2500	40
29.08.2016	4070-7055	800	20
30.08.2016	5870-6875	2500	40
06.11.2016	5695-7360	1500	45
28.11.2016	4025-6995	800	30
20.12.2016	4025-6995	800	45
21.12.2016	5850-6850	2500	30

Table 4.1 Log of the V1686 Cyg spectral observations

Photometric estimations demonstrated that in that period, which lasted probably several months, the brightness of V1686 Cyg unsuspectingly increased for more than two magnitudes in V and then gradually returned to its previous level. Tab. 4.2 presents the results of our BVRI photometry, and the light curve is shown in Fig. 4.1.

To trace the recent variations of V1686 Cyg we checked such sources as images of IPHAS survey [74], as well as SDSS and Gaia DR2 surveys. The brightness estimates, obtained from the IPHAS images, are listed in Tab. 4.3.

The important representation of the recent brightness variations of V1686 Cyg gives the data from AAVSO (American Association of Variable Star Observers), which densely cover the August 2014 - August 2018 period. In Fig. 4.2 we combine the lightcurve in V band from AAVSO with our data and the G magnitudes from Gaia.

Though in 2000-2012 the photometric estimates are scarce, the IPHAS data (Tab. 4.3) allow to assume that V1686 Cyg kept its typical behavior up to 2013, with more or less persistent brightness level near 13.0-13.5 (V). In the first half of 2015 the star demonstrated several characteristic minima. Then, in 2015 Aug. the brightness of V1686 Cyg abruptly lowered, reaching V=16.7 in 2015 Oct.

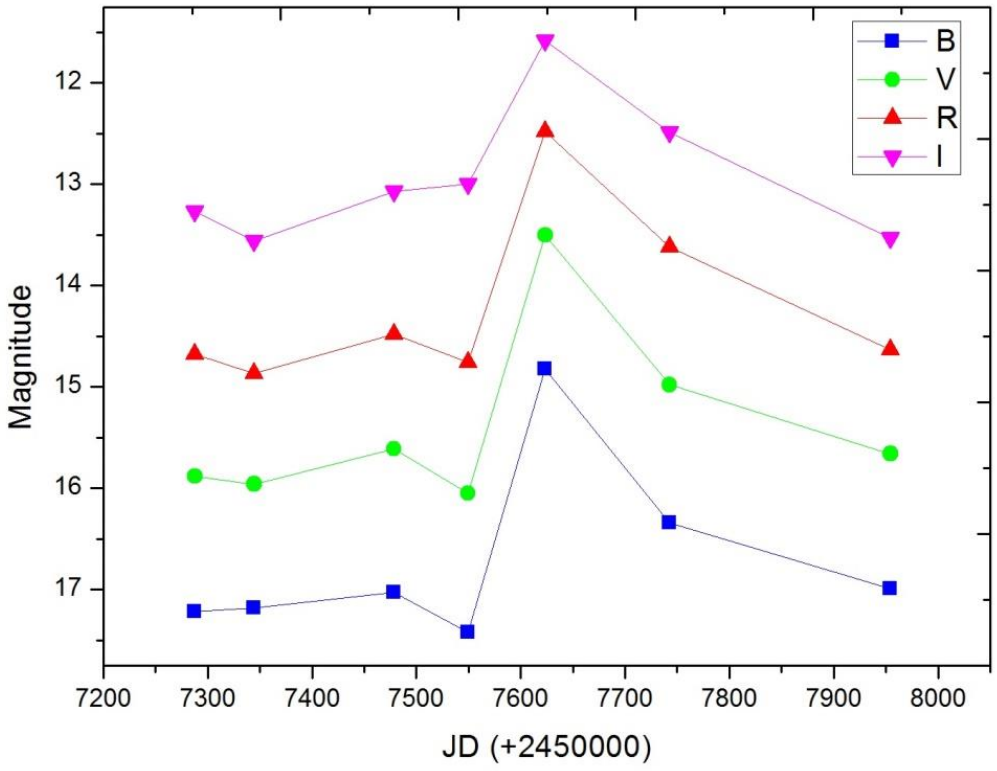

Figure 4.1 BVRI light curve of V1686 Cyg for the period 2015-2017

After that the photometric behavior of the star drastically changed. As one can conclude from the AAVSO lightcurve, at least until the end of 2017 the star remained on the significantly lower level of brightness (about 15.3 in V), with occasional outbursts. During the July-Oct. of 2016 a prominent outburst of at least 2.5 magnitudes in V took place, also traced by our photometry, and which by chance coincided with our spectroscopic observations. One cannot exclude lower amplitude brightening in the first half of 2018.

The pronounced spectral variations, observed by us during the 2016 brightening event, are important. Such spectroscopic variability, related to photometric variations, was expected for V1686 Cyg in [84]. We describe it in the next section.

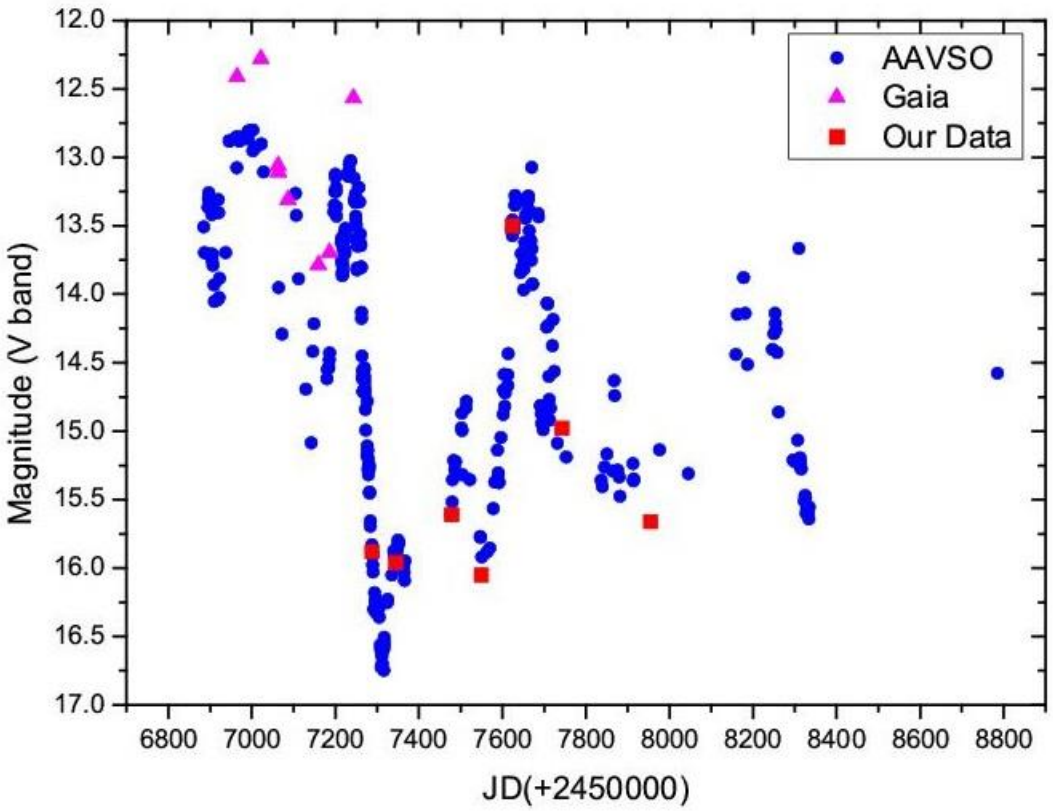

Figure 4.2 The light curve of V1686 Cyg in V band, with combined data from AAVSO, Gaia and our observations

Date	B	V	R	I
22.09.2015	17.22	15.88	14.68	13.27
18.11.2015	17.18	15.96	14.87	13.56
31.03.2016	17.03	15.61	14.48	13.07
10.06.2016	17.42	16.05	14.76	13.00
23.08.2016	14.82	13.50	12.48	11.58
20.12.2016	16.34	14.98	13.62	12.49
20.07.2017	16.99	15.66	14.63	13.53

Table 4.2 The photometry of V1686 Cyg (LkHα 224)

Date	R	I
09.08.2003	13.29	12.17
10.08.2003	13.29	12.15
18.10.2003	14.53	13.37
11.10.2006	14.92	13.79

Table 4.3 The brightness of V1686 Cyg on the IPHAS images

4.3.1 The spectrum of V1686 Cyg in quiescent stage

As was mentioned above, our spectral observations encompassed the whole period of the V1686 Cyg outburst. We selected eight spectra of best S/N quality for the further analysis.

Spectra, taken before the outburst, are quite typical for this star, being similar to the results from [70] and [71]. In the red part of spectral range the most conspicuous line is a broad and strong Hα emission with superposed weak, blue-shifted absorption feature. Forbidden emissions of [OI] also are present, though very strong background emission lines make uncertain the estimations of their intensity. Besides, faint emission lines, mainly belonging to Fe II (40) and not described before, were detected. NaI D lines are not well seen either in emission or absorption; it should be mentioned that previous studies show their pronounced variability.

After the end of the outburst, in Nov.-Dec. 2016, the spectrum returned to the same appearance, with Hα and several Fe II lines in emission; besides, broad-winged Hβ and Hγ absorptions can be seen in the blue range. In fact, the upper lines of Balmer series in absorption, though not strong, probably always are present in the V1686 Cyg spectrum [71,103]. In general, during the time of our observations the spectral type of V1686 Cyg can be assumed as an early Ae, judging by the broad wings of Balmer absorptions and non-detection of He I 5876 line (which also shows prominent variability in V1686 Cyg spectrum, according to [39]). We did not found any other photospheric absorptions, at least with our spectral resolution.

It should be mentioned that in all spectra we detected one of the strongest diffuse interstellar bands (DIB) 6284Å, also mentioned in [84], which is easily distinguished from the nearby atmospheric absorption 6278Å. This band with the similar intensity was previously detected in the spectrum of the nearby LkHα 225 star [102].

4.3.2 The spectrum of V1686 Cyg during the outburst

First significant spectral changes one can see in the spectrum of the star, obtained in May 16 of 2016, when photometric variations were not detected yet. The better S/N spectrum of June 10 2016, still before the photometric brightening, confirms this impression. The central absorption of Hα became much stronger, nearly dividing the

emission line into two almost equal components. Forbidden emission lines of [OI] and [SII] still are present in the spectrum; their width confirms non-background origin.

As can be seen from Tab. 4.2, the maximal brightness of V1686 Cyg was reached in Aug. 2016. Despite the different spectral resolution all our five spectrograms of that period have certain similarity. Especially impressive are the further variations in the profile of Hα line, where absorption component lowers beneath continuum. The strength of iron emissions decreases, forbidden lines of [OI] nearly disappear. On another hand, rather intensive NaI D absorption lines become visible in the spectrum. In the short wave range, which was observed only with lower resolution, besides of Hβ and Hγ with typical shell cores, we see also absorptions of Fe II (42). It is worth to mention that after one week these blue iron absorptions disappeared, though the red part of the spectrum kept the same appearance at least until the end of Aug. of 2016.

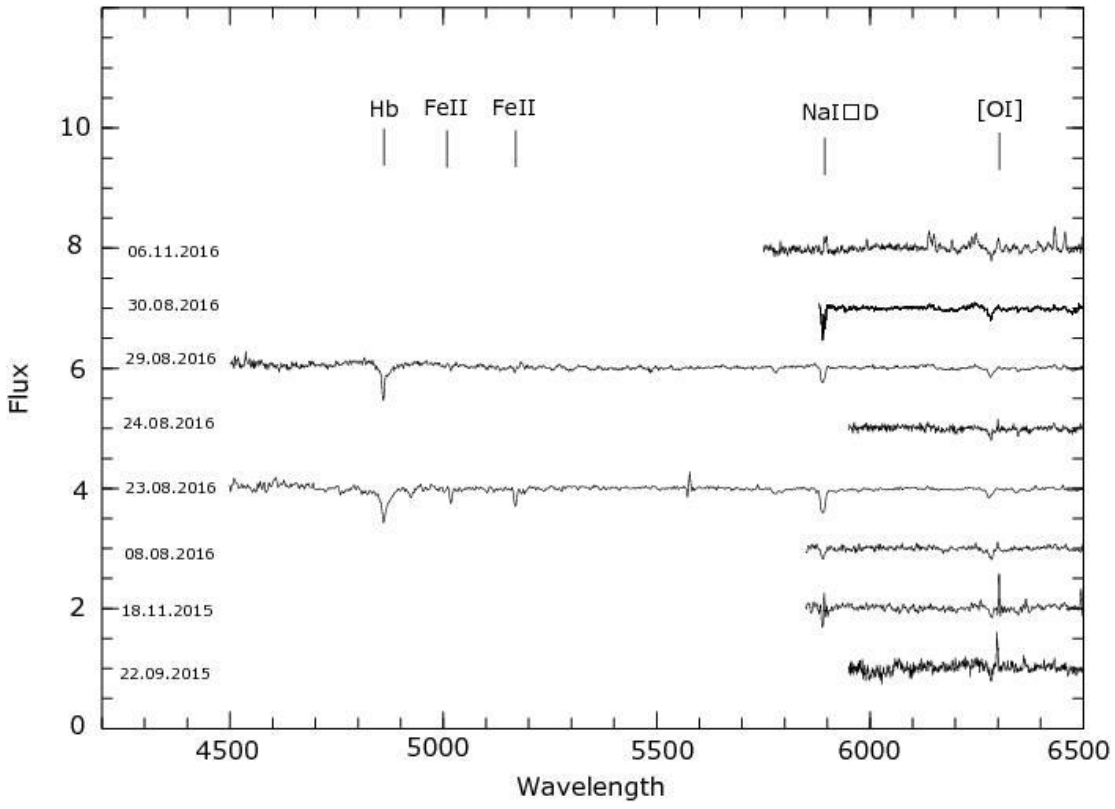

Figure 4.3 The variations of V1686 Cyg spectrum in 2015-2016, in 4500-6500Å range. In the shorter wavelengths the Hα and Fe II absorptions are prominent. Also the obvious increase of the chromospheric emission on 06.11.2016 can be seen.

To better represent the changes, we show the parts of the normalized V1686 Cyg spectra (in the range up to Hα line), in various periods in Fig. 4.3, and the variations in the Hα profile are presented in Fig. 4.4.

In the 2016 Oct. the star started to lower its brightness (see Fig. 4.1). In that relation the spectrum, obtained on Nov. 6, is very interesting. It significantly differs as from the outburst spectra, as well as from the other spectra in quiescent stage. On the one hand, strong NaI D absorptions and Hα line absorption component disappeared. On the other hand, all emission lines became obviously stronger than before the outburst.

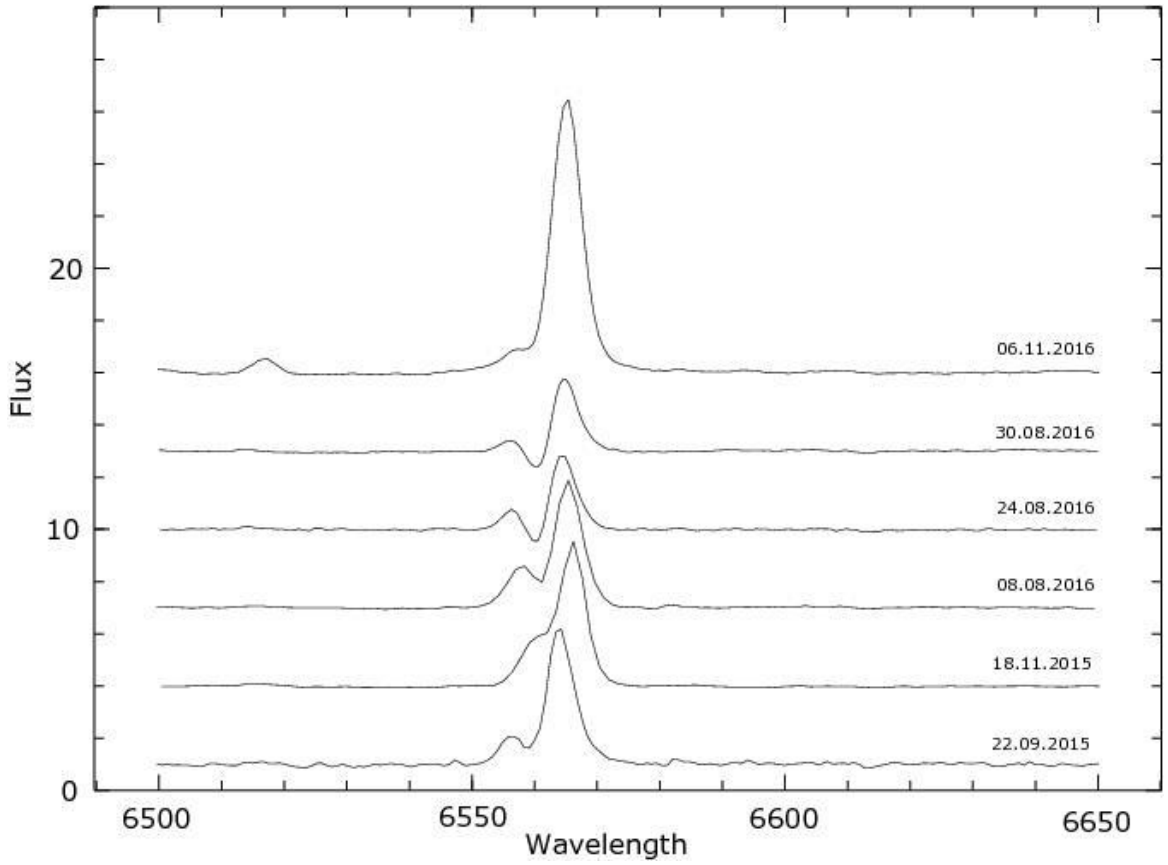

Figure 4.4 The strong variations in the profile of Hα line in the spectrum of V1686 Cyg. During the outburst the absorption component became rather intensive and even lowers below continuum.

The emission line spectrum in 6000-6500Å range appears much richer, with lines of Fe II, Fe I and Ca I. We can note its remarkable similarity to the spectra of PV Cep and V350 Cep, shown in [102]. Subsequent spectra, though of the lower S/N ratio, are more like the pre-outburst spectra, as it was already mentioned in the previous section.

4.3.3 Equivalent widths and radial velocities

For the better representation of the spectral changes, described above, we estimated the equivalent widths of most typical emission and absorption lines. The general picture seems consistent with the mentioned above conclusion that the strength of emission lines relative to continuum significantly lowered during the maximal brightness period. For example, EW of Hα emission component changed from ≈-35Å to ≈-12Å at the end of Aug. 2016; then high values again were restored. In the described above spectrum of Nov. 6, 2016 with very strong emissions EW(Hα) exceeded -50Å. Similar behavior also can be seen for λ6300Å [OI] line. On the other hand, EW of NaI D absorption in the period of the outburst reached 5Å, while it was actually invisible before. Pronounced variability of emission as well as absorption lines in V1686 Cyg spectrum also was previously described [101,84].

We measured the heliocentric radial velocities of several lines and found a pattern very typical for young stellar objects. All measurable absorption lines demonstrated negative velocity. For example, the mean velocity of the absorption component of Hα is -97±47 kms^{-1}. Such large dispersion is natural, because the previous observations also have shown the existence of the blue-shifted absorption components in the Hα line profile with various, but always negative radial velocities. The narrow absorption cores in Hβ and Hγ have similar velocities, though these values cannot be measured with sufficient accuracy because of the lower spectral resolution. Fe II (42) absorptions, seen in only one lower resolution spectrum, also show ambiguous velocities, probably because of the same reason. Both lines of NaI D doublet have velocity near -57 kms^{-1}, similar negative velocity has also λ6300Å [OI] emission. The peak of Hα emission has positive radial velocity: +95±29kms^{-1}. Velocities of

the iron emissions cannot be measured because of their faintness. All these data are in sufficiently good compliance with high-resolution measurements, presented in [104].

4.4 Discussion and Conclusions

Our combined data allow to make several conclusions about the observed spectral variability of V1686 Cyg. These observations fully confirm already described by the listed above authors the pronounced changes in the strength of certain absorption and emission lines, which easily explain the large range of the spectral types, assigned to this object. Actually, V1686 Cyg is one of the most photometrically and spectrally variable HAeBe star, and as one can see (at least in this present case), the spectral and photometric variations of V1686 Cyg are directly related.

As was already stated above, the observed short-time brightening is not typical for the V1686 Cyg. At least similar events cannot be found on the previous long time range light curve, presented in [72]. It can be considered as an outburst, because its accompanying spectral changes could be interpreted as the formation of dense expanding envelope around the star, with its subsequent dissipation during several months. This envelope, emitting mainly in continuum, covered up lower layers of the stellar chromosphere, making invisible the metallic emissions and diminishing even very strong emission component of Hα line. On the other hand, the envelope was sufficiently dense to produce absorption lines with negative radial velocity.

The permanent existence of the blue-shifted absorption components in the Hα line profile, shown by the previous absorptions [71], allow us to conclude, that the similar expanding envelopes, though of much lower density, nearly always are present around V1686 Cyg star.

By now we do not know, how long the V1686 Cyg star will remain in its present lower brightness state. Only the new photometric observations can make the situation clearer. This star definitely deserved continuing monitoring.

Several authors make analogies between V1686 Cyg short-time light drops and UX Ori type variability. However, this question remains to be investigated. In fact, this star may be an object, which combines two types of PMS variability, like V2492 Cyg, V350 Cep or V582 Aur [105,106,107].

5. SPECTRAL STUDY OF V565 MON: PROBABLE FUORI-LIKE OR CHEMICALLY PECULIAR STAR

5.1 Introduction

V565 Mon belongs to a little studied star formation region. As a variable star it was discovered by Hoffmeister [108]. It is the illuminating star of the Parsamian 17 reflection cometary nebula, in which it is deeply embedded [109,110]. The observational data about this star are scarce. The first description of the morphology of the nebula and the multi-band infrared (IR) observations of the central star, which revealed that V565 Mon is a prominent IR source, was given in the work of Cohen [110]. Only after 10 years this object was reobserved photometrically by Neckel & Staude [111]. The spectrum of the star was briefly described in the Herbig & Bell catalog [112], where V565 Mon is listed as HBC 546. The spectral type was very roughly estimated as G, with Hα emission line and very strong Ba II lines in the red part. The next important step in the study of this star was the identification of V565 Mon with the IRAS 06556-0752 source in the catalog of Weintraub [113]. This confirmed that V565 Mon is an extremely bright in the mid-IR range.

The P17 cometary nebula, also known as NGC 2313, PP67 and GN 06.55.6.01 [114], is an object with high surface brightness in the dark cloud LDN 1653, the distance of which is 1060~1200kpc [115,116,117]. P17 has triangular shape and V565 Mon is located in its south-western edge. On deep images with a high spatial resolution one can note traces of the second, opposite cone, which suggests a bipolar structure of the nebula. In the course of the search for Herbig-Haro (HH) objects, group consisting of HH 947 A/B was discovered near the symmetry axis of P17 [118]. Logically, V565 Mon can be considered as a source of this flow.

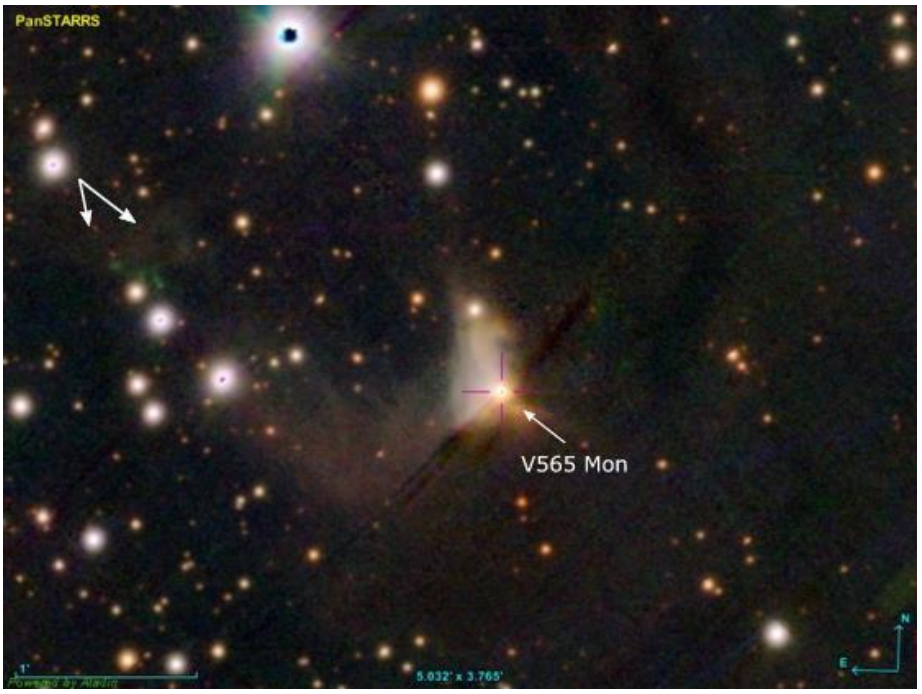

Fig. 5.1 Color image of a field around V565 Mon from PanSTARRS Data Release 1 (DR1) survey (*i*, *r*, *g* filters). HH objects are pointed out by arrows in the left corner. The dark diagonal stripe, visible across the nebula, is an artifact.

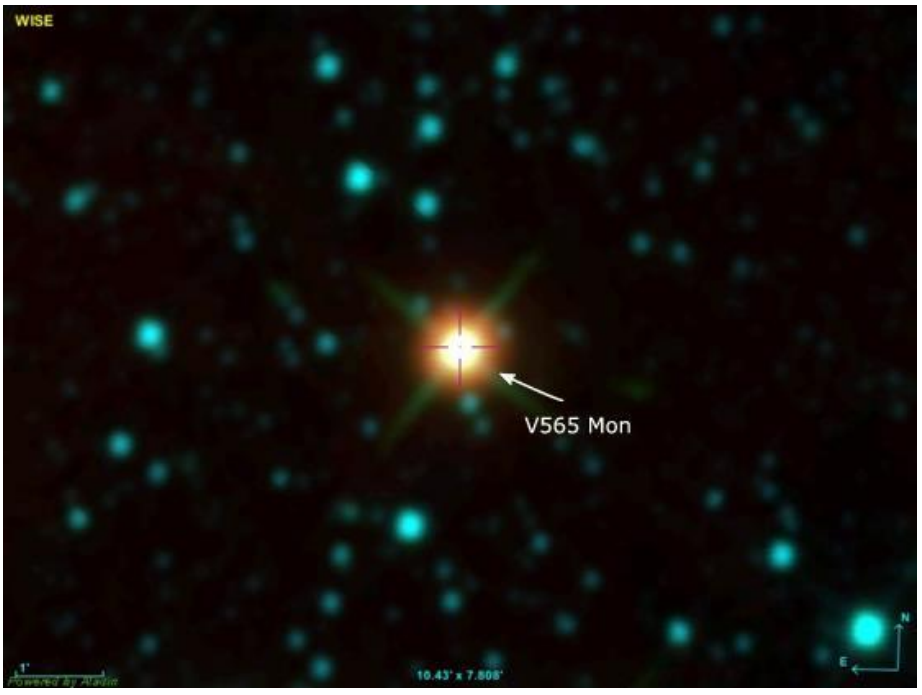

Fig. 5.2 The same field from the AllWISE survey (blue-3.4 μm, green-4.6 μm, red-22 μm). V565 Mon is pointed out by a white arrow.

In the image taken from the Pan-STARRS survey, one can see V565 Mon immersed in dust. The aforementioned HH group is also visible and pointed out by arrows in the left corner of Fig. 5.1. For comparison in Fig. 5.2, we present the same field taken from the AllWISE survey colored chart, which confirms its highly brightness in the mid-IR.

All of the above makes the V565 Mon star an interesting target for further studies. Especially noteworthy is that we still do not have good spectral data on this star. Thus, it was included in our program of spectral studies of selected pre-main sequence (PMS) stars.

5.2 Observations and Data Reduction

Observations of V565 Mon were carried out with the 2.6-m telescope on 2018 February 15. In long-slit mode, the width of the slit was 1.5 ″ (with seeing about 2.5 ″) and the length was about 5′. As a dispersive element, the volume phase holographic grating with 1800g/mm was employed, providing the spectral resolution of about R=2500. Total exposure was 3600 s., which provides signal to noise ratio (S/N) more than 100 in the final spectrum after the processing and optimal extraction. The stellar spectrum was extracted in a 2″ width zone, while background and night-sky emission lines were modeled along the all slit length. Our observations cover the wavelength range of approximately 5800-6900Å. The typical errors for radial velocities are ±13 km s^{-1}.

5.3 Results: General description of the V565 Mon spectrum

During our observations, the visible brightness of V565 Mon was similar to the previously reported values. The reduced spectrum is presented in Fig. 5.3. One can see a red continuum with both emission and absorption lines superposed. Strong Hα emission is divided by a relatively narrow (in comparison with the emission) absorption component, which is going below the continuum. Such a double-peaked profile of the Hα line is typical for young active stars, although such strong central absorption is rare.

Among the most prominent absorption lines is strong but quite narrow NaI D doublet. Besides, two λ6141.71 and λ6496.89 Ba II absorption lines are very noticeable, which were already mentioned in [112]. We also noticed a weak 6707 Li I resonance line, which is a well-known youth indicator for PMS stars [119,120,121]. Also, a variety of Fe II absorption lines exist, but no Fe I absorptions were detected. Besides Hα, the only other emission lines detected are forbidden red doublets of [OI] and [SII]. Taking into account the presence of HH flow, associated with this star, one can assume that they belong to an outflowing envelope or jet near the star.

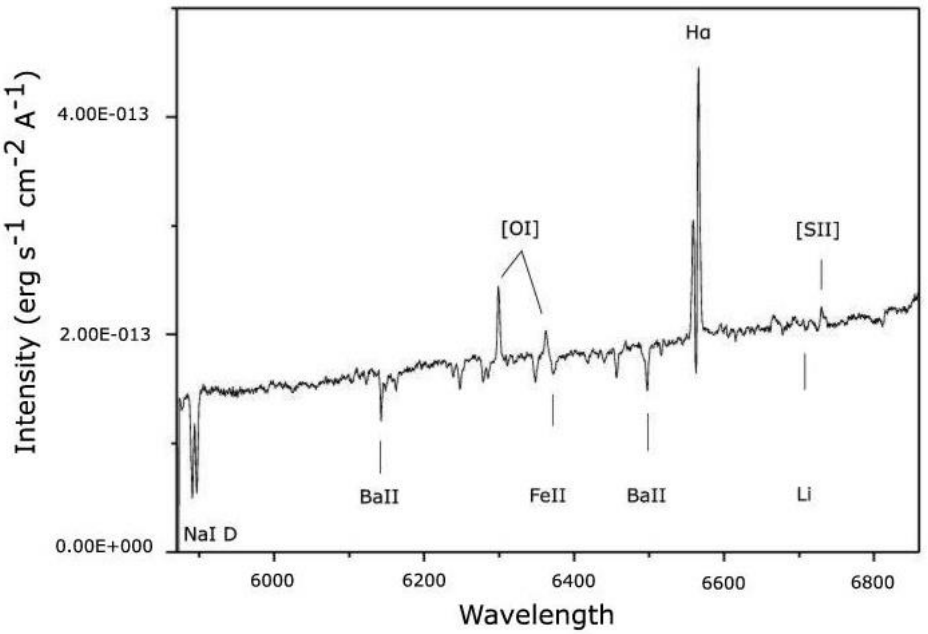

Fig. 5.3 Spectrum of V565 Mon in absolute intensities.

A more or less accurate spectral type of V565 Mon still is difficult to estimate. In any case, the prominent NaI D lines on the one hand, and well-developed Fe II spectrum with absence of Fe I lines on the other hand, lead to a spectral range from late F to early G, confirming Herbig's assumption.

5.3.1 Equivalent Widths and Radial Velocities

We estimated the equivalent widths (EWs) and heliocentric radial velocities of the most prominent absorption and emission lines and present them in Tab. 5.1. In case of Hα we list separate measurements for emission and absorption components. One can see that negative radial velocities are observed only for forbidden lines, which confirms our assumption that these lines are related to HH outflow. Moreover, low absolute values of their velocities point to a large angle of outflow with respect to the line of sight. The absorption component of Hα has near-zero velocity, and all other absorption lines, including NaI D, have positive velocities. In general, the strength of emission lines is not high. Even for Hα emission, the total EW is ≈-7Å.

The mean radial velocity of V565 Mon, computed by the six strongest absorption lines, is +34±14 kms^{-1}. Considering our spectral resolution and the probable blending of several lines, such an error should be considered small enough. The line widths somewhat exceed the instrumental profile of our system, which confirms their photospheric origin.

Errors of the radial velocities of two λ6141.71 and λ6496.89 Ba II absorption lines slightly exceed the mean error value, probably because of their broadness; moreover the λ6141.71 line is blended with the neighbor iron line.

5.4 Discussion and conclusion

First of all, we compared previously obtained estimations of V565 Mon distance and brightness with new data from Gaia Data Release 2 (DR2). The modern distance estimate for V565 Mon, based directly on the newly obtained Gaia parallaxes, is 1150 ± 91 pc, while the statistical estimation from the Bailer-Jones et al. catalog is 1122 pc [122]. This value is in accordance with the previous estimates of LDN 1653 distance (see Sec. 5.1). The brightness of the star also did not change in a noticeable way.

Lines	EW, Å	V_R, kms^{-1}	FWHM
Na I D2 (5889.96)	2.10	36	1.94
Na I D1 (5895.93)	1.88	32	3.84
Ba II (6141.71)	0.83	62	2.62
[OI] (6300.31)	-1.67	-36	3.88
[OI] (6363.82)	-0.58	-51	4.65
Fe II (6456.39)	0.45	24	3.92
Ba II (6496.89)	1.06	32	3.09
Fe II (6516.05)	0.2	17	3.02
Hα (em)	-2.22	-181	3.61
Hα (abs)	0.22	-2	3.92
Hα (em)	-4.64	157	3.05
Li I (6707)	0.08	89	1.48
[S II] (6730.78)	-2.87	-6	2.61

Table. 5.1 EWs and Heliocentric Radial Velocities of Selected Lines in V565 Mon Spectrum.

For the evaluation of main parameters of V565 Mon we obtained photometric data for this object with Vizier VO tools, including the photometry from IRAS and AKARI all-sky surveys [123], WISE survey [124], also [125], MSX catalog [126], 2MASS All-Sky catalog [127,128] and Gaia survey [57]. After making necessary transformations and calculations we produced the spectral energy distribution (SED) of V565 Mon, which is presented in

Fig. 5.4. Of course, one should keep in mind that at longer wavelength (e.g. in AKARI data) a significant amount of emission can have extended origin; however, the SED, obtained by us, is more or less consistent with the star, surrounded by a large mass of heated dust, very likely in the form of a circumstellar disk.

The problem of the extinction value for V565 Mon also is important. In any case, since the star is quite visible in the visual range, its extinction cannot be too high. The Gaia DR2 extinction value for V565 Mon is A_G=2.7. Using visible magnitude of V565 Mon (V=13.72) from [112] and distance of the star (estimated using Gaia DR2), we found M_V=3.05. Comparing this value with standard M_V for a G0 type main sequence star [128], for extinction value one can obtain A_V=1.4. Of course, in case of V565 Mon this value must be higher, because V565 Mon is definitely located above the main sequence.

As can be seen from the SED, V565 Mon emits in the mid and far IR range at least the same, or even a higher amount of energy, as in the optical range. To estimate its total luminosity, we tried several approaches. By integrating the SED curve of V565 Mon we obtained $L_{V565}\approx130\ L_\odot$ for its bolometric luminosity. But even this value is only its lower limit, since, judging by the SED, the star should emit significant energy up to the submillimeter range. By the equation, suggested for IR sources observed by IRAS [130], we find only $75L_\odot$, which in our case can be considered only as an additional correction, to take into account the furthest IR range. We also tried to approximate the SED by Robitaille models [131], but were not satisfied by any of the solutions, because they cannot represent well the nearly flat far-IR side of the SED. The possible reason for this can be significant extended emission in the far-IR range, but the available data do not allow us to check its existence.

Taking 130 $L_\odot$ as an initial estimate for the V565 Mon bolometric luminosity and making the assumption that the flux in all observed ranges is a result of the radiation of a G0 type central star, we can use general equations like

$$M_{bol,*} - M_{bol,\odot} = -2.5log_{10}(L_*/L_\odot) \qquad (5.1)$$

and

$$m - M = 5\log d - 5 + A_v \quad (5.2)$$

to convert the bolometric luminosity of V565 Mon to absolute magnitude. As a result we ascertain M_{bol}=-0.58. We have to add the bolometric correction, which for the G0 star is rather small [129], hence, M_v=-0.55. We know the observed visible magnitude of V565 Mon (m=13.72, see above), so from Eq. 5.2 the value of extinction for V565 Mon should be A_v=2.86. The similarity of this result with the Gaia estimate is remarkable. One can assume that $A_v \approx 3$ is a reasonable estimate for the V565 Mon extinction.

It is obvious, that V565 Mon is indeed located in the LDN 1653 cloud, because our estimate of its radial velocity is in perfect accordance with a velocity (converted to heliocentric) of +29 km s^{-1}, measured by the ^{13}CO line [115]. Thus, we see that all main features of V565 Mon, described above, point to the PMS nature of this star.

However, it is not easy to classify this object, because its significant luminosity (higher than a great majority of T Tau stars) suggests that it has intermediate mass and, consequently, belongs to the HAeBe star class. On the other hand, its spectral type is probably too late for such classification and its spectrum corresponds to T Tau stars. Nevertheless, V565 Mon could belong to some intermediate class between T Tau and HAeBe stars.

However, the most unusual feature of V565 Mon is the presence of two strong λ6141.71 and λ6496.89 Ba II absorption lines in its spectrum. Although this fact was mentioned in the Herbig-Bell catalog [112], nowhere was stressed the peculiarity of barium overabundance in such a young star.

Meanwhile, though it is assumed that for low and intermediate ($1M_\odot \leq M \leq 3M_\odot$) mass stars barium emerges through **s-process**, recent studies have found the distinct excess of barium abundance in young stellar clusters [132,133,134,135,136]. The main trend, described in these works, is in favor of the anticorrelation between barium enrichment and the age of the cluster. In [136] a new mechanism of barium enrichment in young open clusters was suggested. Some possible explanations of barium abundance linked it to chromospheric activity, however significant correlation was not detected [138]. Despite all

these various approaches, the processes producing barium in young stars still are hardly understandable.

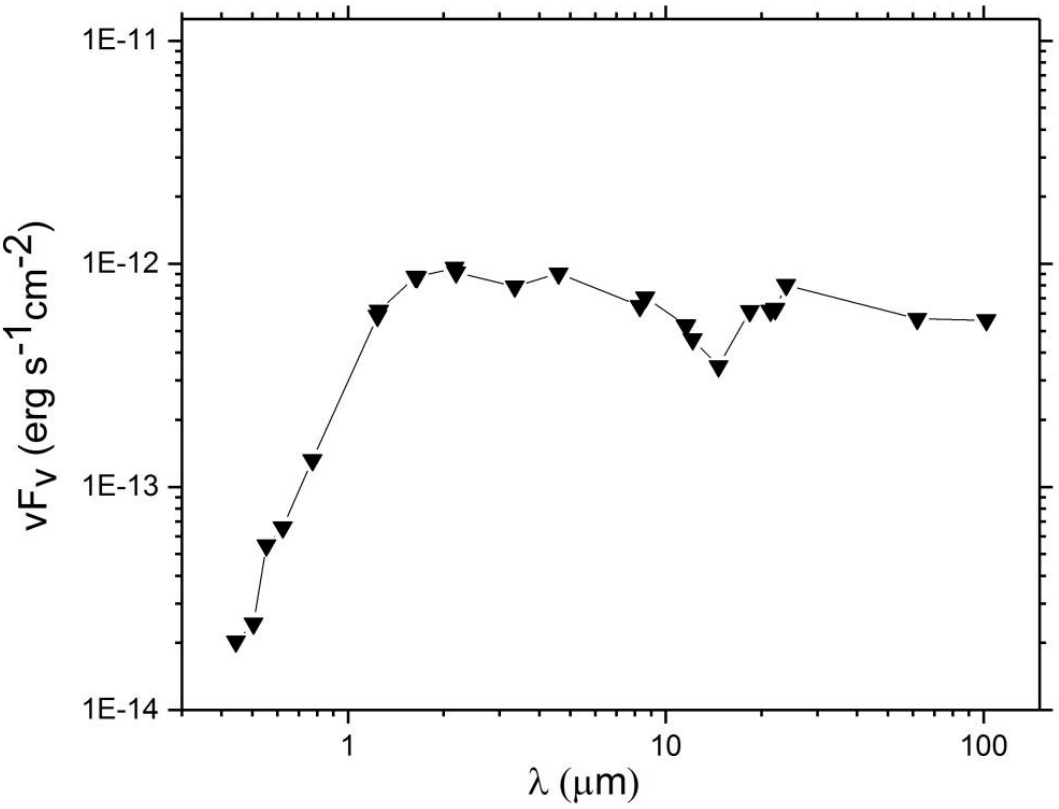

Fig. 5.4 SED of V565 Mon

The most obvious difference of V565 Mon with these studies listed above is that even the youngest open clusters described in these works have ages of 10^8 years, while the age of V565 Mon cannot exceed several million years. On the other hand, EW of Ba II line (1.06) is even larger than the upper limit of the curve of growth in [137] (see their fig. 1). We screened the spectra of several hundred PMS stars from the Cohen and Kuhi atlas [86], but did not found any object with similar strength of Ba II lines.

Besides, we also considered the possibility that a V565 Mon star can be a FU Ori-like object. Actually, this possibility was the reason why we included this star in our observational program. The spectral type of V565 Mon and the scarcity of emission lines in its spectrum are in favor of the FUor hypothesis. Also, it is well known that the existence of Ba II (especially λ6497) lines is one of the most typical features in spectra of FUors.

However, there are several reasons against such a suggestion, in particular: the photospheric absorption lines definitely are wider than in bona fide FUors and FU Ori-like stars; the Hα profile does not show characteristic wide P Cyg type absorption; radial velocities of all absorptions, including even the NaI D doublet, are positive, i.e. indicate the absence of significant outflowing activity. Of course, one cannot exclude the possibility that V565 Mon can represent some non-typical case of FU Ori-like stars, or that its spectral characteristics are due to its orientation with respect to the line of sight.

Anyway, for the last 25 years little study was carried out to reveal the nature of V565 Mon. A few previous spectral investigations give only a general view, without going into details. Scarce photometric data that we have in hand also give a very generic and not complete picture, which does not allow us to draw a conclusion about the variability of V565 Mon. Meanwhile, as our spectral study revealed, this somewhat neglected object could be an important step in understanding the nucleosynthesis problems in young stars. In this sense, the case of V565 Mon is unique and it deserved a detailed high resolution spectral study in the optical and near-IR range.

6. PV CEP AND V350 CEP: STARS ON THE WAY BETWEEN FUORS AND EXORS

6.1 Introduction

The variability of PV Cep and the nebula GM1-29 (RNO 125), connected with this star, was discovered in 1977 [139,140] (see Fig. 6.1). The sharp increase in the brightness of PV Cep resembled an outburst of FU Ori, but even the first spectra of this star showed a similarity with classical stars of the T Tau type [140,141,142]. Subsequently, Herbig tentatively assigned PV Cep to the class of EXors [25], but later excluded this object from the list [143] (Herbig, 2008), since further studies indicated too noticeable differences between PV Cep and typical EXors. Note that in following years PV Cep underwent several rises and falls in the brightness (see below). Like many other active T Tau stars, it is the source of the extended Herbig-Haro flow [144,145] and bipolar molecular outflow [146]. Despite the considerable number of subsequent studies (e.g., [80,147,148,149]) it is worth mentioning that, PV Cep remains largely an enigmatic object.

The variable star V350 Cep, located in a cluster within the NGC 7129 nebula (see Fig. 6.1), was first mentioned in [150]. The authors noticed that this object was not visible on the maps of the Palomar Atlas (1954), but in 1977 it reached 16.5 magnitudes (in the V band). In [151] the historical light curve of V350 Cep is presented.

More recent data were collected by Herbig [143]. The results unambiguously indicate that the increase in the brightness of this star began approximately in 1972 and it has reached its maximum since 1978. The star remains at the same level of brightness for almost 50 years, showing only weak fluctuations. Deeper minima (up to V = 17.7) with a length of several months were observed twice (in 2009 and 2016) with a subsequent return of the brightness to the mean value [152,153].

However, it turns out that V350 Cep is also not a FUor type star, at least in classical terms, since already the first spectral observations showed that it is a T Tau type star, with a strong and very developed emission spectrum [141].

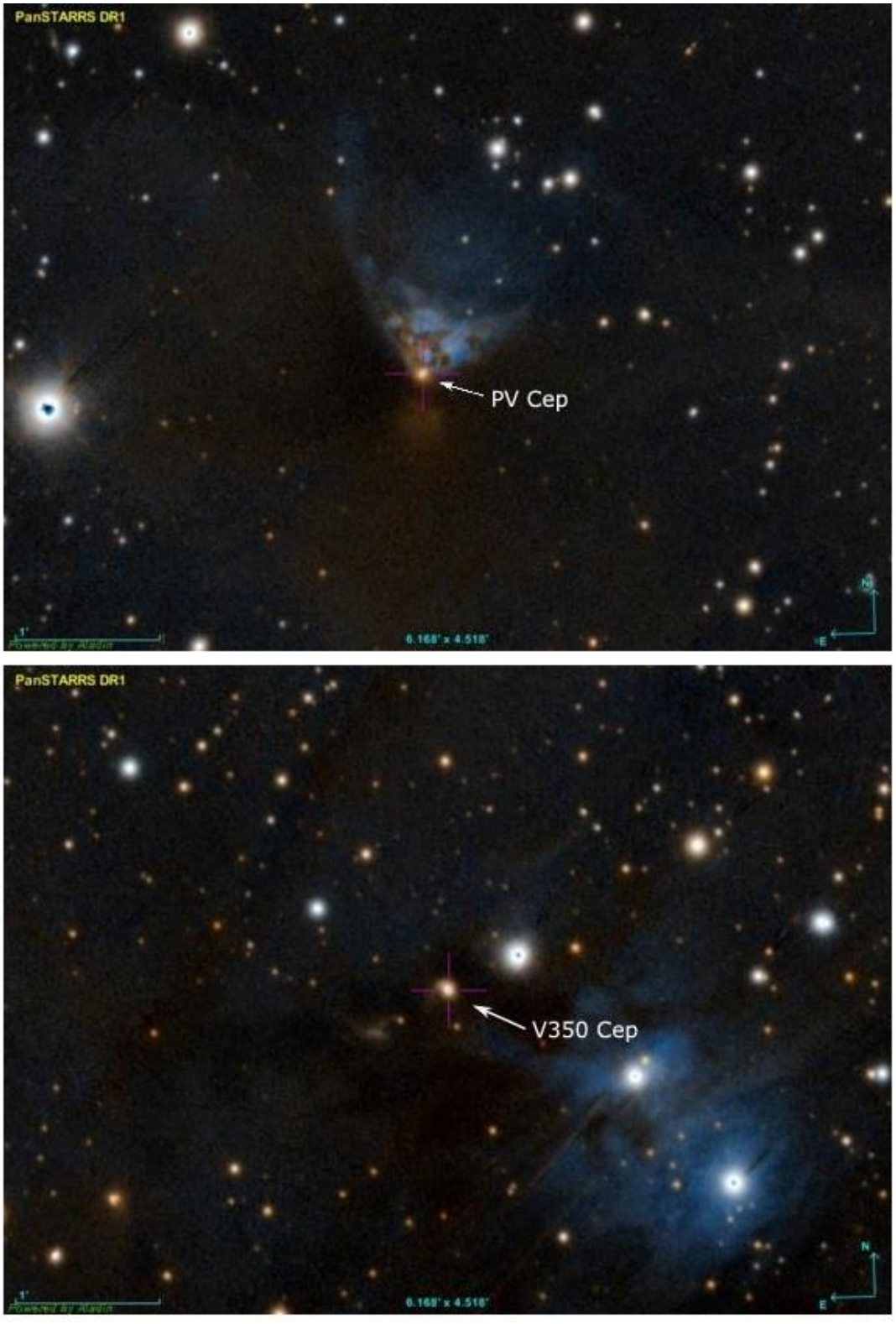

Figure 6.1 The color images of the fields around the PV Cep and associated nebula GM 1-29 (at the top) and the V350 Cep star (at the bottom). Both taken from PanSTARRS Data Release 1 (DR1) survey (*i*, *r*, *g* filters).

This was subsequently confirmed by the following numerous observations, for example ones made in [154,155,156]. All authors note the emission spectrum of V350 Cep, with strong Balmer lines, forbidden lines [OI] and many lines of both ionized and neutral iron. A detailed analysis of V350 Cep, carried out with the high-resolution spectrographs [143,157], showed obvious signs of an outflow of matter from the star. Herbig (2008) pointed out that V350 Cep can hardly be attributed to EXors, since, in particular, this star does not show outbursts characteristic for the latter ones, but it is almost constantly at the maximum brightness level [143]. The spectral type of V350 Cep was reliably enough assessed as M2 [154,143].

In this chapter, we present the new spectra of PV Cep and V350 Cep obtained over the past five years and compares these results with available data.

6.2 Observations and Data Reduction

Observations of both objects were carried out with the 2.6-m telescope. When obtaining the spectra, the width of the slit was 1.5″ and the length was about 5′. The field of view in the direct imaging mode was about 11′ at a scale of 0.67″ / pixel. As a dispersing element volume phase holographic gratings with 600 g/mm and 1800 g/mm were used, providing a spectral resolution R of about 800 and 2500, respectively.

The total exposure time is calculated in such a way that a signal-to-noise ratio of more than 100 is provided in the spectra after processing and optimal extraction. Table 6.1 gives a summary of all spectral observations of PV Cep in BAO and SAO. For the V350 Cep, one spectrum was obtained on 22 Sept. 2015 with a total exposure of 20 min and a resolution of about 2500.

The errors of resulting radial velocities presented here for PV Cep and V350 Cep are ±23 and ±21 km s^{-1} respectively.

Date	Spectral Range (Å)	Resolution (λ/Δλ)	Total Exosure (min.)
20.09.2015	4100-6800	800	30
10.06.2016	5800-6800	2500	40
24.08.2016	5800-6800	2500	15
21.12.2016	5800-6900	2500	45
24.06.2017	5800-6900	2500	40
25.06.2017	5800-6900	2500	40
20.06.2018	5800-6800	2500	60
23.12.2020	3650-7300	1300	40

Table 6.1. The log of the observations of PV Cep with 2.6-m and 6-m telescopes

In addition, at 23 December 2020, one spectrum was obtained at the 6-m telescope of the SAO. The width of the slit was 1″ with the length of about 6′.

The equivalent widths and radial velocities of all main lines were measured for both stars.

6.3 Results: PV Cep: Photometric data and the lightcurve of PV Cep

Although we were periodically obtaining direct images of PV Cep, which clearly show strong fluctuations in the brightness of the star and changes in the shape of the associated nebula GM 1-29 (RNO 125), photometric estimates of the brightness were not done, since this star is constantly monitored by the AAVSO group.

The AAVSO data concerning PV Cep start from 2010, and the photometry for 2004-2010 is presented in [148].

The resulting light curve of PV Cep, compiled on the basis of these data, shows that since 2006 the star began to fall in brightness from $m_R \approx 13.5$ to $m_R \approx 15.5$, and after 2008 it quickly went to a minimum ($m_R \approx 16.5$-17.4) (Fig. 6.2).

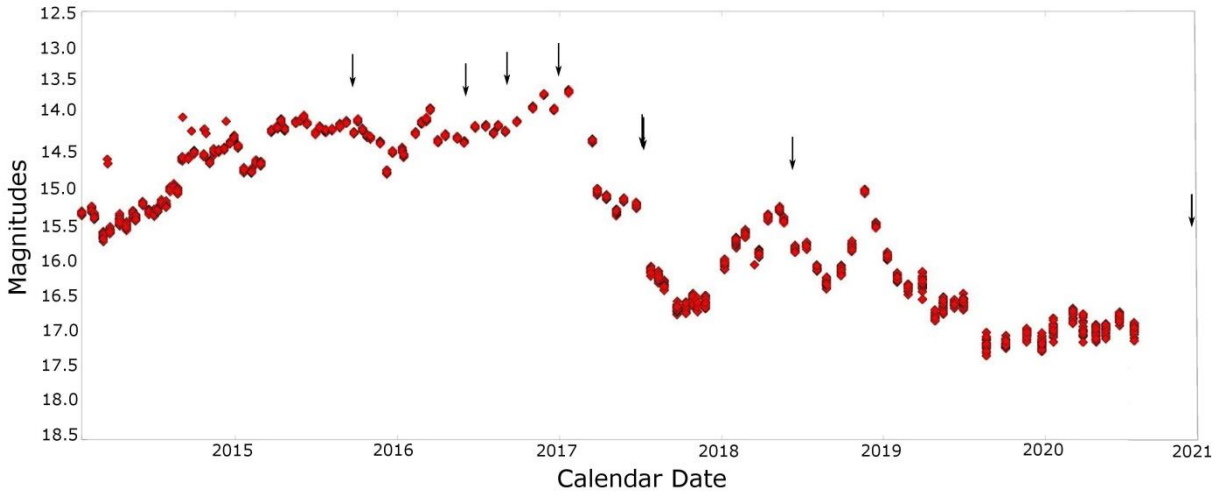

Fig. 6.2 The lightcurve of PV Cep in R color, generated with AAVSO database. The arrows indicate our spectral observations.

During 2010, the brightness of PV Cep was increasing in waves, and then has descended with amplitude of about 1-1.5^m. Finally, practically from the beginning of 2011, the star began to gradually and almost continuously rise in brightness, reaching almost its maximum ($R \approx 13.6$) by the end of 2016. After that, a rapid decline in brightness had begun, which was superimposed by individual local and short-term minima (the most noticeable of which occurred in the fall of 2017). By the middle of 2019, the star finally lowered to a minimum ($R \approx$ 17-17.3), where it remains up to the present time (end of 2020). Thus, over the past 15 years, PV Cep has undergone two large-scale (both in the amplitude - 3-4^m, and in the length - several years) brightness increases. The analysis of the earlier literature data makes it possible to distinguish other maxima during 1950 – 2005. However, one can suspect that PV Cep reached its maximal brightness (on the order of R = 11) only during its most powerful eruption on 1976-1978, when it was discovered [142].

6.3.1 General description of the spectra of PV Cep and its changes

In general, the spectrum of PV Cep in the optical and the near infrared ranges has been described in detail in [142,80,148,149]. Briefly, these results can be summarized as follows. It has the spectral characteristics of very active stars, namely, with very strong emission in the Hα line, also noticeable emissions from the Paschen and Brackett series, the Ca II IR triplet, numerous Fe II and Fe I lines, and in the IR range, of many other elements, as well as very noticeable NaI D absorption lines. The highest level of excitation in PV Cep spectrum have He I λ5875 and λ6678 lines, not strong, but clearly visible.

In addition, the spectrum of PV Cep contains a considerable number of forbidden lines of shock excitation: in the optical range, these are [OI] and [SII] emissions, and in the near-IR there are also numerous [Fe II].

It should be noted that the star is very red, and as a result the short-wavelength part of the optical range was rarely observed. Therefore, the discovery of a strong K CaII emission line and fluorescence in Fe I lines, typical for the most active T Tau stars [80] during the epoch of the highest brightness rise (1978) remains the only example. We will consider the question of the spectral type of PV Cep separately. Previous studies have also revealed a noticeable variability of individual spectral lines, apparently associated with the brightness level of the star.

Comparing the Tab. 6.1 and the PV Cep light curve, we see that the spectra we obtained correspond to almost all brightness levels of the star. For comparison, we present in Fig. 6.3 the PV Cep spectra at the maximum and the minimum brightness. Comparing with the data of other authors, no very important changes were detected; however, the several differences between the spectra are quite obvious. First of all, the greatly increased intensity of the forbidden lines is striking, while the classical Fe I and Fe II emission lines do not undergo any special changes. In particular, despite the weakened level of the continuum, it is clearly noticeable that in the blue-green (5000-5500 Å) region of the spectrum, the structure of the “forest” of numerous metal lines is practically the same. Note that the

intensity of the 5875 He I line also remains almost unchanged; that is, the level of excitation in the chromosphere of the star also persisted during brightness fluctuations.

Since the H and K Ca II lines did not fall into the spectral range of our observations, we could not verify whether the fluorescence in the Fe I lines is retained in the spectrum. However, we note that the neutral iron lines in the red spectral range (λ6138 Fe I and λ6592.91 Fe I), which are subjects to fluorescence, are constantly present. Although their equivalent widths are twice less in comparison with the spectrum of the star LkHα 120, with which PV Cep is often compared, and where this phenomenon is clearly expressed [158].

The most intense emission in the PV Cep spectrum, the Hα line, shows well-seen profile changes depending on the brightness level. As noted in practically all previous studies, it consists of two components, separated by the central absorption. Note that a two-peaked structure was also observed in the first members of the Paschen series in the near IR [149].

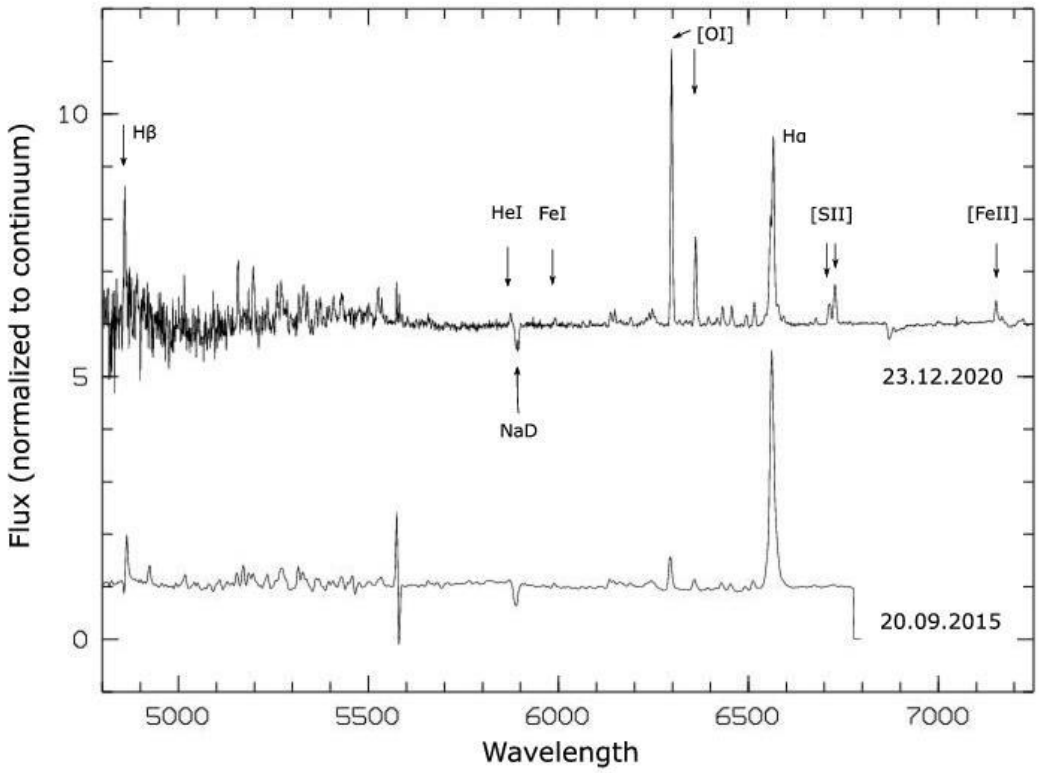

Figure 6.3 The spectrum of PV Cep on September 20, 2015 (at maximum) and on December 23, 2020 (at minimum). For convenience, both spectra are normalized to the continuum.

Fig. 6.4 shows sections of our spectra normalized to the continuum, including the Hα line. It is easy to see, that as the brightness decreases, the central absorption component becomes weaker and weaker, while on June 10 and especially on December 21, 2016 (just at the moment of maximum brightness), it lowered even below the continuum level (EW was about 0.8 Å). However, a really pronounced profile of P Cyg was observed only during the period of the absolute maximum in 1977-78 [142].

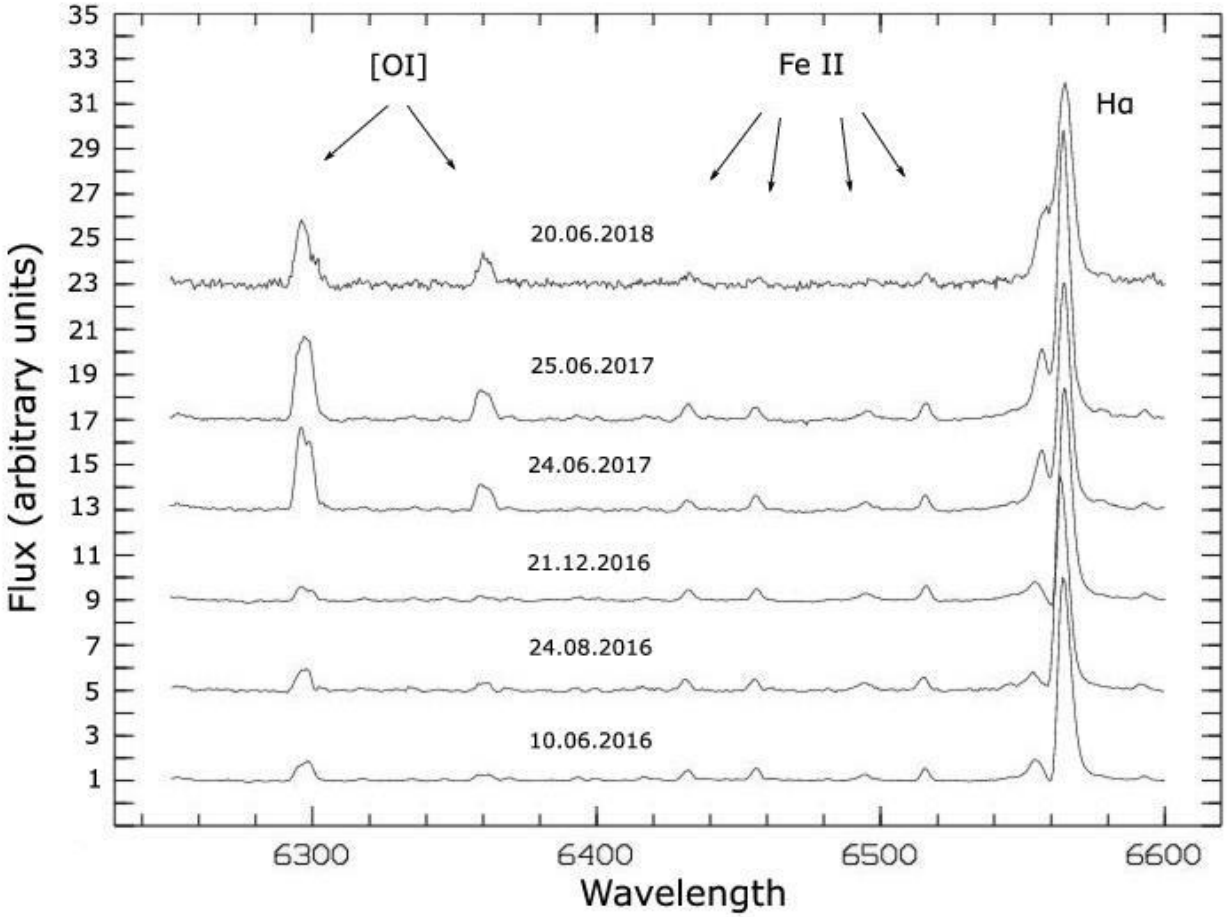

Figure 6.4 Sections of the PV Cep spectrum normalized to the continuum corresponding to different observation dates. Strong changes in the profiles and intensities of the Hα and of the [O I] lines are seen, while the Fe II emissions remain unchanged. The spectra from the 2016-2017 shifted by 4 units in relation to each other, and the spectrum of the 2018 - by 6 units.

For the visual representation of the behavior of the typical lines in the PV Cep spectrum, the variations in EWs as a function of time are shown in fig. 6.5. For a comparison of these variations with the apparent brightness of the star, the dependence of the EWs of the Hα and of the [OI] on m(R) is shown in fig. 6.6. From fig. 6.5 and 6.6 it is easy to see, that the equivalent widths of the forbidden lines unambiguously increase with decreasing brightness, while the equivalent width of one of the strongest permitted emissions (λ6516 Å Fe II) practically does not change. The Hα line behaves, apparently, in an ambiguous manner. The authors of previous studies have come to approximately the same conclusions. It should be noted that according to [148] the equivalent width of Hα was very high (> 100 Å) in 2004-2009, almost near the maximal value in 1977-1979 (see the summary graph in [80]; in recent years, it has not reached such values.

6.3.2 Radial velocities

From the very first observations, it became apparent that the PV Cep was surrounded by an expanding envelope. In addition, it gradually became clear that this star is the source of bipolar outflow. Therefore, the question of whether the lines in its spectrum belong to certain emitting regions (chromosphere, inner disk, outflowing matter, collimated jet) is quite important. Radial velocities can clarify the picture. When comparing our data with previous measurements, we have reduced all results to heliocentric radial velocities, which are used below.

Since the photospheric absorptions are not observed in the PV Cep spectrum, the velocity closest to the radial velocity of the star itself should have the deep chromospheric emission lines of Fe II and Fe I. We obtained the average velocity of five Fe II and Fe I lines to be -15 ± 11 kms^{-1}, which is in excellent agreement with the Herbig measurements (-19 kms^{-1}, see [142]), and -13 kms^{-1} [159], as well as with the velocities of the permitted emissions in the near infrared region [160,149].

The emission components of the Hα line are apparently formed mainly in the expanding envelope created by the strong stellar wind. Note the very large total emission width (our estimates give an FWZI of the order of 1200-1500 km s^{-1}), which was also pointed out by other authors.

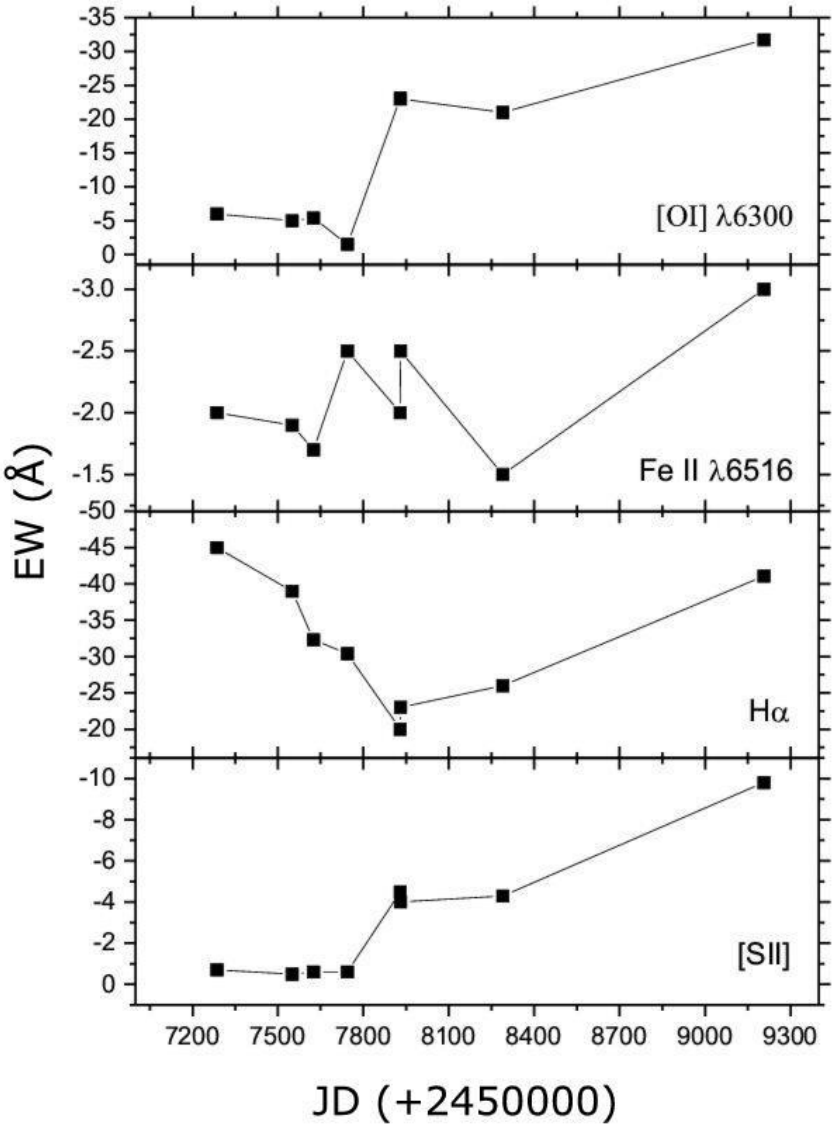

Figure 6.5 The equivalent widths of some lines in the PV Cep spectrum as a function of time. For the Hα line, the total emission EW was measured; for the [SII] lines, the total EW of both lines of the doublet is given.

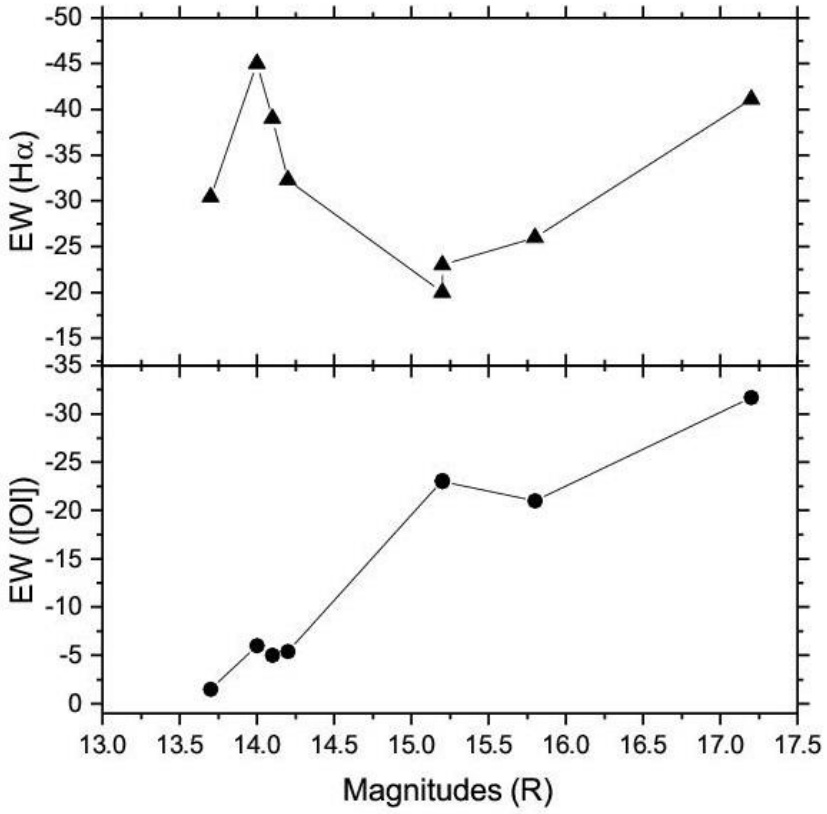

Fig. 6.6 The equivalent widths of Hα and [OI] lines as a function of an apparent brightness of the PV Cep in R color.

As can be seen from Fig. 6.4, it practically does not depend on the brightness level, as well as from the velocity of the main emission component (+84±19 km s^{-1}). Whereas the absorption component of Hα changes not only in intensity (from the P Cyg profile to almost complete disappearance), but also in the radial velocity. Estimates for the spectra obtained at 2016-2018 give values in the range from -120 to -180 km s^{-1} (note that even larger shifts were observed during the 1977 maximum [158]. At the star's minimum brightness at the end of 2020, the Hα absorption shift was only -80 km s^{-1}.

Strong and narrow absorptions of NaI D, like in many similar stars, are also formed, undoubtedly, in an expanding envelope. It is noteworthy that their intensity changes very noticeably, up to complete disappearance, but it does not depend on the level of apparent brightness. Their radial velocity remains negative all the time, but its absolute value changes beyond the limits of measurement errors. In particular, in our spectra of 2016-2017 years it

was in the range of -118 to -159 km s^{-1}, and at the end of 2020 it was -45 km s^{-1}, thus, it decreased in parallel with the absorption component of Hα.

Such variations indicate that the intensity and the speed of the stellar wind outflow fluctuate quite noticeably and are probably related also to the changes in the apparent brightness of the star.

6.3.3 Forbidden lines

Strong and wide forbidden lines [O I] and [S II] are typical, as it turned out later, for objects with collimated outflow. They were found in the spectrum of PV Cep immediately after its discovery. Neckel et al. were the first to draw attention to their multicomponent structure [159]. Not only the total equivalent width of these lines changes noticeably, but also the radial velocities and relative intensities of the components. These phenomena are especially pronounced for the [S II] lines [80].

Often, with the sufficient resolution, four components can be distinguished in each of the lines of the doublet. On the other hand, sometimes they blend together into one very wide (> 400 km s^{-1}) emission line. The [O I] lines are also subdivided into components, but due to their greater intensity and width, they are less expressed.

These features are complicating the accurate measurements, but on average, the radial velocities of the [S II] components in the spectra, considered in this work, can be estimated by the following values: -230, -170, -50, and +70 km s^{-1} (moreover, the component with a positive velocity changes especially noticeably and often it is completely absent). See it in the Fig. 6.7.

Taking into account aforesaid, when comparing these results with those of the previous work, we find rather good agreement. Thereby, in [159] authors distinguish components with -246, -133, and -55 km s^{-1} in the [O I] line; in [161] authors give -275 and -60 km s^{-1} for [OI] (for a total line width of -455 to +255 km s^{-1}) and -300 and -75 km s^{-1} for [S II]; in [162] for [O I] with a total range from -400 to +50 km s^{-1}, the components -300, -170, -

100, and -50 km s^{-1} are listed. Thus, components with positive radial velocity are rarely observed, apparently due to their low intensity.

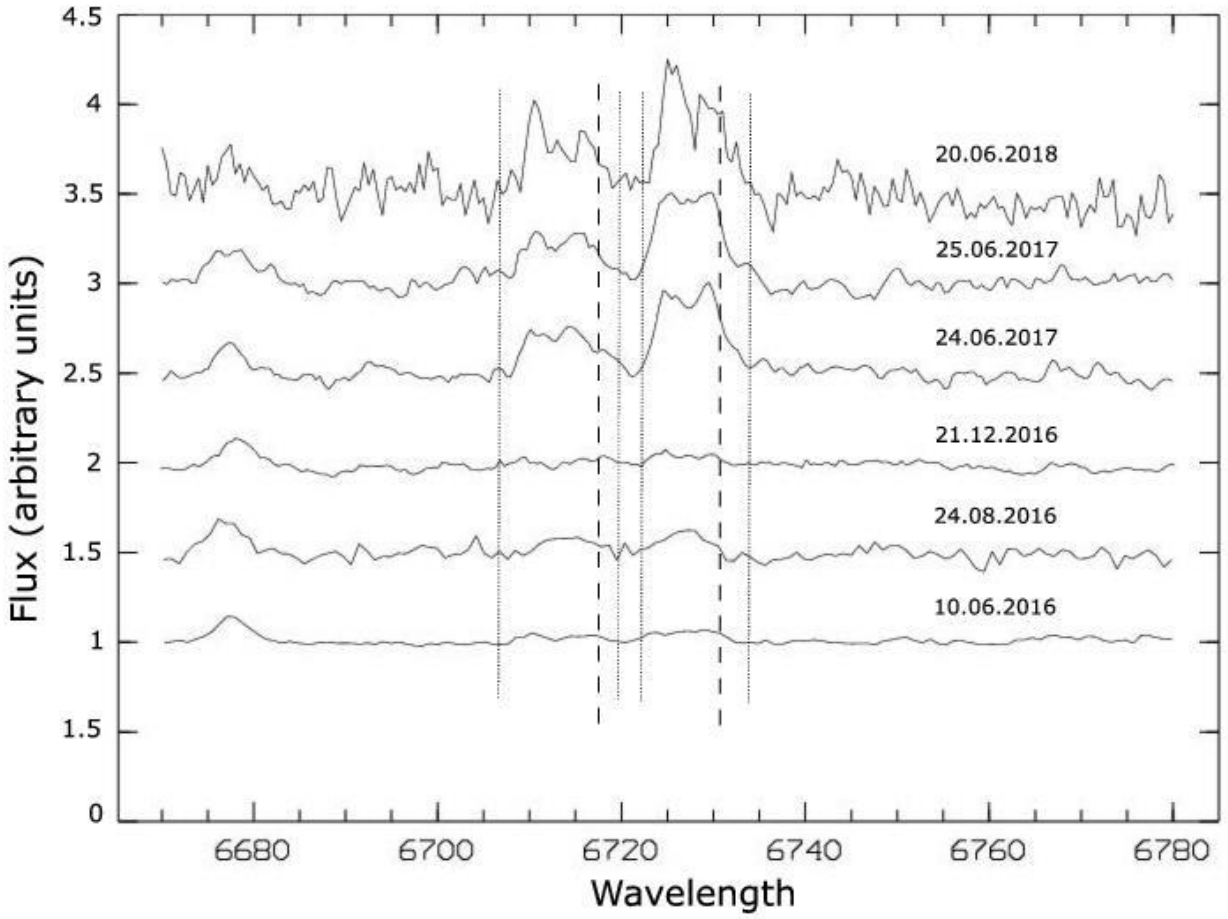

Figure 6.7 Appearance of [S II] lines and its changes in the spectrum of PV Cep from 2016-2018. The wavelength values corresponding to the zero radial velocity are shown by the dotted line. The limits for the FWZI lines are also indicated. The spectra are normalized to the continuum and shifted relative to each other along the ordinate axis by 0.5 arbitrary flux units.

To understand this phenomenon, it is extremely important to point that a similar split is observed also in the strong [Fe II] emission lines, which are quite numerous in the near-IR region of the spectrum, and their intensity varies greatly [149]. Components are especially clearly detected in 1.257 and 1.644 μm lines [Fe II], with radial velocities of –265, –99, +50, and +165 km s^{-1}. In the same work, it was shown that the emitted components with a high

absolute velocity actually belong to a collimated outflow from PV Cep, while those with a low one are concentrated around the star.

Thus, it is natural to assume that the multicomponent structure of the [O I] and [S II] lines has the same origin. However, as we can see, a really good agreement on the velocities between them and [Fe II] is observed only for the high-velocity blue-shifted component, which, moreover, is the least of all subject to fluctuations of the intensity. On the other hand, the high-speed redshifted component has never been observed in the optical range.

This fact is quite naturally explained by a combination of two factors. First, in the immediate vicinity of PV Cep, there are constant and rather short-term variations in circumstellar extinction caused by the formation and redistribution of dust particles in the disk during the processes of outflow and individual ejections of matter [148]. The average value of this absorption, estimated from the [Fe II] lines, is about A_V = 10 mag [149]. About the influence of a circumstellar dust clouds indicated by the dependence of EW of Hα emission from the brightness of PV Cep, characteristic for UXor type stars. Since the inclination of the axis of the circumstellar disk PV Cep to the sky plane is insignificant [163], it is straightforward that near the star the radiation of the redshifted (i.e., opposite from us) branch of the outflow in the optical range is simply screened by this disk and becomes clearly distinguishable only in the near IR. Secondly, as it is reasonably suggested in [149], the observed small (2-3″) emission knot (actually a miniature jet) could have been ejected by PV Cep during the 2004-2005 outburst recorded in [148]. This makes one to suspect that even during the lower-amplitude manifestations of activity around the star (at least along the outflow axis), small condensations appear, emitting in forbidden lines. Differences in their densities, velocities and sizes create rather rapidly varying profiles of the [O I] and [S II] lines.

A conclusion from the above discussions is the assumption that after the maximum described in Section 6.3 at the turn of 2016-2017 one can expect the appearance of a similar knot, which in the coming years will become possible to observe directly (and thereby obtain the confirmation of this hypothesis). Similar observations of the formation of new initial clumps in jets after bursts are extremely rare and, as far as we know, have been

noted so far only for the companion of the Z CMa [164] and the newly discovered FUor V2494 Cyg [165]. As an object experiencing fairly frequent and powerful outbursts, PV Cep offers a good opportunity to test and explore its mechanism of occurrence.

6.4 Results: V350 Cep

The stars PV Cep and V350 Cep were not only discovered at the same time, but they are quite similar in terms of the spectra, so it is worth to compare both objects. As mentioned above, the V350 Cep keeps its maximal brightness almost all the time. Accordingly, the spectrum obtained by us and considered in this work belongs to the quiet period in the state of a star. By its general appearance, it is quite consistent with the results of previous observations. Some fragments are shown in Fig. 6.8.

The measured equivalent widths of the most characteristic lines of Fe I, Fe II, and He I show excellent agreement with the 1990s values given in [155]. The intensities of the Fe I fluorescent lines in our spectrum are somewhat lower than in the period of 1978-1994 [156]. Also, the intensities of the forbidden lines [OI] and [S II] have remained almost unchanged. The Hα line in our 2015 spectrum has a pronounced P Cyg profile (Fig. 6.8). The equivalent width (about -24 Å for the main emission component, and 0.2 Å for the absorption component, which falls below the continuum level), corresponds to the data of 1990, 1994, 2005, and 2007 [155, 143, 157]. The radial velocities of forbidden emissions turned out to be negative: -117 km s^{-1} for [O I] and -97 km s^{-1} for [S II]. For the Hα line, the values +46 and -270 km s^{-1} (emission peaks) and -167 km s^{-1} (absorption component) were obtained. These values of Hα are in very good agreement with the results of 2005 and 2007.

Thus, the chromospheric activity of V350 Cep has remained at almost unchanged level since its brightness rise (i.e. for more than 40 years). However, a comparison of the available literature data on the Hα line profile leads us to an interesting and previously unmentioned conclusion.

Namely, from the moment of the first observations in 1978 to July 1985 inclusively [154,166,156], the P Cyg profile in the Hα line was not observed, while since October 1986 it has been constantly present [156,155,143,157 and the present work].

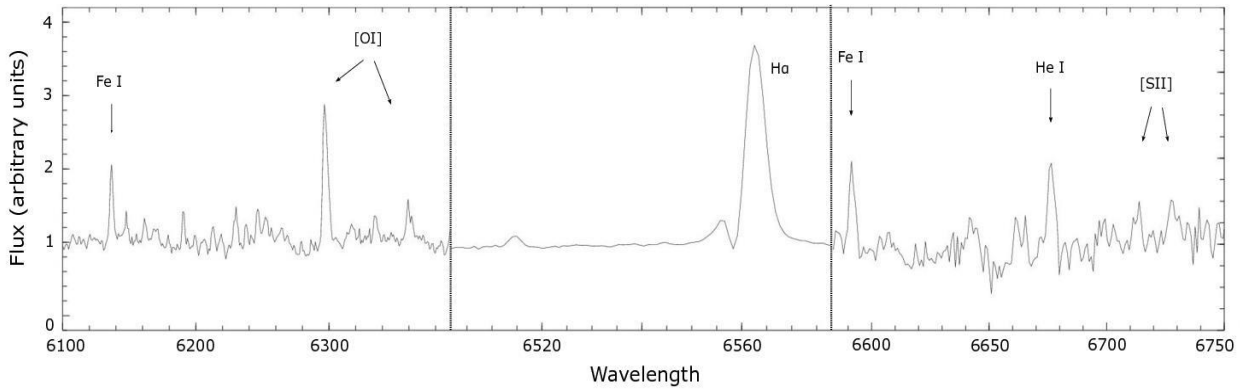

Fig. 6.8 Fragments of the V350 Cep spectrum normalized to the continuum: the P Cyg profile of Hα line, forbidden lines [OI] and [S II], and Fe I fluorescent lines are presented.

The above facts indicate that V350 Cep is surrounded by an accreting disk, which not only creates an excess in the far-infrared range, but also sometimes manifests itself in UXor-like brightness dips [106]. However, the presence of a disk does not strongly affect the extinction: A_V = 1.2 [167]. After the rise in the brightness, a rather dense expanding envelope with a velocity range of several hundred kilometers per second was formed around the star, and its density gradually increased so much that the outflow led to the formation of a profile of the P Cyg type. The question of the existence of a collimated flow in V350 Cep is still open. On the one hand, such a flow was not detected by direct observations (the results in [155] are not entirely convincing). On the other hand, it is possible that V350 Cep may be the source of the Herbig-Haro object HH 235 [168], although the rather weak forbidden lines [O I] and [S II] indicate an insignificant intensity of shock excitation in the shell of a star itself.

6.5 Discussion

The absence of any photospheric lines in the PV Cep spectrum makes it very difficult to classify it and to determine other parameters. The spectral type A5 was estimated in [142] rather arbitrarily. Absorption lines were observed only in one spectrum obtained in 1978, corresponding to the late spectral type (G8-K0) [80]. Since a similar spectrum has never been observed again, this estimate should also be treated with caution. In the same way, the distance estimates of the PV Cep are also (taken by the authors mainly from various stellar astronomical studies) differs: 500 pc [142], 440 pc [162], 280 pc [167], and 325 pc [148]. Nowadays, due to the availability of Gaia data, the PV Cep parallax is known very accurately; it corresponds to a distance of 340 pc [122].

Also, the estimation of the extinction in the direction of PV Cep is a rather difficult task. The color of the star and the rapid drop in the intensity of the continuum in the blue region indicate that the absorption is significant. Most of it undoubtedly arises in the circumstellar disk. It changes noticeably over time, significantly affecting the observed brightness fluctuations of PV Cep. Moreover, as shown in [149], there is a significant difference in the absorption between the northern and the southern parts of the outflow (radiation of latter passes through the whole disk).

Unsurprisingly, estimating the bolometric luminosity of PV Cep is not an easy task. If we consider the most recent works, then in [148] the bolometric luminosity of the star itself was estimated to be ≈17 $L_\odot$ (adopting G8 for the spectral type, taken from [80]), and the luminosity of the accretion disk, which creates a significant part of the total radiation of PV Cep, turned out to be much higher: ≈40 $L_\odot$ at low brightness and ≈80 $L_\odot$ at the 2006 maximum. However, in [149] the accretion luminosity estimate (based on the 2012 data) turned out to be an order of magnitude lower: ≈5.7 L⊙, which the authors explain by a further decrease in the accretion rate. If we take into account that in [149] authors clearly overestimated the distance to the object (500 pc vs 340 pc), then this discrepancy is even stronger. Thus, it can be assumed that in the current state of a deep minimum, the

brightness of PV Cep is determined practically only by the radiation of the star itself, i.e. $L_{bol} \approx 20\ L_{\odot}$.

The situation with the V350 Cep, spectral type of which is reliably known, is simpler. The distance to the cluster NGC 7129, to which the star belongs, was estimated by various authors and it varies from 800 to 1260 pc. However, the parallaxes obtained with the Gaia space observatory made it possible to obtain a fairly accurate value of 900 pc [169]. Estimating the average V for V350 Cep from the light curve of 1993-2014 as 16.1 [152] and taking the above values of distance and absorption, and also taking into account the bolometric correction for the spectral type M2 [170], we obtained an estimate of 3.3 $L_{\odot}$ for the post-outburst luminosity of this object. Unfortunately, with the available data in hand, it is not possible to find, which part of this value comprises the accretion luminosity.

The main question remains in the unusual character of the variability of both stars and their classification. Let us consider the V350 Cep first. Obviously, the rise in the star's brightness is caused by a sharp increase in the accretion rate, but the subsequent stable state at the maximum level is unique in its way. Recently published historical light curve from 1970-85 confirms that the increase in the brightness began precisely in 1971-72 and no other noticeable bursts have occurred since 1885 [106].

V350 Cep was tentatively assigned to the class of possible EXors [25], but it was later excluded from those [143], primarily due to the absence of recurrent bursts (although in terms of luminosity it corresponds to typical EXors). On the other hand, in terms of the light curve, the object exactly corresponds to classical FUors with a slow increase in luminosity (similarly with the V1515 Cyg). Moreover, an even more slow decrease in brightness, characteristic for many FUors, is observed after 1997 [152]. A possible connection with a collimated outflow also makes the V350 Cep similar to the FUors. It is also worth to note the impressive stability of the spectral characteristics for almost 40 years (besides the Hα line). The P Cyg components in the Hα and NaI D lines with a wide and almost rectangular profile also resemble FUors [143,157]. The rather low luminosity of V350 Cep is atypical for FUors, but still not exceptional. However, the rest of the abundant emission spectrum of V350 Cep corresponds to CTTS stars, rather than FUors. We tend to agree with the assumption made

in [152] about the similarity between V350 Cep and V1647 Ori, which is a recently discovered eruptive object that combines features of both FUor and EXor.

The observational facts collected to date allow us to conclude with sufficient confidence that there is a whole class of intermediate objects between FUors and EXors, to which (at least presumably) almost two dozen objects can be attributed, and half of them are visible only in the infrared range. Apparently, the V350 Cep is also one of them. If subsequent observations confirm the stability or further development of the P Cyg component in the Hα line, it can be assumed that V350 Cep gradually develops towards a typical FUor state. In conclusion, we note that important information for the classification of FUors and FUor-like objects can be obtained from infrared spectra. Unfortunately, as far as we know, an IR spectroscopy of the V350 Cep has not yet been performed.

PV Cep, which, in contrary to V350 Cep, shows repeated outbursts, also cannot be attributed to EXors for a number of reasons, which were discussed in detail in studies [171] and [149]. We will only mention the main arguments. PV Cep is an object of greater mass and luminosity than classical EXors. It is surrounded by a rather massive accretion disk. According to calculations made in [172] and [148], during and immediately after the outburst, the accretion rate was approximately 10^{-6} $M_{\odot}$ y^{-1}, and subsequently it decreased to 10^{-7} $M_{\odot}$ y^{-1} [149], but even this value is higher, than for classic CTTS stars. Undoubtedly, PV Cep is at an earlier evolutionary stage than EXors. Finally, it is associated with a biconical cometary nebula and generates a powerful and extended (2.6 pc) collimated flow [144], which is completely uncharacteristic for EXors.

However, it is quite remarkable, that practically all of the properties listed above, on the contrary, are characteristic of FUors. PV Cep differs from classical FUors by a very developed emission spectrum and, of course, repeated eruptions. Thus, PV Cep, like V350 Cep, turns out to be an object resembling V1647 Ori, as an intermediate object between FUors and EXors. The number of such "intermediate" objects has been growing in recent years. They may include, in particular, V346 Nor, V2492 Cyg, V1180 Cas.

7. GENERAL CONCLUSIONS

This thesis is dedicated to the proper investigation of diverse manifestations of phenomena of eruptive variability of YSO's, such as FUors, EXors, intermediate and UXors. An accurate description and differences of them were presented in *Sec. Introduction*.

Thesis is based on 4 published articles:

- "New powerful outburst of the unusual young star V1318 Cygni S (LkHα 225)", Astronomy & Astrophysics (chapter 3) [102]
- "Simultaneous photometric and spectral analysis of a new outburst of V1686 Cyg", Research in Astronomy and Astrophysics (chapter 4) [173]
- "Spectral study of V565 Mon: Probable FU Ori-like or chemically peculiar star", Research in Astronomy and Astrophysics (chapter 5) [174]
- "PV Cep and V350 Cep: Stars on the way between FUors and EXors", Astrophysics (chapter 6) [175]

Here I will bring brief conclusions on each chapter and make general remarks.

Chapter 3 [Magakian et al., 2019]: Our investigation on eruptive variable stars begins with V1318 Cyg. This young double star is associated with a small isolated star-forming region around HAeBe star BD+40°4124 and it has very unusual photometric and spectral behavior. We present results of photometric and spectroscopic observations in the optical range. We carried out BVRI photometric observations of V1318 Cyg from 2015 Sept. to 2017 July. For the same period we acquired medium- and low-resolution spectra. Observations were performed with the 2.6m telescope of the Byurakan observatory. We also analyze the images of this field in IPHAS and other surveys.

We analyze the historical light curve for V1318 Cyg and demonstrate that the southern component, V1318 Cyg S, after being rather bright in the 1970s (V≈14 mag.) started to lower its brightness and in 1990 became practically invisible in the optical. After its reappearance in the second half of the 1990s the star started very slowly brightening. Between 2006 and 2010 V1318 Cyg S this process quickened, and in 2015 the star became brighter than in minimum by more than five magnitudes in visible light. Since that time V1318 Cyg S remains at maximum. Its spectrum shows little variability and consists of a mixture of emission and absorption lines, which has allowed us to estimate its spectral type as early Ae, with an obvious evidence of a matter outflow. We derive its current Av≈7.2 and $L=750L_{\odot}$, thus confirming that V1318 Cyg S belongs to the Herbig Ae stars, making it, along with BD+40°4124 and V1618 Cyg, the third luminous young star in the group. It is very probable that we observe V1318 Cyg S near the pole and that the inclination of its dense and slow ($\approx 100 kms^{-1}$) outflow is low.

Our group was the first that noticed and described the exceptional brightening of V1318 Cyg S star. New observations confirm that the star keeps its high brightness level until now (at least 6 years) [176]. Moreover, its spectrum develops towards to classical FUor type spectrum.

Chapter 4 [Andreasyan et al., 2020]: We present an analysis of the optical observations of Herbig AeBe star V1686 Cyg, which is associated with a small isolated star-forming region around HAeBe star BD+40°4124.

Observations were held on 2.6m telescope of Byurakan Astrophysical Observatory from 2015 to 2017. For this period we obtained direct images and 14 medium- and low-resolution spectra of V1686 Cyg. In the course of observations we noticed that this star underwent a non-typical brightness outburst. We were able to trace the whole period of the outburst photometrically and spectrally. After data reduction we found that the full rise and decline of V1686 Cyg brightness had almost 3 magnitudes amplitude and lasted about 3 months. We were also able to trace the changes of the stellar spectrum during the outburst,

which are correlated with the photometric variations. Corresponding changes in the spectrum are explained by the formation of expanding envelope around the star, existence of which was responsible for the short-duration visibility of the blue-shifted absorption component in the profile of Hα line.

It is difficult to ascribe V1686 Cyg to one of the well-known classes of eruptive variables, as this short-time burst is not typical for it, however it gives an impression of an EX Lupi type variability.

Chapter 5 [Andreasyan 2021]: We present a detailed spectroscopic study of pre-main-sequence star V565 Mon, which is an illuminating star of the Parsamian 17 cometary nebula. Observations were performed with the 2.6m. telescope in Byurakan Astrohysical Observatory on 2018 February 15. Radial velocities and equivalent widths of the most prominent lines of V565 Mon are presented. We build the spectral energy distribution and estimate the main parameters of the star. We obtained $L_{V565} \approx 130\ L_{\odot}$ as a bolometric luminosity of V565 Mon, which, although, is its lower limit. Also, based on the Gaia DR2 distance, we evaluate the extinction value for V565 Mon as $A_V \approx 3$. Examining the spectrum of V565 Mon we note the presence of strong absorption Ba II lines, which is very unusual for a young star. Possible explanations of the mechanisms responsible for barium abundance in young open clusters are discussed. The existence of Ba II lines is an indicative feature in the spectra of FUors, thus we also consider this possibility.

Hence, we think that V565 Mon is a unique example, further investigation of which can help us to understand some open questions involved in the problem of nucleosynthesis in young stars.

Chapter 6 [Andreasyan et al., 2021]: Based on the new observations executed during 2015-2020 and the literature data, unusual eruptive variables PV Cep and V350 Cep were examined.

We trace the whole period of the new outburst of PV Cep, which generally lasted from 2011 to 2019. Currently, it is in a deep minimum. The outburst was accompanied by significant changes in the intensity and profiles of a number of lines, including Hα, [S II], and [O I]. The forbidden lines generally have negative radial velocities and have multicomponent profiles. [SII] lines are divided into four components, the velocities and relative intensities of which are variable. PV Cep can represent an intermediate type object, between the FUor and EXor classes, like V1647 Ori.

V350 Cep practically all the time remains at the maximal brightness level and its spectrum virtually does not change. The available data suggest that the pronounced P Cyg profile of the Hα line in the spectrum of V350 Cep appeared several years after the brightening, in 1986. The luminosities of stars in the current state are estimated as 20 L⊙ and 3.3 L⊙, respectively. In case of further development of P Cyg profile of the Hα line, it could be assumed that V350 Cep slowly develops towards to FUor type stars.

On the example of aforementioned 5 stars: *V1318 Cyg*, *V1686 Cyg*, *V565 Mon*, *PV Cep* and *V350 Cep* we demonstrated a difficulty of the definite classification of YSO's. In course of time, some previously identified EXor turns out to be a FUor, and vice versa, FUor-like object turn to be an EXor. Or, it happens, that a certain classification is clarified by observations performed over several, maybe even decades after. For example, our prediction in FUor nature of V1318 Cyg seems to be confirmed by our American colleagues [176]. Also, there are doubts in the classification of the other eruptive variables, such as V2493 [177], V2492 [178], V1647 Ori (as an intermediate object; [179]). Such uncertainties and modifications happen all the time. Consequently, a regular update of the lists of various classes of eruptive young variables is indeed necessary. For that reason the whole scientific community, including our group, constantly emphasize the importance of monitoring programs on objects showing eruptive variations. Even the observations performed by amateur astronomers, like a group of AAVSO, can play a big role.

Let us stress that FUor and EXor type outbursts are linked to the mass accretion rate from the disk, while in the UXor events they refer to obscuring dusty cloud oriented in the

line of sight. Therefore, for example EXor bursts can be combined with an UXor event as well. This complicates the general picture even more.

On the other hand, concerning FUor (also FUor-like) and EXor sources, it should be noted that although the usually accepted mechanisms responsible for such different manifestations of outburst phenomena are similar, the real differences should exist. In view of this let us note, that, according to the recent data, the FUors discs are noticeably more massive than EXors [180]. Moreover, the discs around the FUors are more compact than in EXors. Along with the absence of the outflowing activity in EXors, this, once again, confirms the idea that FUor events happen in the earlier stage of the disc evolution than EXor.

All this demonstrates that the studies of intermediate type objects (and my thesis is devoted to just that type of eruptive variables) can bring more light on the nature and the origin of this still not well understood phenomenon.

ACKLOWLEDGEMENTS

First and foremost I would like to express my sincere gratitude to my scientific advisor **Dr. Tigran Yu. Magakian** for his constant support! During our cooperative work Dr. Magakian has keeping the golden mean: giving me sufficient independence, but always ready to help. It was a great honor for me to get to know him and to have an opportunity to share many conversations about various topics (not only about science) with such a polymath person. I would like to thank a member of our scientific group **Dr. Tigran Movsessian** for helping me with the observations and for being a professional in it. I thank my **colleagues in BAO** for their kind attitude towards me.

I am thankful to **G. Oganesyan** for being a real motivator for me in science and in life. He is a language editor of this thesis.

Finally, I am eternally grateful to my family: **Ruben**, **Nella**, **Marianna**, **Lusine**, **Tatevik**, **Andranik** and the sweetest baby girl **Armine**, for believing in me and always lift me up in every circumstance, throughout every step of my life. I couldn't be luckier!

REFERENCES

1. Амбарцумян, В., “Звездные Ассоциации”, 1947, Астрономический Журнал, 26, 3
2. Амбарцумян, В. А., “Проблемы эволюции Вселенной”, 1968, Издательство Академии наук Армянской ССР
3. Strom, Karen M.; Strom, Stephen E.; Edwards, Suzan; Cabrit, Sylvie; & Skrutskie, Michael F., “Circumstellar Material Associated with Solar-Type Pre-Main-Sequence Stars: A Possible Constraint on the Timescale for Planet Building” 1989, Astronomical Journal, 97, 1451
4. Barsony, M., “Class 0 Protostars” 1994, Astronomical Society of the Pacific Conference Series, 65, 197
5. Andre, P. & Montmerle, T., “From T Tauri Stars to Protostars: Circumstellar Material and Young Stellar Objects in the ρ Ophiuchi Cloud”, 1994, Astrophysical Journal, 420, 837
6. Joy, Alfred H., “T Tauri Variable Stars”, 1945, Astrophysical Journal, 102, 168
7. Herbig, G. H., “The Properties and Problems of T Tauri Stars and Related Objects”, 1962, Advances in Astronomy and Astrophysics, 1, 47
8. Appenzeller, I. & Mundt, R., “T Tauri stars” 1989, The Astronomy and Astrophysics Review, 1, 291
9. Bertout, C., “T Tauri stars: wild as dust” 1989, Annual Review of Astronomy&Astrophysics, 27, 351
10. Herbst, W., Herbst, D. K., Grossman, E. J. & Weinstein, D., “Catalogue of UBVRI Photometry of T Tauri Stars and Analysis of the Causes of Their Variability” 1994, Astronomical Journal, 108, 1906
11. Hoffmeister, C., “Analyse der Lichtkurven von vier RW Aurigae-Sternen”, 1965, Veroeff. der Sternwarte in Sonneberg, 6, 97
12. Bouvier, J. & Bertout, C., “Spots on T-Tauri Stars” 1989, Astronomy&Astrophysics, 211, 99

13. Bibo, E. A., & The, P. S., “The type of variability of Herbig Ae/Be stars”, 1991, Astronomy and Astrophysics, Supplement Series, 89, 319
14. Audard, M., Ábrahám, P., Dunham, M. M., Green, J. D., Grosso, N., Hamaguchi, K., Kastner, J. H., Kóspál, Á., Lodato, G., Romanova, M. M., Skinner, S. L., Vorobyov, E. I. & Zhu, Z., “Episodic Accretion in young stars”, 2014, Protostars and Planets VI, eds. H. Beuther, R. S. Klessen, C. P. Dullemond, & T. Henning (Tucson: Univ. Arizone Press), 387
15. Herbig, G. H., “On the interpretation of FU Orionis”, 1966, Vistas in Astronomy, 8, 109
16. Herbig, G. H., “Eruptive phenomena in early stellar evolution”, 1977, Astrophysical Journal, 217, 693
17. Амбарцумян, В. А., “Фуоры”, 1971, Астрофизика, 7, 557
18. Clarke, C., Lodato, G., Melnikov, S. Y. & Ibrahimov, M. A., “The photometric evolution of FU Orionis objects: disc instability and wind-envelope interaction”, 2005, Monthly Notices of Royal Astronomical Society, 361, 942
19. Hartmann, L. & Kenyon, S. J., “On the nature of FU Orionis objects” 1985, Astrophysical Journal, 299, 462
20. Hartmann, L. & Kenyon, S. J., “The FU Orionis Phenomenon”, 1996, Annual Review of Astronomy&Astrophysics, 34, 207
21. Larson, R. B., “The FU ORI mechanism”, 1980, Monthly Notices of Royal Astronomical Society, 190, 321
22. Herbig, G., H., Petrov, P. P. & Duemmler, R., “High-Resolution Spectroscopy of FU Orionis Stars”, 2003, Astrophysical Journal, 595, 384
23. Aspin, C. & Reipurth, B., “Two Embedded Young Stellar Objects in NGC 2264 with FU Orionis Characteristics”, 2003, Astronomical Journal, 126, 2936
24. Greene, T. P., Aspin, C. & Reipurth, B., “High-Resolution Near-Infrared Spectroscopy of Fuors and Fuor-Like Stars”, 2008, Astronomical Journal, 135, 1421

25. Herbig, G. H., “FU Orionis eruptions”, In ESO Workshop on Low Mass Star Formation and Pre-Main Sequence Objects (B. Reipurth, ed.), ESO, Garching, 1989, 33-233
26. Weintraub, D. A., Sandell, G. & Duncan, W. D., “Are FU Orionis Stars Younger than T Tauri Stars? Submillimeter Constraints on Circumstellar Disks”, 1991, Astrophysical Journal, 382, 270
27. Sandell, G. & Weintraub, D. A., “On the Similarity of FU Orionis Stars to Class I Protostars: Evidence from the Submillimeter”, 2001, Astrophysical Journal Supplement Series, 134, 115
28. Reipurth, B. & Bally, J., “Herbig-Haro Flows: Probes of Early Stellar Evolution”, 2001, Annual Review of Astronomy and Astrophysics, 39, 403
29. Reipurth, B. & Aspin, C., “Infrared Spectroscopy of Herbig-Haro Energy Sources”, 1997, Astronomical Journal, 114, 2700
30. Парсамян, Э. С. и Гаспарян, К. Г., “О фуорообразных изменениях блеска звезд ассоциации Ориона”, 1987, Астрофизика, 27, 447
31. Bell, K. R. & Lin, D. N. C., “Using FU Orionis Outbursts to Constrain Self-regulated Protostellar Disk Models”, 1994, Astrophysical Journal, 427, 987
32. Bonnell, I. & Bastien, P., “A Binary Origin for FU Orionis Stars”, 1992, Astrophysical Journal, 401, L31
33. Antoniucci, S., Arkharov, A. A., Di Paola, A., Giannini, T., Kishimoto, M., Kloppenborg, B., Larionov, V. M., Li Causi, G., Lorenzetti, D., Vitali, F., “EXORCISM: EXOR optiCal Infrared Systematic Monitoring”, 2013, in Protostars and Planets VI, Heidelberg, July 15–20, 2013. Poster #2B055, 55
34. Lorenzetti, D., “The EXor phenomenon”, 2016, arXiv160303034
35. Herbig, G. H., “The Spectra of Be- and Ae- Type Stars Associated with Nebulosity”, 1960, Astrophysical Journal Supplement, 4, 337
36. Bastian, U.; Finkenzeller, U.; Jaschek, C. & Jaschek, M.; “The definition of T Tauri and Herbig Ae/Be stars”, 1983, Astronomy&Astrophysics, 126, 438

37. Finkenzeller, U. & Mundt, R., “The Herbig Ae/Be stars associated with nebulosity”, 1984, Astronomy&Astrophysics Supplement Series, 55, 109
38. Oudmaijer, R. D.; Palacios, J.; Eiroa, C. & Davies, J. K., “EXPORT: Optical photometry and polarimetry of Vega-type and pre-main sequence stars”, 2001, Astronomy&Astrophysics, 379, 564
39. Mendigutía, I., Eiroa, C., Montesinos, B., Mora, A., Oudmaijer, R. D., Merín, B., and Meeus, G., “Optical spectroscopic variability of Herbig Ae/Be stars”, 2011, Astronomy&Astrophysics, 529, 34
40. Vioque, M., Oudmaijer, R. D.; Baines, D.; Mendigutia, I. & Perez-Martinez, R., “Gaia DR2 study of Herbig Ae/Be stars”, 2018, Astronomy&Astrophysics, 620, 128
41. Gorti, U., Dullemond, C. P., & Hollenbach, D., “Time Evolution of Viscous Circumstellar Disks due to Photoevaporation by Far-Ultraviolet, Extreme-Ultraviolet, and X-ray Radiation from the Central Star”, 2009, The Astrophysical Journal, 705, 1237
42. Natta, A., Grinin, V.P., Mannings, V., Ungerechts, H., “The Evolutionary Status of UX Orionis-Type Stars”, 1997, The Astrophysical Journal, 491, 885
43. Lause, F., “UX Orionis” 1930, Astronomische Nachrichten; 239, 303
44. Grinin, V. P., Kiselev, N.N., Minikulov, N. Kh., Chernova, G. P. & Voshchinnikov, N. V., “The investigations of zodiacal light of isolated Ae-Herbig stars with non-periodic Algol-type minima” 1991, Astrophysics and Space Science, 186, 283
45. Grinin, V.P., “Polarimetric activity of Herbig Ae/Be stars”, 1994, Astronomical Society of the Pacific Conference Series, 62, 63
46. Natta, A. & Whitney, B.A., “Models of scattered light in UXORs” 2000, Astronomy&Astrophysics, 364, 633
47. Wenzel, W., “Extremely young stars. Introductory report”, 1969, Communications of the Konkoly Observatory, 65, 61
48. Bibo, E. A. & The, P. S., “A study of the Herbig Ae-type star UX Orionis: its remarkable behaviour in the colour-magnitude diagram, and the properties of its dust shell”, 1990, Astronomy&Astrophysics, 236, 155

49. The, P. S., de Winter, D., & Perez, M. R., “A new catalogue of members and candidate members of the Herbig Ae/Be (HAEBE) stellar group”, 1994, Astronomy & Astrophysics Supplements, 104, 315
50. https://www.aavso.org/
51. Afanasiev, V. L. & Moiseev, A. V., “The SCORPIO Universal Focal Reducer of the 6-m Telescope”, 2005, Astronomy Letters, 31, 194
52. Afanasiev, V. L. & Moiseev, A.V., “Scorpio on the 6-m Telescope: Current State and Perspectives for Spectroscopy of Galactic and Extragalactic Objects”, 2011, Baltic Astronomy, 20, 363
53. Bonnarel, F., Fernique, P., Bienaymé, O., Egret, D., Genova, F., Louys, M., Ochsenbein, F.; Wenger, M., Bartlett, J. G., “The ALADIN interactive sky atlas. A reference tool for identification of astronomical sources”, 2000, Astronomy and Astrophysics Supplement, 143, 33
54. Wenger, M., Ochsenbein, F., Egret, D., Dubois, P., Bonnarel, F., Borde, S., Genova, F., Jasniewicz, G., Laloë, S., Lesteven, S., Monier, R., “The SIMBAD astronomical database. The CDS reference database for astronomical objects” 2000, Astronomy and Astrophysics Supplement, 143, 9
55. Ochsenbein, F.; Bauer, P.; Marcout, J, “The VizieR database of astronomical catalogues”, 2000, Astronomy and Astrophysics Supplement, 143, 23
56. Gaia Collaboration (Prusti, T., et al.), “The Gaia mission”, 2016, 595, A1
57. Gaia Collaboration, Brown, A. G. A., Vallenari, A., Prusti, T., & de Bruijne, J. H. J., “Gaia Data Release 2. Summary of the contents and survey properties”, 2018, Astronomy&Astrophysics, 616, 1
58. https://www.originlab.com/
59. https://inkscape.org/
60. Romano, G., “New Variable Stars in Field Centered on Gamma Cygni”, 1967, Information Bulletin on Variable Stars, 229, 1
61. Romano, G., “Researches with the Schmidt telescopes. III. Variable stars in the field of gamma Cygni”, 1969, Memorie della Societa Astronomica Italiana, 40, 375

62. Wenzel, W., “Observations of the Extremly Young Stellar Group LkHα 224 and 225”, 1972, Information Bulletin on Variable Stars, 713, 1
63. Strom, K.M., Strom, S. E., Breger, M., et al., “Infrared and Optical Observations of a Young Stellar Group Surrounding BD+40°4124”, 1972, Astrophysical Journal, 173, L65
64. Allen, D. A., “Near infrared magnitudes of 248 early-type emission-line stars and related objects”, 1973, Monthly Notices of the Royal Astronomical Society, 161, 145
65. Wenzel, W., “Note on the extremely young stars LkHα 224 and 225”, 1980, Mitt. Verand. Sterne, 8, 182
66. Ибрагимов, М. А., Мельников, С. Ю., Чернышев, А. В., Шевченко, В. С., “Необычные цветовые изменения V 1318 Cyg=LkHα 225”, 1988, Астрофизика, 29, 633
67. Шевченко, В. С., Ибрагимов, М. А. & Чернышева, Т. Л., “Область звездообразования RSF 2 CYG, связанная с чрезвычайно молодым скоплением NGC 6910 и звездами Ae / Be Herbig BD+40°4124 и BD+41°3731” 1991, Астрономический Журнал, 68, 466
68. Shevchenko, V. S., Grankin, K. N., Ibragimov, M. A., Mel’Nikov, S.Y., & Yakubov, S.D., “Periodic Phenomena in Ae/Be Herbig Stars Lightcurves – Part One Lightcurves Classification and Digital Analysis Methods”, 1993, Astrophysics&Space Science, 202, 121
69. Aspin, C., Sandell, G., & Weintraub, D. A., “The remarkable pre-main sequence object V1318 Cygni”, 1994, Astronomy&Astrophysics, 282, L25
70. Hillenbrand, L. A., Meyer, M. R., Strom, S. E., & Skrutskie, M. F., “Isolated Star Forming Regions Containing Herbig Ae/Be Stars. I. The Young Stellar Aggregate Associated With BD+40°4124” 1995, The Astronomical Journal, 109, 280
71. Магакян, Т. Ю. & Мовсесян, Т. А., “LkHα 225: свидетельство коллимированного истечения в оптическом спектре”, 1997, Письма в Астрономический Журнал, 23, 764

72. Herbst, W. & Shevchenko, V. S., “A Photometric Catalog of Herbig AE/BE Stars and Discussion of the Nature and Cause of the Variations of UX Orionis Stars”, 1999, The Astronomical Journal, 118, 1043
73. Lang, D., Hogg, D. W., Mierle, K., Blanton, M., Roweis, S., “Astrometry.net: Blind Astrometric Calibration of Arbitrary Astronomical Images”, 2010, The Astronomical Journal, 139, 1782
74. Drew, J. E., Greimel, R., Irwin, M. J., et al., “The INT Photometric Hα Survey of the Northern Galactic Plane (IPHAS)”, 2006, Monthly Notices of Royal Astronomical Society, 362, 753
75. Alam, S., Albareti, F. D., Allende Prieto, C., et al., “The Eleventh and Twelfth Data Releases of the Sloan Digital Sky Survey: Final Data from SDSS-III”, 2015, The Astrophysical Journal Supplement Series, 219, 12
76. Chambers, K. C., Magnier, E. A., & Metcalfe, N., “The Pan-STARRS1 Surveys” 2016, ArXiv e-prints [arXiv:1612.05560]
77. Jester, S., Schneider, D. P., Richards, G. T., et al., “The Sloan Digital Sky Survey View of the Palomar-Green Bright Quasar Survey”, 2005, AJ, 130, 873
78. Petrov, P. P., & Babina, E. V., “The photospheric spectrum of the pre-FUor V1331 Cyg: Is it a star or a disk?”, 2014, Bulletin of the Crimean Astrophysical Observatory, 110, 1
79. Herbig, G. H., “The Diffuse Interstellar Bands”, 1995, ARA&A, 33, 19
80. Магакян, Т. Ю. & Мовсесян, Т. А., “Спектр PV Cep и GM1-29 (RNO125) в 1976 1977гг.”, 2001, Астрофизика, 44, 515
81. Herbig, G. H., “The Unusual Pre-Main-Sequence Star VY Tauri”, 1990, Astrophysical Journal, 360, 639
82. Palla, F., Testi, L., Hunter, T. R., et al., “The active source in the region of the Herbig star BD+40°4124”, 1995, Astronomy&Astrophysics, 293, 521
83. van den Ancker, M. E., Wesselius, P.R. & Tielens, A. G. G. M., “ISO spectroscopy of young intermediate-mass stars in the BD+40°4124 group”, 2000, Astronomy&Astrophysics, 355, 194

84. Hernández, J., Calvet, N., Briceňo, C., Hartmann, L., Berlind, P., "Spectral Analysis and Classification of Herbig Ae/Be Stars", 2004, AJ, 127, 1682
85. Gray, R. O. & Corbally, C. J., "Stellar Spectral Classification", 2009, Princeton University Press, ISBN: Â 978-0-691-12511-4
86. Cohen, M. & Kuhi, L. V., "Observational studies of pre-main-sequence evolution", 1979, Astrophysical Journal Supplement Series, 41, 743
87. Rodgers, B., Wooden, D., H., Grinin, V., Shakhovsky, D., & Natta, A., "Spectroscopic Variability of the UXOR Star RR Tauri", 2002, Astrophysical Journal, 564, 405
88. Loren, R. B., "The star-formation process in molecular clouds associated with Herbig Be/Ae stars. I. LkHα 198, BD+40°4124, and NGC 7129", 1977, Astrophysical Journal, 218, 716
89. Davies, R. I., Tecza, M., Looney, L. W., et al., "Adaptive Optics Integral Field Spectroscopy of the Young Stellar Objects in LkHα 225", 2001, Astrophysical Journal, 552, 692
90. Looney, L. W., Wang, S., Hamidouche, M., Safier, P.N., & Klein, R., "Colliding Clouds: The Star Formation Trigger of the Stellar Cluster around BD+40°4124", 2006, Astrophysical Journal, 642, 330
91. Sandell, G., Wiesemeyer, H., Requena-Torres, M.A., et al., "GREAT [C II] and CO observations of the BD+40°4124 region", 2012, Astronomy&Astrophysics, 542, L14
92. Matthews, B. C., Graham, J. R., Perrin, M. D. & Kalas, P., "The Molecular Gas Environment around Two Herbig Ae/Be Stars: Resolving the Outflows of LkHα 198 and LkHα 225S", 2007, Astrophysical Journal, 671, 483
93. Kurosawa, R., Harries, T. J., & Symington, N. H., "On the formation of Hα line emission around classical T Tauri stars", 2006, Monthly Notices of Royal Astronomical Society, 370, 580
94. Reipurth, B., Pedrosa, A., & Lago, M. T. V. T., "Hα emission in pre-main sequence stars. I. an atlas of line profiles", 1996, Astronomy and Astrophysics Supplement, 120, 229

95. Perrin, M. D., Graham, J. R., Kalas, P., et al., “Laser guide star adaptive optics imaging polarimetry of Herbig Ae/Be stars”, 2004, Proceedings of the SPIE, 5490, 309
96. Johnson, H. L., Photometric Systems, 1963, In Basic Astronomical Data, edited by K.A. Strand (Chicago: Chicago University Press), 204
97. Johnson, H. L., Astronomical Measurements in the Infrared, 1966, Annual Review of Astronomy and Astrophysics, 4, 193
98. Connelley, M. S. & Reipurth, B., “A Near-infrared Spectroscopic Survey of FU Orionis Objects”, 2018, The Astrophysical Journal, 861, 145
99. Lorenzetti, D., Antonucci, S., Giannini, T., et al., “On the Nature of EXor Accretion Events: An Infrequent Manifestation of a Common Phenomenology”, 2012, Astrophysical Journal, 749, 188
100. Semkov, E. H. & Peneva, S. P., “Optical photometry of GM Cep: evidence for UXor type of variability”, 2012, Astrophysics and Space Science, 338, 95S
101. Mora, A., Merín, B., Solano, E., et al., “EXPORT: Spectral classification and projected rotational velocities of Vega-type and pre-main sequence stars”, 2001, Astronomy&Astrophysics, 378, 116
102. Magakian, T. Yu., Movsessian, T.A., Andreasyan, H.R. & Gevorgyan, M.H., “New powerful outburst of the unusual young star V1318 Cygni S (LkHα 225)”, 2019, Astronomy&Astrophysics, 625, A13
103. Donehew, B. & Brittain, S., “Measuring the Stellar Accretion Rates of Herbig Ae/Be Stars”, 2011, The Astronomical Journal, 141, 46
104. Cauley, P.W & Johns-Krull, C.M., “Optical Mass Flow Diagnostics in Herbig Ae/Be Stars”, 2015, The Astrophysical Journal, 810, 5
105. Giannini, T., Munari, U., Antoniucci, S., Lorenzetti, D., Arkharov, A.A., Dallaporta, S., Rossi, A. & Traven, G., “The 2016-2017 peak luminosity of the pre-main sequence variable V2492 Cygni”, 2018, Astronomy&Astrophysics, 611 54

106. Jurdana-Šepić, R., Munari, U., Antoniucci, S., Giannini, T. & Lorenzetti, D., "Towards a better classification of unclear eruptive variables: the cases of V2492 Cyg, V350 Cep, and ASASSN-15qi" 2018, Astronomy&Astrophysics, 614, 9
107. Ábrahám, P., Kóspál, Á., Kun, M., Fehér, O., Zsidi, G., Acosta-Pulido, J.A., Carnerero, M. I. et al., "An UXor among FUors: Extinction-related Brightness Variations of the Young Eruptive Star V582 Aur", 2018, The Astrophysical Journal, 853, 28
108. Hoffmeister, C., "Mitteilungen über neuentdeckte Veränderliche Sterne (S 10153 S10375)", 1968, Astronomische Nachrichten, 290, 277
109. Парсамян, Э. С., "Список кометарных туманностей, обнаруженных на Паломарских картах", 1965, Известия АН АРМ. ССР, 18, 146
110. Cohen, M., "Infrared Observations of New Cometary Nebulae", 1974, Publications of the Astronomical Society of the Pacific, 86, 813
111. Neckel T. & Staude H. J., "A survey of bipolar and cometary nebulae. Photographic and photometric observations", 1984, Astronomy&Astrophysics, 131, 200
112. Herbig, G. H. & Bell, K. R., "Third Catalog of Emission-Line Stars of the Orion Population", 1988, Lick Observatory Bulletin, 1111
113. Weintraub, D. A., "A Catalog of Pre-Main Sequence Emission-Line Stars with IRAS Source Associations", 1990, Astrophysical Journal Supplement, 74, 575
114. Magakian, T. Yu., "Merged catalogue of reflection nebulae", 2003, Astronomy&Astrophysics, 399, 141
115. Kim, B. G., Kawamura, A., Yonekura, Y., Fukui, Y., "^{13}CO (J=1-0) Survey of Molecular Clouds toward the Monoceros and Canis Major Region", 2004, Publications of the Astronomical Society of Japan, 56, 313
116. Maddalena R. J., Morris M., Moscowitz J. & Thaddeus P., "The Large System of Molecular Clouds in Orion and Monoceros", 1986, The Astrophysical Journal, 303, 375
117. Hilton, J. & Lahulla, J. F., "Distance measurements of Lynds galactic dark nebulae" 1995, Astronomy and Astrophysics Supplement, 113, 325

118. Магакян, Т. Ю., Мовсесян, Т. А., Никогосян, Е. Г., “Поиски НН объектов и эмиссионных вед в областях звездообразования. IV. Новые потоки и объекты Хербига-Аро, связанные с кометарными туманностями”, 2008, Астрофизика, 51, 15
119. Herbig, G. H., “Apparent Lithium Isotope Ratios in F5-G8 Main Sequence Stars” 1964, Astronomical Journal, 69Q, 141
120. Takeda, Y. & Kawanomoto, S., “Lithium Abundances of F, G, and K-Type Stars: Profile-Fitting Analysis of the Li I 6708 Doublet”, 2005, Publications of the Astronomical Society of Japan, 57, 45
121. Любимков, Л. С., “Литий в звездных атмосферах: наблюдения и теория”, 2016, Астрофизика, 59, 459
122. Bailer-Jones, C., Farnocchia D., Meech K., Brasser R., Micheli M., Chakrabarti S., Buie M. & Hainaut O., “Estimating Distance from Parallaxes. IV. Distances to 1.33 Billion Stars in Gaia Data Release 2”, 2018, The Astronomical Journal, 156, 58B
123. Abrahamyan, H., Mickaelian, A. & Knyazyan, A., “The IRAS PSC/FSC Combined Catalogue”, 2015, Astronomy and Computing, 10, 99
124. Cutri, R. M. & et al., “VizieR Online Data Catalog: WISE All-Sky Data Release”, 2012, VizieR Online Data Catalog, 2311, 0C
125. Fischer, W. J., Padgett, D. L., Stapelfeldt, K. L., Sewilo, M., “A WISE Census of Young Stellar Objects in Canis Major”, 2016, The Astrophysical Journal, 827, 96
126. Egan, M. P., Price, S. D., Kraemer, K. E., Mizuno, D. R., Carey, S. J., Wright, C. O., Engelke, C. W., Cohen, M. & Gugliotti, M. G., “VizieR Online Data Catalog: MSX6C Infrared Point Source Catalog. The Midcourse Space Experiment Point Source Catalog Version 2.3 (October 2003)”, 2003, VizieR Online Data Catalog, 5114, 0E
127. Cutri, R. M., Skrutskie, M. F., van Dyk. S., Beichman, C. A., Carpenter, J. M., Chester, T., Cambresy, L., Evans, T., Fwoler, J., Gizis, J., Howard, E., Huchra, J., Jarrett, T., Kopan, E. L., Kirkpatrick, J. D., Light, R. M., Marsh, K. A., McCallon, H., Schneider, S., Stiening, R., Sykes, M., Weinberg, M., Wheaton, W. A., Wheelock,

S., & Zacarias, N., “VizieR Online Data Catalog: 2MASS All-Sky Catalog of Point Sources”, 2003, Vizier Online Data Catalog, 2246, 0C

128. Tian, Hai-Jun, Gupta, P., Sesar, B., Rix, H., Martin, N., Liu, Ch., Goldman, B., Platais, I., Kudritzki, R. & Waters, Ch., “A Gaia-PS1-SDSS (GPS1) Proper Motion Catalog Covering ¾ of the Sky”, 2017, The Astrophysical Journal Supplement Series, 232, 4
129. Allen, C. W., “Astrophysical Quantities”, 1975, Astrophysical Quantities (3rd ed.; Athlone: London)
130. Connelley, M., Reipurth, B. & Tokunaga, A., “Infrared Nebulae around Young Stellar Objects”, 2007, The Astronomical Journal, 133, 1528
131. Robitaille, T. P., Whitney, B. A., Indebetouw, R. & Wood, K., “Interpreting Spectral Energy Distributions from Young Stellar Objects. II. Fitting Observed SEDs Using a Large Grid of Precomputed Models”, 2007, The Astrophysical Journal Supplement Series, 169, 328
132. D’Orazi V., Magrini L., Randich S., Galli D., Busso M. & Sestito P., “Enhanced Production of Barium in Low-Mass Stars: Evidence from Open Clusters”, 2009, The Astrophysical Journal Letters, 693L, 31D
133. Desidera S., Covino E., Messina, S., D’Orazi V., Alcalá, J. M., Brugaletta, E.; Carson, J., Lanzafame A. C. & Launhardt R., “The debris disk host star HD 61005: a member of the Argus association”, 2011, Astronomy&Astrophysics, 529A, 54D
134. Maiorca E., Randich S., Busso M., Magrini L. & Palmerini S., “s-processing in the Galactic Disk. I. Super-solar Abundances of Y, Zr, La, and Ce in Young Open Clusters”, 2011, The Astrophysical Journal, 736, 120M
135. D’Orazi V., Biazzo K., Desidera S., Covino E., Andrievsky S. M. & Gratton R. G., “The chemical composition of nearby young associations: s-process element abundances in AB Doradus, Carina-Near and Ursa Major”, 2012, Monthly Notices of Royal Astronomical Society, 423, 2789

136. Mishenina T., Korotkin S., Carraro G., Kovtyukh V. V. & Yegorova I. A., “Barium and yttrium abundance in intermediate-age and old open clusters”, 2013, Monthly Notices of Royal Astronomical Society, 433, 1436M
137. Mishenina T., Pignatari M., Carraro G., Kovtyukh V., Monaco L., Korotkin S., Shereta E., Yegorova I. & Herwig F., “New insights on Ba overabundance in open clusters. Evidence for the intermediate neutron-capture process at play?”, 2015, Monthly Notices of Royal Astronomical Society, 446, 3651M
138. D’Orazi V., De Silva G. M. & Melo C. F. H., “First determination of s-process element abundances in pre-main sequence clusters. Y, Zr, La, and Ce in IC 2391, the Argus association, and IC 2602”, 2017, Astronomy&Astrophysics, 598A, 86D
139. Гюльбудагян, А. Л. & Магакян, Т. Ю., “Новая Кометарная Туманность”, 1977, Письма в Астрономический Журнал, 3, 113
140. Cohen, M., Kuhi, L.V., Harlan, E.A., “A remarkable structural change in a faint cometary nebula”, 1977, Astrophysical Journal, 215, L127
141. Магакян, Т. Ю., Амирханян, А. С., “О спектрах двух переменных звезд в Цефее”, 1977, Астрономический Циркуляр, № 1038, 6
142. Cohen, M., Kuhi, L.V., Harlan, E.A., Spinrad, H., “Continuing changes in the peculiar nebulous object PV Cep”, 1981, Astrophysical Journal, 245, 920,
143. Herbig, G.H., “History and Spectroscopy of EXor Candidates”, 2008, The Astronomical Journal, 135, 637,
144. Reipurth B., Bally J., Devine D., “Giant Herbig-Haro Flows”, 1997, The Astronomical Journal, 114, 2708,
145. Gomez, M., Whitney, B.A., Kenyon, S. J., “A survey of optical and near-infrared jets in taurus embedded sources”, 1997, The Astronomical Journal, 114, 1138,
146. Levreault, R.M., “Interactions between pre-main-sequence objects and molecular clouds. II. PV Cephei”, 1984, Astrophysical Journal, 277, 634,
147. Мовсесян, Т. А., Магакян, Т. Ю., Саргсян, Д. М., Никогосян, Е. Г., “Интегральная спектроскопия туманности GM 1-29 и зведы PV Cep”, 2008, Астрофизика, 51, 461

148. Kun, M., Szegedi-Elek, E., Moór, A. et al., “Inner disc rearrangement revealed by dramatic brightness variations in the young star PV Cep”, 2011, Monthly Notices of Royal Astronomical Society, 413, 2689,
149. Caratti o Garatti, A., Garcia Lopez, R., Weigelt, G. et al., “LBT/LUCIFER near infrared spectroscopy of PV Cephei. An outbursting young stellar object with an asymmetric jet” 2013, Astronomy&Astrophysics, 554, A66,
150. Гюльбудагян, А. Л., Саркисян, Р. А., “Новая переменная СПЗ 2246 вблизи туманности NGC 7129”. 1977, Астрономический Циркуляр, № 972, 7
151. Pogosyants. A. Yu., “The Unusual T Tauri Type Star V350 Cephei”, 1991, IBVS 3624, 1
152. Ibryamov, S., Semkov E., Peneva S., “A long-term UBVRI photometric study of the pre-main sequence star V350 Cep”, 2014, Research in Astronomy and Astrophysics, 14, 1264
153. Semkov, E. H., Ibryamov S. I., Peneva S. P., “A deep decrease event in the brightness of the PMS star V350 Cep”, 2017, Bulgarian Astronomical Journal, 27, 75
154. Cohen, M. & Fuller, G. A., “Optical spectroscopy of known and suspected Herbig Haro objects”, 1985, Astrophysical Journal, 296, 620
155. Miranda, L. F., Eiroa, C., Fernandez, M., Gomez de Castro A. I., “Long-slit spectroscopy and direct imaging of the PMS objects GGD 33 and V350 Cephei in NGC 7129”, 1994, Astronomy&Astrophysics, 281, 864
156. Магакян, Т. Ю., Мовсесян, Т. А., Оганесян, Е., “Спектр V350 Cep: наблюдения 1978-1994гг.”, 1999, Астрофизика, 42, 121
157. Dahm, S. E., Hillenbrand, L. A., “An Optical Survey of the Partially Embedded Young Cluster in NGC 7129”, 2015, Astronomical Journal, 149, 200
158. Penston, M. V., Keavey, P. M., “The spectrum of the T Tauri star LkHα 120”, 1977, Monthly Notices of Royal Astronomical Society, 180, 407
159. Neckel, T., Staude, H. J., Sarcander, M., Birkle, K., “Herbig-Haro emission in two bipolar reflection nebulae” 1987, Astronomy&Astrophysics, 175, 231

160. Hamann, F., Persson, S. E., “Emission-Line Studies of Young Stars. II. The Herbig Ae/Be Stars”, 1992, Astrophysical Journal Supplement, 82, 285
161. Corcoran, M., Ray, T. P., “Forbidden emission lines in Herbig Ae/Be stars”, 1997, Astronomy&Astrophysics, 321, 189
162. Acke, B., van den Ancker M. E., Dullemond C. P., “[OI] 6300Å emission in Herbig Ae/Be systems: Signature of Keplerian rotation”, 2005, Astronomy&Astrophysics, 436, 209
163. Hamidouche, M., “Aperture Synthesis Imaging of V892 Tau and PC Cep: Disk Evolution”, 2010, Astrophysical Journal, 722, 204
164. Whelan, E. T., Dougados, C., Perrin, M.D., et al., “The 2008 Outburst in the Young Stellar System Z CMa: The First Detection of Twin Jets”, 2010, The Astrophysical Journal Letters, 720, L119
165. Magakian, T. Yu., Movsessian, T. A., Nikogossian, E. H. et al., “V2494 Cyg: a unique FU Ori type object in the Cygnus OB7 complex”, 2013, Monthly Notices of Royal Astronomical Society, 432, 2685
166. Goodrich, R. W., “New observations of Herbig-Haro objects and related stars”, 1986, Astronomical Journal, 92, 885
167. Kun, M., Balog, Z., Kenyon, S. J., Mamajek, E. E., Gutermuth, R. A., “Pre-Main Sequence Stars in the Cepheus Flare Region”, 2009, The Astrophysical Journal Supplement, 185, 451
168. Мовсесян, Т. А., Магакян, Т. Ю., Моисеев, А. В., Геворгян, М. Г., “Детальное кинематическое исследование объектов Хербига-Аро в северо-восточной области NGC 7129”, 2015, Астрофизический Бюллетень, 70, 215
169. Cantat-Gaudin, T., Jordi, C., Vallenari, A., et al., “A Gaia DR2 view of the open cluster population in the Milky Way”, 2018, Astronomy&Astrophysics, 618, A93
170. Hartigan, P., Strom, K. M., Strom, S. E., “Are Wide Pre-Main-Sequence Binaries Coeval”, Astrophysical Journal, 1994, 427, 961

171. Lorenzetti, D., Giannini, T., Larionov, V.M. et al., “Simultaneous Monitoring of the Photometric and Polarimetric Activity of the Young Star PV Cep in the Optical/Near infrared Bands”, 2011, The Astrophysical Journal, 732, 69
172. Lorenzetti, D., Larionov, V. M., Giannini, T. et al., “Near-Infrared Spectroscopic Monitoring of EXor Variables: First Results”, 2009, The Astrophysical Journal, 693, 1056
173. Andreasyan, H., Magakian, T., Movsessian, T., “Simultaneous photometric and spectral analysis of a new outburst of V1686 Cyg”, 2020, Research in Astronomy and Astrophysics, 20, 53
174. Andreasyan, H., “Spectral study of V565 Mon: Probable FU Ori-like or chemically peculiar star”, 2021, Research in Astronomy and Astrophysics, 21, 64
175. Андреасян, А. Р., Магакян, Т. Ю., Мовсесян, Т. А., Моисеев, А. В., “PV CEP и V350 CEP: Звезды на пути между Фуорами и Эксорами”, 2021, Астрофизика, 64, 213
176. Hillenbrand, L. A., Isaacson H., Rodriguez, A. C., Connelley M., Reipurth B., Kuhn, M. A., Beck T., Perez, D. R., 2021 (in preparation)
177. Miller, K. A., Smith, W. W., Ehrenreich, T., et al. 2011, ApJ, 730, 80
178. Ibryamov, S. I., Semkov, E. H., Peneva, S. P., “V2492 Cygni: Optical BVRI Variability During the Period 2010-2017”, 2018, Publications of the Astronomical Society of Australia, 35, 7
179. Aspin, C., “The Continuing Outburst of V1647 Orionis: Winter/Spring 2011 Observations”, 2011, The Astronomical Journal, 142, 135
180. Cieza, L. A., Ruíz-Rodríguez, D., Perez, S., Casassus, S., Williams, J. P., Zurlo, A., Principe, D. A., Hales, A., Prieto, J. L., Tobin, J. J., Zhu, Z., Marino, S., “The ALMA early science view of FUor/EXor objects- V. Continuum disc masses and sizes”, 2018, Monthly Notices of the Royal Astronomical Society, 474, 4347